HIV

CD4 binding site immunogens elicit heterologous anti–HIV-1 neutralizing antibodies in transgenic and wild-type animals

Harry B. Gristick[1]†, Harald Hartweger[2]†, Maximilian Loewe[2], Jelle van Schooten[1]‡, Victor Ramos[2], Thiago Y. Oliveira[2], Yoshiaki Nishimura[3], Nicholas S. Koranda[1], Abigail Wall[4,5]§, Kai-Hui Yao[2], Daniel Poston[2]||, Anna Gazumyan[2], Marie Wiatr[2], Marcel Horning[2], Jennifer R. Keeffe[1], Magnus A. G. Hoffmann[1], Zhi Yang[1], Morgan E. Abernathy[1]¶, Kim-Marie A. Dam[1], Han Gao[1], Priyanthi N. P. Gnanapragasam[1], Leesa M. Kakutani[1], Ana Jimena Pavlovitch-Bedzyk[1]#, Michael S. Seaman[6], Mark Howarth[7], Andrew T. McGuire[4,5], Leonidas Stamatatos[4,5], Malcolm A. Martin[3], Anthony P. West Jr.[1], Michel C. Nussenzweig[2,8]*, Pamela J. Bjorkman[1]***

Passive transfer of broadly neutralizing anti–HIV-1 antibodies (bNAbs) protects against infection, and therefore, eliciting bNAbs by vaccination is a major goal of HIV-1 vaccine efforts. bNAbs that target the CD4 binding site (CD4bs) on HIV-1 Env are among the most broadly active, but to date, responses elicited against this epitope in vaccinated animals have lacked potency and breadth. We hypothesized that CD4bs bNAbs resembling the antibody IOMA might be easier to elicit than other CD4bs antibodies that exhibit higher somatic mutation rates, a difficult-to-achieve mechanism to accommodate Env's N276$_{gp120}$ N-glycan, and rare five-residue light chain complementarity-determining region 3. As an initial test of this idea, we developed IOMA germline–targeting Env immunogens and evaluated a sequential immunization regimen in transgenic mice expressing germline-reverted IOMA. These mice developed CD4bs epitope–specific responses with heterologous neutralization, and cloned antibodies overcame neutralization roadblocks, including accommodating the N276$_{gp120}$ glycan, with some neutralizing selected HIV-1 strains more potently than IOMA. The immunization regimen also elicited CD4bs-specific responses in mice containing polyclonal antibody repertoires as well as rabbits and rhesus macaques. Thus, germline targeting of IOMA-class antibody precursors represents a potential vaccine strategy to induce CD4bs bNAbs.

INTRODUCTION

A successful vaccine against HIV-1 would be the most effective way to contain the AIDS pandemic, which, so far, is responsible for >36 million deaths in total and 1 to 2 million new infections each year (https://unaids.org/en/resources/fact-sheet). Clinical trials of vaccine candidates have revealed disappointing outcomes, and, as a result, there is no currently available protective vaccine against HIV-1 (*1*), in part due to the large number of circulating HIV-1 strains (*2*). For the past decade, a major focus of HIV-1 vaccine design has been on eliciting broadly neutralizing antibodies (bNAbs), which neutralize a majority of HIV-1 strains in vitro at low concentrations (*1*). Multiple studies have demonstrated that passively administered bNAbs can prevent HIV-1 or simian/human immunodeficiency virus (SHIV) infection (*3*–*15*), suggesting that a vaccination regimen that elicits bNAbs at neutralizing concentrations would be protective.

The HIV-1 envelope (Env) protein, a trimeric membrane glycoprotein comprising gp120 and gp41 subunits that is found on the surface of the virus, is the sole antigenic target of NAbs (*16*). An impediment to HIV-1 vaccine design is that most inferred germline (iGL) precursors of known bNAbs do not bind with detectable affinity to native Envs on circulating HIV-1 strains (*17*–*28*). As a result, potential Env immunogens must be modified to bind and select for bNAb precursors in vivo during immunization (i.e., a "germline-targeting" approach). This approach has been used to activate precursors of the VRC01 class of bNAbs that target the CD4 binding site (CD4bs) on gp120 (*25*, *29*). Eliciting VRC01-class bNAbs that target the CD4bs would be desirable because of their breadth and potency (*30*). However, the VRC01 class of bNAbs may be difficult to elicit because of their requirement for rare short light chain (LC) complementarity-determining region 3 (CDRL3) loops of five residues (present in only ~1% of human

[1]Division of Biology and Biological Engineering, California Institute of Technology, Pasadena, CA 91125, USA. [2]Laboratory of Molecular Immunology, Rockefeller University, New York, NY 10065, USA. [3]Laboratory of Molecular Microbiology, National Institute of Allergy and Infectious Diseases, National Institutes of Health, Bethesda, MD 20892, USA. [4]Vaccine and Infectious Disease Division, Fred Hutchinson Cancer Research Center, Seattle, WA 98109, USA. [5]Department of Global Health, University of Washington, Seattle, WA 98195, USA. [6]Center for Virology and Vaccine Research, Beth Israel Deaconess Medical Center, Boston, MA 02215, USA. [7]Department of Biochemistry, University of Oxford, South Parks Road, Oxford OX1 3QU, UK. [8]Howard Hughes Medical Institute, Rockefeller University, New York, NY 10065, USA.
*Corresponding author. Email: bjorkman@caltech.edu (P.J.B.); nussen@rockefeller.edu (M.C.N.)
†These authors contributed equally to this work.
‡Present address: Department of Medical Microbiology, Amsterdam UMC, University of Amsterdam, Amsterdam, Netherlands.
§Present address: Sage Bionetworks, Seattle, WA 98121, USA.
||Present address: Laboratory of Retrovirology, Rockefeller University, New York, NY 10065, USA.
¶Present address: 290 Jane Stanford Way, ChEM-H/Neuro Building, Stanford, CA 94305, USA.
#Present address: Department of Microbiology and Immunology, Stanford University School of Medicine, Stanford, CA 94305, USA.
**Present address: Department of Pharmacology, University of Cambridge, Tennis Court Road, Cambridge CB2 1PD, UK.

Abs) (*31*) and many somatic hypermutations (SHMs), including a difficult-to achieve sequence of mutations to sterically accommodate the highly conserved $N276_{gp120}$ glycan (*32*).

Crystal structures of a natively glycosylated HIV-1 soluble Env trimer derived from the clade A BG505 strain (BG505 SOSIP.664) (*33*) complexed with the Ab IOMA revealed that this CD4bs bNAb exhibits distinct properties from VRC01-class bNAbs (*34*). In common with VRC01-class bNAbs, IOMA is derived from the heavy chain variable domain 1-2 (VH1-2) immunoglobulin (Ig) heavy chain (HC) gene segment, and it binds Env with a similar overall pose as other VH1-2–derived CD4bs bNAbs, but it is not as potent or broad as many of the VRC01-class Abs (*34*). However, unlike VRC01-class bNAbs, IOMA includes a normal-length (eight residues) CDRL3 (*34*) and is less mutated, with 9.5% HC and 7% LC nucleotide mutations to its iGL, compared with VRC01, with 30% HC and 19% LC nucleotide mutations (*35*, *36*). In addition, IOMA accommodates the $N276_{gp120}$ glycan, a roadblock for raising VRC01-class bNAbs (*32*), using a relatively easy-to-achieve mechanism involving a short helical CDRL1, and four amino acid changes (including a single mutated glycine) that each require single-nucleotide substitutions. By contrast, the CDRL1s of VRC01-class bNAbs include either a three- to six-residue deletion or large numbers of SHMs that introduce multiple glycines and/or other insertions to create flexible CDRL1 loops (*32*). Thus, IOMA-like Abs likely represent an easier pathway for vaccine-induced maturation of CD4bs precursors to mature CD4bs bNAbs.

Here, we report immunogens engineered to elicit IOMA and other CD4bs bNAbs. Using these immunogens, we devised a sequential immunization strategy that elicited broad heterologous serum neutralization in both IOMA iGL knock-in and wild-type (WT) mouse models. This was achieved using fewer than half of the immunizations in other studies (*37*, *38*). Moreover, IOMA-like bNAbs elicited in knock-in mice were more potent than IOMA against some strains. Last, the immunization regimen developed in knock-in mice also elicited CD4bs-specific responses in multiple WT animals, including mice, rabbits, and rhesus macaques, providing a rationale for using the IOMA-targeting immunogens described here as part of an effective HIV vaccine.

RESULTS

Design of IOMA-targeting immunogens

To create the IOMA iGL Ab, we reverted the HC and LC sequences of mature IOMA (*34*) to their presumptive germline sequences. The IOMA iGL HC sequence was based on human *IGHV1-2*02, IGHD3-22*01*, and *IGHJ6*02* and contained 22 amino acid changes compared with the HC of IOMA, all within the V gene. The HC complementarity-determining region 3 (CDRH3) was unaltered because of uncertainty with respect to D gene alignment and potential P and N nucleotides—the IOMA iGL HC sequence maintains one gp120-contacting residue (W100F, Kabat numbering) (*39*) found in mature IOMA (*34*). The sequence of the IOMA iGL LC was derived from human *IGLV2-23*02* and *IGLJ2*01* containing 16 amino acid changes compared with mature IOMA, including three SHMs in CDRL3. Of the three mutations in CDRL3, two non-contact amino acids (V96 and A97; Kabat numbering) (*39*) at the VJ junction were left as in mature IOMA (fig. S1A and table S1).

No currently available germline-targeting CD4bs immunogens bind IOMA iGL with detectable affinity (fig. S1B), and IOMA iGL does not neutralize primary HIV-1 strains (fig. S1C). We therefore used in vitro selection methods to identify potential IOMA-targeting immunogens (Fig. 1A). We chose *Saccharomyces cerevisiae* yeast display for selecting an IOMA-targeting immunogen for two reasons: (i) Yeast libraries can contain up to 1×10^9 variants (*40*, *41*) and therefore allow screening a large number of immunogen constructs, a necessity because we were starting with no detectable binding of IOMA iGL to any CD4bs-targeting immunogens, and (ii) *S. cerevisiae* attaches different forms of N-linked glycans to glycoproteins than mammalian cells, e.g., yeast can add up to 50 mannoses to $Man_{8\text{-}9}GlcNAc_2$ (*42*). Such glycan differences may be an advantage because N-glycosylated immunogens selected in a yeast library to bind IOMA iGL and increasingly mature forms of IOMA might stimulate an Ab maturation pathway that is relatively insensitive to the form of N-glycan at any potential N-linked glycosylation site (PNGS) on HIV-1 Env. Promiscuous glycan recognition is desired because Env trimers on viruses exhibit heterogeneous glycosylation at single PNGSs, even within one HIV-1 strain (*43*–*45*). Using yeast display for immunogen selection, we sought to achieve promiscuous N-glycan accommodation through recognition of a glycan's core pentasaccharide, a common feature of both complex-type and high-mannose glycans, which we observed as being recognized at some N-glycan sites in structures of Ab Fab-Env complexes (*21*, *46*, *47*).

Yeast display libraries were produced using variants of the 426c.NLGS.TM4ΔV1-3 monomeric gp120 immunogen (hereafter referred to as 426c.TM4 gp120), a modified clade C gp120 that was designed to engage VRC01-class precursor Abs (*25*, *48*, *49*). We started with a gp120-based immunogen instead of the engineered outer domain immunogens (eODs) previously used to select for VRC01-class bNAb precursors (*27*, *29*, *50*) because, unlike certain other CD4bs bNAbs, IOMA contacts the inner domain of gp120 (*34*), which is absent in the eOD constructs (*27*, *29*, *50*). To aid in determining which immunogen residues should be varied to achieve IOMA iGL binding, we solved a 2.07 Å crystal structure of IOMA iGL Fab (fig. S1D and table S2), which was nearly identical (root mean square deviation of 0.64 Å for 209 Cα atoms) to the mature IOMA Fab structure complexed with BG505 Env trimer (fig. S1E) (*34*). On the basis of modeling the IOMA iGL Fab structure (Fig. 1, B and C, and fig. S1D) into the mature IOMA Fab-Env structure (*34*), we varied seven positions in 426c.TM4 gp120. A library with ~10^8 variants was produced using degenerate codons so that all possible amino acids were incorporated at the selected positions (see Materials and Methods). $R278_{gp120}$ was varied because this position might select for IOMA iGL's unique CDRL1 conformation (*34*). In addition, we introduced a $D279N_{gp120}$ substitution because IOMA is about two- to threefold more potent against HIV-1 viruses that have an N at this position (*34*). Next, $V430_{gp120}$ was varied to increase the interaction with the HC of IOMA iGL. Last, residues 460_{gp120}-464_{gp120} were varied in the V5 loop of 426c gp120 to accommodate and select for IOMA iGL's normal-length CDRL3.

After three rounds of fluorescence-activated cell sorting (FACS) using one fluorophore for IOMA iGL and another against a C-terminal Myc tag to monitor gp120 expression, there was a >100-fold enrichment for gp120 variants that bound IOMA iGL (fig. S1F, middle), demonstrated by increased staining for IOMA iGL compared with the starting 426c.TM4 gp120 (Fig. 1, B and C, and fig. S1F, left and middle). Two clones (from ~100 sequenced after the

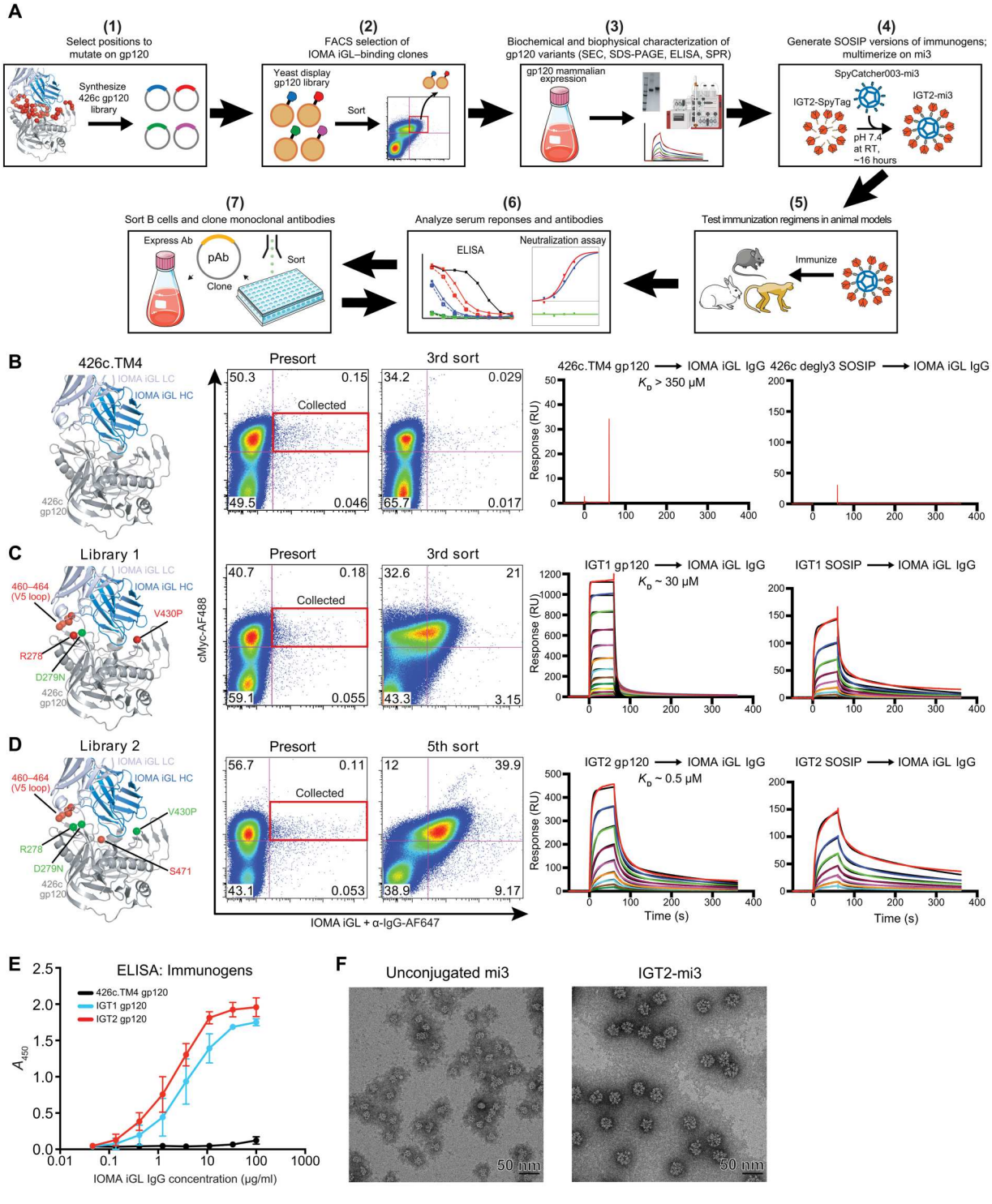

Fig. 1. Design and characterization of IOMA iGL targeting immunogens. (**A**) Overview of strategy to engineer and test immunogens designed to elicit IOMA-like Abs. pAb, antibody expression plasmids. (**B** to **D**) Residues selected from the unmutated starting protein 426c.TM4 gp120 to mutate in yeast display library (left), FACS summary (second and third panels), and SPR data for the highest affinity immunogen selected from each library as gp120 (fourth panel) and SOSIP (fifth panel) are shown (B), as well as in library 1 (C) and library 2 (D). Residues shown in red represent degenerate positions in the library, whereas residues shown in green represent point mutations from 426c.TM4 gp120. Representative sensorgrams are shown in colors, with the 1:1 binding model fits shown in black. IgG was immobilized to the CM5 chip, and gp120 at varying concentrations (the highest concentration in red and dilutions in various colors) was flowed over the chip surface (IGT2 gp120: 4.9 to 5000 nM; IGT1 gp120: 2.3 to 150,000 nM; 426c.TM4 gp120: 7000 to 609,000 nM; IGT2 SOSIP: 31 to 2000 nM; IGT1 SOSIP: 78 to 10,000 nM; 426c degly2 SOSIP: 313 to 40,000 nM). RU, response units. (**E**) ELISA demonstrating binding of CD4bs IgGs to various Env proteins. Bars indicate means and 95% confidence interval. (**F**) Representative negative stain EM micrographs of unconjugated SpyCatcher003-mi3 nanoparticles (left) and IGT2-SpyTag SOSIP conjugated to SpyCatcher003-mi3 nanoparticles (right). Scale bars, 50 nm.

third sort) accounted for 50% of the sequences, suggesting that IOMA iGL-binding activity was enriched. IOMA germline–targeting 1 (IGT1), the best variant identified by the initial yeast display library, had an affinity of ~30 μM for IOMA iGL, as determined by a surface plasmon resonance (SPR)–based binding assay (Fig. 1C, right). IGT1 was then used as a guide to construct a second yeast library to select for an immunogen with higher affinity to IOMA iGL (Fig. 1D). On the basis of their selection in IGT1, we maintained residues $R278_{gp120}$, $N279_{gp120}$, and $P430_{gp120}$ while allowing amino acids R/N/K/S to be sampled at position 460. In addition, residues 461 to 464 and 471 were allowed to be fully degenerate and sample all possible amino acids. After seven rounds of sorting, multiple clones were selected, including IGT2, which bound to IOMA iGL with a 0.5 μM affinity (Fig. 1D, right, and fig. S1F, right).

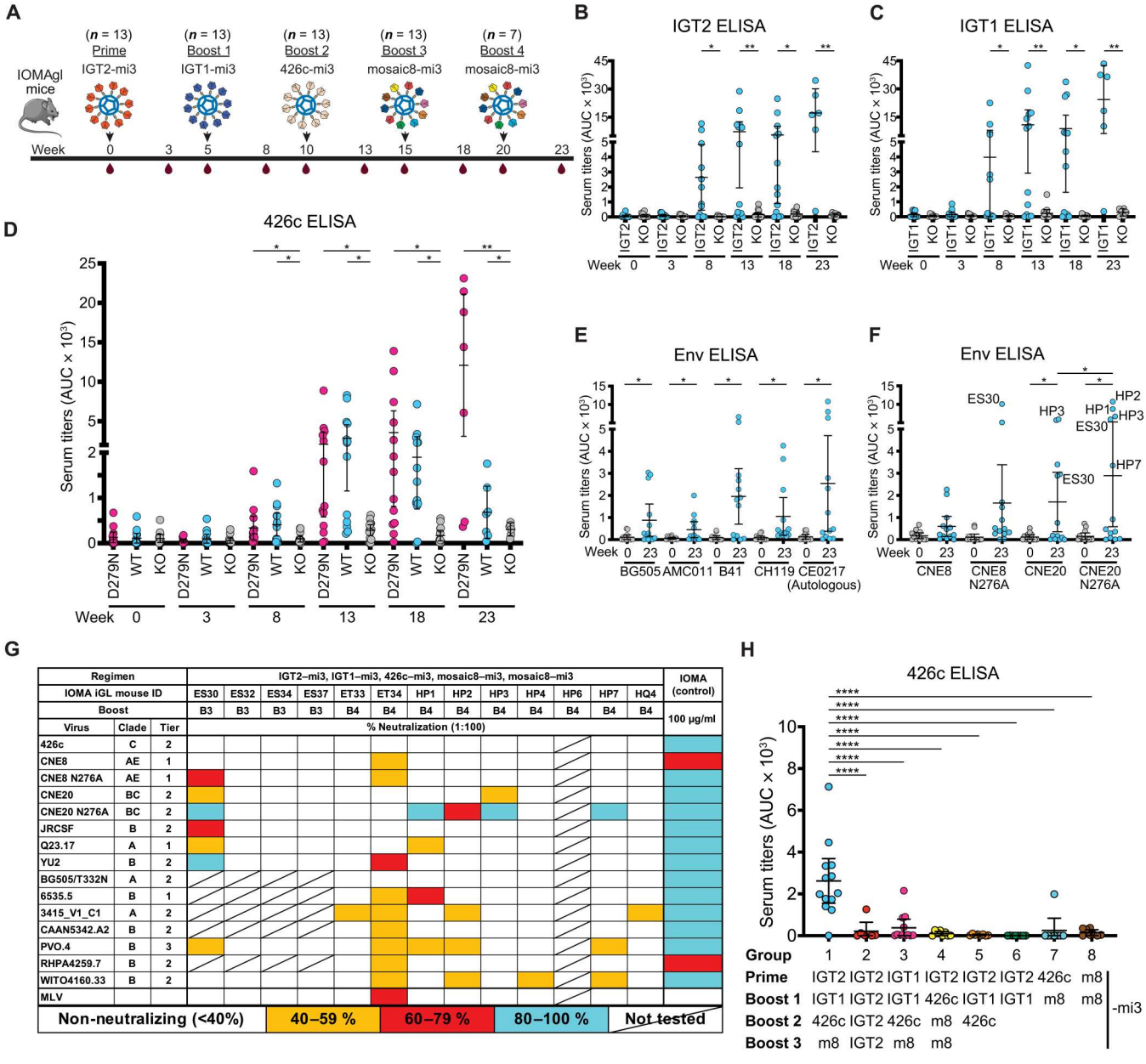

Fig. 2. Sequential immunization with IOMA-targeting immunogens elicits heterologous neutralizing serum responses in IOMA iGL transgenic mice. (**A**) Schematic and timeline of immunization regimen for IOMA iGL knock-in mice. (**B** to **F**) Serum ELISA binding at the indicated time points for IGT2 and IGT2 KO (B), IGT1 and IGT1 KO (C), 426c D279N, 426c, and 426c KO (D) and to a panel of WT and N276A versions of SOSIP-based Envs (E and F). (**G**) Serum neutralization activity against a panel of 18 HIV pseudo-viruses and a murine leukemia virus (MLV) control after terminal bleed. (**H**) 426c-binding serum IgG ELISA using serum samples isolated from mice at the end of the different sequential immunization regimens indicated underneath and detailed in fig. S4. Animal immunization studies were performed as three independent experiments. Each dot represents results from one mouse. Bars indicate means and 95% confidence interval. Significance was demonstrated using an unpaired *t* test ($P \leq 0.05$), except when comparing CNE20 vs CNE20 N276A (F), which used a paired analysis. AUC, area under the curve; *n*, number of animals; m8, mosaic8.

IOMA-targeting mutations selected by yeast display were transferred onto a 426c-soluble native-like Env trimer (a SOSIP.664 construct) (*33*) to hide potentially immunodominant off-target epitopes within the Env trimer core that are exposed in a monomeric gp120 protein. The SOSIP versions of IGT1 and IGT2 were well behaved in size exclusion chromatography (SEC) and SDS–polyacrylamide gel electrophoresis (PAGE) (fig. S1, G and H). IGT1 and IGT2 SOSIPs bound to IOMA iGL IgG with higher apparent affinities than IGT1 and IGT2 gp120s due to avidity effects (Fig. 1, C and D). IGT1 and IGT2 SOSIP- and gp120-based immunogens were also evaluated for binding to a panel of VRC01-class iGL Abs (VRC01, 3BNC60, and BG24) (*27*). IGT2 bound all the iGLs tested, making it the only reported immunogen that binds to iGLs from both IOMA- and VRC01-class CD4bs bNAbs (Fig. 1E and fig. S1, I and J). Last, using the SpyCatcher-SpyTag system (*51*), we covalently linked our SpyTagged SOSIP-based immunogens to the designed 60-nucleotide oligomer nanoparticle SpyCatcher003-mi3 (Fig. 1, A and F) (*52*), thereby enhancing antigenicity and immunogencity through avidity effects from multimerization (fig. S1I) (*53*, *54*) while also reducing the exposure of undesired epitopes at the base of soluble Env trimers (*55*–*57*). Efficient covalent coupling of the immunogens to SpyCatcher003-mi3 was demonstrated by SDS-PAGE (fig. S1H), and negative stain electron microscopy (EM) showed that these nanoparticles were densely conjugated and uniform in size and shape (Fig. 1F).

Sequential immunization of transgenic IOMA iGL knock-in mice elicits broad heterologous neutralizing serum responses

To evaluate whether our immunogens induced IOMA-like Ab responses, we generated transgenic mouse models expressing the full, rearranged IOMA iGL V_H or V_L genes in the mouse *Igh* (*Igh*^{IOMAiGL}) and *Igk* loci (*Igk*^{IOMAiGL}) (fig. S2, A and B). Mice homozygous for both chains, termed IOMAgl mice, showed overall normal B cell development, with reduced numbers of pre-B cells and late up-regulation of CD2 (suggesting accelerated B cell development due to the already rearranged V(D)J and VJ genes), a preference for the IOMA iGL Igκ as seen by a reduction of mouse Igλ-expressing cells, and a reduction in IgD expression indicative of low autoreactivity (fig. S2, C to H) (*58*). The total B cell numbers in IOMAgl mice were grossly normal, making them suitable to test IOMA germline-targeting immunogens (fig. S2, D and G).

We primed the IOMAgl mice using mi3 nanoparticles coupled with the SOSIP version of the immunogen with the highest affinity to IOMA iGL (Fig. 2A, IGT2-mi3) adjuvanted with the saponin/MPLA nanoparticles (SMNP) adjuvant (*59*) and compared binding by enzyme-linked immunosorbent assay (ELISA) to IGT2 and a CD4bs knockout mutant IGT2 (CD4bs KO: G366R/D368R/D279N/A281T). Priming the IOMAgl mice with IGT2-mi3 elicited only weak responses to the priming and boosting (IGT1-mi3) immunogens (Fig. 2, B and C). However, boosting with mi3 nanoparticles coupled with IGT1, which bound IOMA iGL with a lower affinity than IGT2 (Fig. 1C, middle), increased the magnitude and specificity of the serum responses, as demonstrated by an increase in binding to IGT2 and IGT1 compared with IGT2- and IGT1-CD4bs KO (Fig. 2, B and C). A comparable level of differential binding was preserved throughout the remaining immunizations (group 1) after boosting with 426c degly2 D279N (degly2: removal of $N460_{gp120}$ and $N462_{gp120}$ PNGSs), followed by mosaic8-mi3, a nanoparticle coupled with eight different WT SOSIPs chosen from a global HIV-1 reference panel used to screen bNAbs (table S1) (*60*). Serum binding also increased throughout the immunization regimen for 426c and 426c D279N, a mutation preferred by IOMA, compared with 426c-CD4bs KO (Fig. 2D). Terminal bleed sera showed binding to a panel of heterologous WT and N276A Env SOSIPs (Fig. 2, E and F), and, when screened against a panel of IOMA-sensitive HIV-1 strains, 8 of 12 IOMA iGL knock-in animals neutralized up to 9 of 15 strains (Fig. 2G; fig. S3, A to M; and table S3). However, one of these mice (ET34) also neutralized the murine leukemia virus control, suggesting that the neutralization activity from this mouse is at least partially nonspecific for HIV.

To determine whether a shorter immunization regimen could elicit heterologous neutralizing responses, we tested seven other immunization regimens in IOMA iGL knock-in mice (Fig. 2H and fig. S4, groups 2 to 8). ELISA binding titers against 426c degly2 and 426c SOSIPs using serum from group 1, which was primed with IGT2-mi3 and sequentially boosted with IGT1-mi3, 426c degly2 D279N-mi3, and mosaic8-mi3, were significantly higher than binding titers from the other groups ($P < 0.0001$) (Fig. 2H and fig. S4B). These results demonstrate the requirement for germline targeting through sequential immunization to induce IOMA-like Abs.

bNAbs isolated from IOMA iGL knock-in mice

To analyze immunization-induced Abs, we isolated B cells from the spleens and mesenteric lymph nodes of three IOMA iGL knock-in mice of group 1 (ES30, HP1, and HP3) after the final boost (week 18 or 23; Fig. 2G). We sorted immunization-induced germinal center B cells or used antigen-bait combinations of 426c degly2 D279N or CNE8 N276A together with 426c degly2 D279N-CD4bs KO (table S1) to sort epitope-specific B cells (fig. S5). Among the identified HC and LC sequences, we noted a correlation ($R^2 = 0.78$ for HCs and $R^2 = 0.62$ for LCs) between the total number of V region amino acid mutations and V region mutations with identical or chemical similarity to IOMA. We compared this with unbiased VH1-2*01 or VL2-23*02 sequences derived from peripheral blood of HIV-negative human donors, which showed both a lower rate and correlation ($R^2 = 0.52$ for HCs and $R^2 = 0.55$ for LCs) of IOMA-like mutations, indicating that the immunization regimen induced maturation of IOMA iGL toward IOMA (*61*), particularly of the HC that constitutes the majority of contact surface between IOMA and Env-based immunogens (Fig. 3A) (*34*). Fifty-five paired sequences were selected for Ab production on the basis of mutation load and similarity to mature IOMA (fig. S6). In addition, 10x Genomics V(D)J analysis of germinal center B cells revealed 5207 paired HC and LC sequences, of which another 12 were chosen for recombinant Ab production (figs. S5 to S7, A and B).

The selected monoclonal Abs were tested for binding to a panel of heterologous Envs by ELISA (fig. S8A). Isolated IOMA-like Abs that demonstrated binding to the Envs were then evaluated in pseudo-typed in vitro neutralization assays (*62*), and several exhibited similar neutralization potencies as mature IOMA on a small panel of heterologous HIV-1 strains. Some Abs neutralized the tier 2 strain 25710, which IOMA does not neutralize, and IO-010 neutralized Q842.D12 better than IOMA (Fig. 3B). We also noted that among the Env-binding monoclonal Abs, stronger

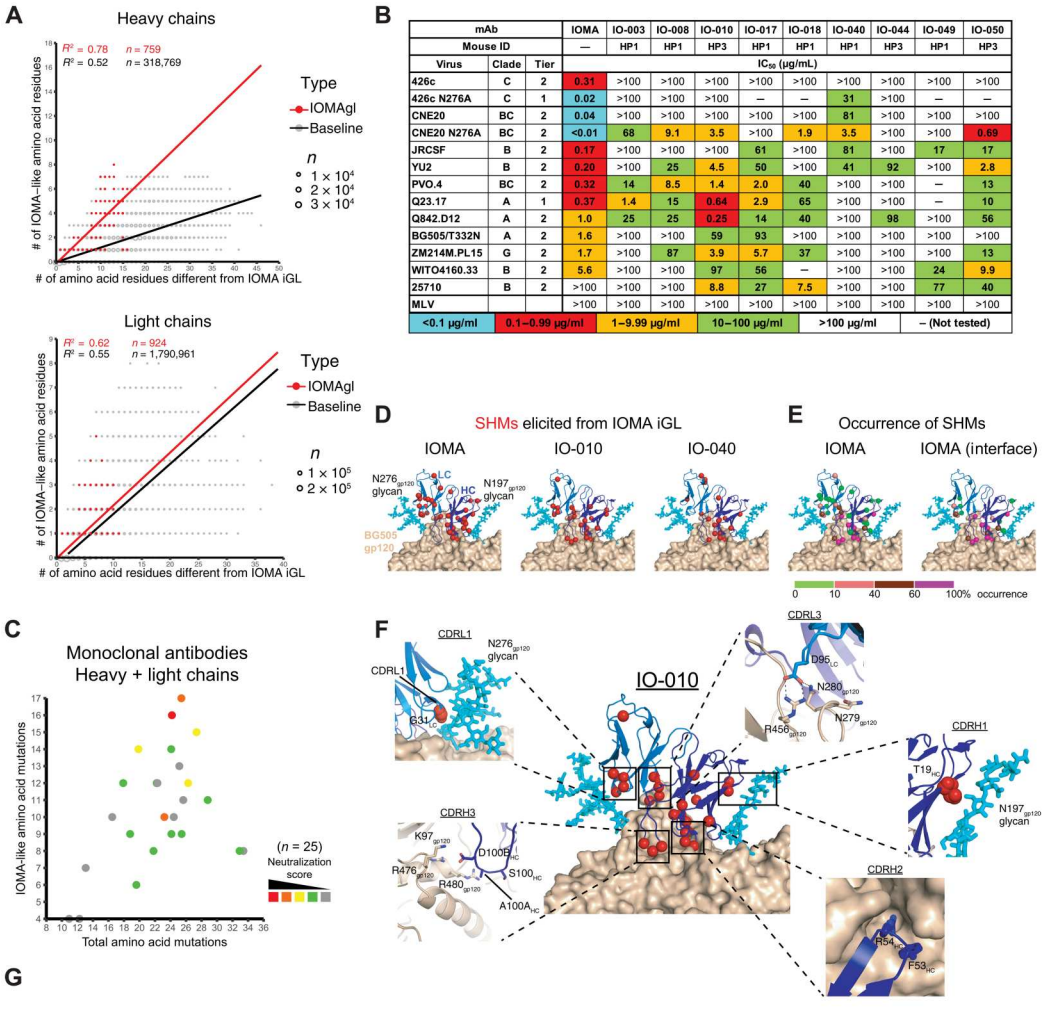

mAb			IOMA	IO-003	IO-008	IO-010	IO-017	IO-018	IO-040	IO-044	IO-049	IO-050
Mouse ID			—	HP1	HP1	HP3	HP1	HP1	HP1	HP3	HP1	HP3
Virus	Clade	Tier	IC_{50} (μg/mL)									
426c	C	2	0.31	>100	>100	>100	>100	>100	>100	>100	>100	>100
426c N276A	C	1	0.02	>100	>100	>100	–	–	31	>100	–	–
CNE20	BC	2	0.04	>100	>100	>100	>100	>100	81	>100	>100	>100
CNE20 N276A	BC	2	<0.01	68	9.1	3.5	>100	1.9	3.5	>100	>100	0.69
JRCSF	B	2	0.17	>100	>100	>100	61	>100	81	>100	17	17
YU2	B	2	0.20	>100	25	4.5	50	>100	41	92	>100	2.8
PVO.4	BC	2	0.32	14	8.5	1.4	2.0	40	>100	>100	–	13
Q23.17	A	1	0.37	1.4	15	0.64	2.9	65	>100	>100	–	10
Q842.D12	A	2	1.0	25	25	0.25	14	40	>100	98	>100	56
BG505/T332N	A	2	1.6	>100	>100	59	93	>100	>100	>100	>100	>100
ZM214M.PL15	G	2	1.7	>100	87	3.9	5.7	37	>100	>100	>100	13
WITO4160.33	B	2	5.6	>100	>100	97	56	–	>100	>100	24	9.9
25710	B	2	>100	>100	>100	8.8	27	7.5	>100	>100	77	40
MLV			>100	>100	>100	>100	>100	>100	>100	>100	>100	>100

<0.1 μg/ml | 0.1–0.99 μg/ml | 1–9.99 μg/ml | 10–100 μg/ml | >100 μg/ml | – (Not tested)

Fig. 3. Monoclonal Abs cloned from IOMA iGL transgenic mice neutralize heterologous HIV strains. (**A**) Graphs show the total number of V region (excluding CDR3) amino acid mutations in HC (top) and LC (bottom) of all Ab sequences (*x* axis) versus the number of mutations that are identical or chemically equivalent to mutations in IOMA for amino acid positions where IOMA and IOMA iGL differ (*y* axis). Sequences derived from IOMAgl mice HP1, HP3, and ES30 from immunization group 1 (red) and baseline human VH1-2*01 or VL2-23*02 sequences from peripheral blood of HIV-negative human donors (gray). The size of the dot is proportional to the number of sequences. Number of sequences (*n*), determination coefficient (Pearson, R^2), and linear regression lines are indicated. Chemical equivalence classified in seven groups as follows: (i) G = A = V = L = I; (ii) S = T; (iii) C = M; (iv) D = N = E = Q; (v) R = K = H; (vi) F = Y = W; and (vii) P. (**B**) Neutralization titers (IC_{50} values) of nine representative monoclonal Abs (mAbs) isolated from IOMA iGL transgenic mice against a panel of 14 viruses and an MLV control. IC_{50}s for IOMA are shown on the far left. (**C**) 3D plot showing neutralization activity (color-coded), total number of amino acid mutations in both HC and LC V(D)Js (*x* axis), and the number of mutations that are identical or chemically equivalent to mutations in the IOMA (*y* axis) for all Env-binding monoclonal Abs from IOMAgl mice HP1, HP3, and ES30 from immunization group 1. Chemical equivalence is as in (A). For each Ab, a neutralization score was calculated (see Materials and Methods). Red indicates higher neutralization activity and score. The number of sequences (*n*) is indicated. (**D**) Residues mutated from IOMA iGL are shown as red spheres mapped onto the crystal structure of mature IOMA (shown in cartoon representation) bound to BG505 gp120 (depicted in surface representation) (Protein Data Bank 5T3Z). SHMs are depicted for mature IOMA (left) and two Abs isolated from IOMAgl mice: the more potent IO-010 (middle) and a weaker IO-040 (right). (**E**) Total SHMs for mature IOMA (left) or SHMs found in the IOMA-gp120 interface (right) are colored according to their percentages of occurrence from green to magenta (left). Structures are depicted as in (D). (**F**) Key mutations essential for IOMA binding to Env that were elicited in our immunization strategy are mapped onto Ab IO-010 and highlighted in each inset box. IO-010 depicted as in (D). Each inset represents a different interaction between IOMA and gp120. (**G**) Amino acid sequence alignment of IOMA V_H and V_L and monoclonal Abs from (B) with IOMA iGL as a reference.

G

HC

```
                 ————————FR1———————  —CDRH1—  ———FR2———  ———CDRH2———  ————————FR3————————  ————CDRH3————  ——FR4——
                  5   10   15   20   25   30   35   40   45   50   55   60   65   70   75   80   85   90   95   100  105 110
                  •    •    •    •    •    •    •    •    •    •    •    •    •    •    •    •    •    •    •    •    •   •
IOMA_iGL  QVQLVQSGAEVKKPGASVKVSCKASGYTFTGYYMHWVRQAPGQGLEWMGWINPNSGGTNYAQKFQGRVTMTRDTSISTAYMELSRLRSDDTAVYYCAREMFDSSADWSPWRGMVAWGQGTLVTVSS
IOMA      E....E...Q.......T...T....K....H.........R..........FR.AVK.P.N.R...S......MEIF.......T.......................................
IO-003    ................T...........D.FI..................FR.AVD.....R...........T.....................A.....DE....H.L.............
IO-008    ................T............EL..................YR.AVK.......................V.NG............D.....DE..............P.....
IO-010    ................T............HL..................FR.AIG.....R...........I......RG.........F........DDE...................
IO-017    ................T............HL..................FR.AIG.....R...........N......RG.........F........DD....................
IO-018    ................T..........ID..I.................YR..PG.....R....L......N......N..K.......F....L..RDD...................
IO-040    ................T...........D.FI....V.............RF.V.DS...R...........T.....................T....D......C.L.............
IO-044    .........M......T...A......ADHFI..................RF.N.DS...R...........T.....................T..VS.........L.............
IO-049    ................T...R........D................R...FR..IE.....................................I.....E...................
IO-050    ................R...........D.EI..................FR.AVK.R............P..T...............R..........D.E...................
```

LC

```
                 ————————FR1———————  —CDRL1—  ———FR2———  ———CDRL2———  ————————FR3————————  —CDRL3—  —FR4—
                  5   10   15   20   25   30      35   40   45   50   55   60   65   70   75   80   85   90   95   100  105
                  •    •    •    •    •    •       •    •    •    •    •    •    •    •    •    •    •    •    •    •    •
IOMA_iGL  QSALTQPASVSGSPGQSITISCTGTSSDVGSYNLVSWYQQHPGKAPKLMIYEVSKRPSGVSNRFSGSKSGNTASLTISGLQAEDEADYYCCSYAGSVAFGGGTKLTVL
IOMA      ......................A.S.R...GFD...............I....N.....I.S...A..............E....H...Y...DG...........
IO-003    .......................R.I..F.................D.................D.M...I...F......E.F...F...L...........
IO-008    ..........................D.....................................................D.LV......V.G.
IO-010    ........................I.G...................D.N.......................F..............DTLV..........
IO-017    ........................I.G.D.................D.N.......................F..............DTLV..........
IO-018    ........................I...D.................D.........................F..............DTLV..........
IO-040    ..........................................V.........................S.........T..V........GDNLV.....R....
IO-044    ................S........N.I...D.................D.T................K........F.T........W...D...........G.
IO-049    ......................P...I.T.....................NR.............C........DF.........S..E.TL..........
IO-050    ..........................................R.......................F..............DTLI..........
```

neutralization activity tended to occur with Abs that shared a larger number of critical residues with IOMA (Fig. 3C).

Two mature IOMA residues, CDRH2 residues $F53_{HC}$ and $R54_{HC}$, interact with the CD4bs Phe^{43} binding pocket (*63*) on gp120 and are critical for Env recognition (*34*) (Fig. 3, D to G, and fig. S6). Twenty-nine of 67 clones chosen for Ab production (fig. S6) contained both mutations, and another 15 contained $R54_{HC}$, 5 of which were in combination with $Y53_{HC}$, which is chemically similar to $F53_{HC}$. $N53F_{HC}$ is a rare mutation that is found in only ~0.13% of VH1-2*02–derived Abs (*64*, *65*). In contrast, our immunization regimen elicited this mutation in ~45% of Abs, a ~350-fold increase. S54R is elicited at slightly higher frequencies in VH1-2*02–derived Abs (~2.7%). However, our immunization regimen elicited this mutation at an ~24-fold higher rate compared with the random frequency of this mutation in VH1-2*02–derived Abs (table S4) (*64*). In addition, our sequential immunization regimen selected for a negatively charged DDE motif in CDRH3 (replacing the IOMA sequence of S100, A100A, and D110B) in 23 of 63 sequences and another 27 sequences with at least one of the three mutations, which was likely selected for by a highly conserved patch of positively charged residues found at the IOMA-contacting interface of the Envs used in our immunization regimen [$K97_{gp120}$ (90% conserved), $R476_{gp120}$ (R: 64% conserved and R/K: 98% conserved), and $R480_{gp120}$ (99% conserved)] (Fig. 3, D to G, and fig. S6). To accommodate the $N276_{gp120}$ glycan, IOMA acquired three mutations in CDRL1 ($S29G_{LC}$, $Y30F_{LC}$, and $N31D_{LC}$). The group 1 immunization regimen elicited all three of these substitutions; however, none of the clones contained all these mutations. Of 63 Abs, 7 contained two and another 25 contained one of these mutations (Fig. 3, D and E, and fig. S6). Two of the most potent Abs elicited by our immunization regimen, IO-010 and IO-017, acquired the $S31G_{gp120}$ mutation, suggesting that this mutation is more critical to accommodate the $N276_{gp120}$ glycan (Fig. 3, D to G) and generating Ab breadth and potency. Although accommodation of the N276 glycan is critical for CD4bs bNAbs to develop breadth and potency, CD4bs bNAbs must also acquire mutations to better interact with the N197 glycan, such as $K19T_{HC}$ in FR1. Our immunization strategy elicited the $K19T_{HC}$ mutation in 31 of 67 monoclonal Abs (~46%), which is ~20-fold higher compared with the random frequency of this mutation in VH1-2*02–derived Abs (table S4) (*64*). Within the CDRL3, VRC01-class bNAbs acquire a $G96E_{LC}$ mutation that enables interactions with the CD4bs loop, whereas IOMA acquires a similar $G95D_{LC}$ mutation. Once again, this mutation was elicited in 22 of 67 Abs (~33%) by our immunization regimen (Fig. 3, D to G, and fig. S6). An essential interaction of VRC01-class bNAbs involves the germline-encoded N58 residue in $FR3_{HC}$, which makes backbone contacts to the highly (~95%) conserved $R456_{gp120}$. Because of a shift away from gp120 in CDRL2, IOMA acquires an $N58K_{HC}$ substitution such that the longer lysine sidechain can access $R456_{gp120}$ (*34*). Our immunization regimen elicited substitutions at $N58_{HC}$ to amino acids with longer sidechains in 39 of 67 (~58%) Abs and was mutated to $N58K_{HC}$ in 17 of 67 (~24%) Abs, a ~1.5-fold increase over the random frequency of the $N58K_{HC}$ mutation (Fig. 3, D to G; fig. S6; and table S4). Our immunization regimen elicited additional IOMA-like mutations within CDRH2: $G56A_{HC}$ (~30%) and $T57V_{HC}$ (~31%), ~3-fold and ~74-fold increases over the random frequency in other VH1-2*02–derived Abs (table S4). The 10x Genomics V(D)J analysis produced an unbiased view of the extent of SHM elicited in the germinal center over the course of the immunization regimen, which, excluding frame shifts, reached up to 26 amino acid mutations in the HC, exceeding the number of mutations of the IOMA HC, and up to 10 mutations in the LC (fig. S7, C to E).

Sera from prime-boosted WT mice targeted the CD4bs and displayed heterologous neutralizing activity

We next investigated the same immunization regimen in WT mice (Fig. 4A). Because IOMA does not have the same sequence requirements as VRC01-class bNAbs (*34*), we hypothesized that a prime boost with IGT2-IGT1 could induce IOMA-like Abs (which we define as recognizing the CD4bs and including a normal-length CDRL3) (*34*) in WT mice, although these mice do not contain the VH1-2 germline gene segment. Priming with IGT2-mi3 in WT mice elicited strong serum-binding responses that were CD4bs specific ($P \leq 0.05$; Fig. 4B) compared with the IOMA iGL knock-in mice, which only responded robustly after a boost with IGT1-mi3 (Fig. 2, B and C). As in the IOMA iGL knock-in mice, the magnitude of these responses increased after boosting with IGT1-mi3, and a significant fraction of the response was still epitope specific ($P \leq 0.001$). To characterize Abs in immunized serum, we measured binding to anti-idiotypic monoclonal Abs raised against IOMA iGL. Although naïve serum did not react with either of the anti-idiotypic Abs, priming with IGT2-mi3 elicited serum responses that bound both anti-idiotypic Abs, and boosting with IGT1-mi3 increased these responses (Fig. 4C). After further boosting with 426c-mi3 and mosaic8-mi3 (Fig. 4A), we measured binding to heterologous WT Envs. Our immunization regimen elicited significantly increased binding responses to all nine Envs ($P \leq 0.05$ to $P < 0.001$; Fig. 4, D and E) in the majority of mice. Serum binding to CNE8 $N276A_{gp120}$ and CNE20 $N276A_{gp120}$ was significantly higher compared with CNE8 and CNE20 ($P \leq 0.05$), suggesting that these responses were at least partially specific to the CD4bs (Fig. 4E). Last, we evaluated neutralization activity against a panel of heterologous HIV-1 strains and detected a weak heterologous neutralization in the sera of 7 of 16 WT animals (Fig. 4F; fig. S3, N to X; and table S5).

Immunization of rabbits and rhesus macaques elicited CD4bs-specific responses

To evaluate this immunization regimen in other WT animals with more potential relevance to humans, we started by immunizing rabbits and rhesus macaques with IGT2-mi3, followed by IGT1-mi3 (Fig. 5A). For these experiments, we assayed only for binding Ab responses because we did not achieve heterologous neutralization after a prime or a prime/single boost of a different HIV-1 immunogen in rabbits or nonhuman primates (NHPs) (*57*, *66*). As with the WT mouse immunizations, the IGT2-mi3 immunization elicited robust responses that were partially epitope specific as evaluated by comparing binding to IGT1 versus to IGT1-CD4bs KO (Fig. 5B). When boosted with IGT1-mi3, the responses showed significant increases in epitope specificity to the CD4bs in both rabbits and NHPs ($P \leq 0.05$) (Fig. 5B). In addition, postprime and postboost sera exhibited potent neutralization of pseudo-viruses generated from the IGT2 and IGT1 immunogens (Fig. 5C). As stated above, we did not evaluate neutralization of heterologous pseudoviruses because our previous results using a different HIV-1 immunogen in rabbits and NHPs showed heterologous neutralization

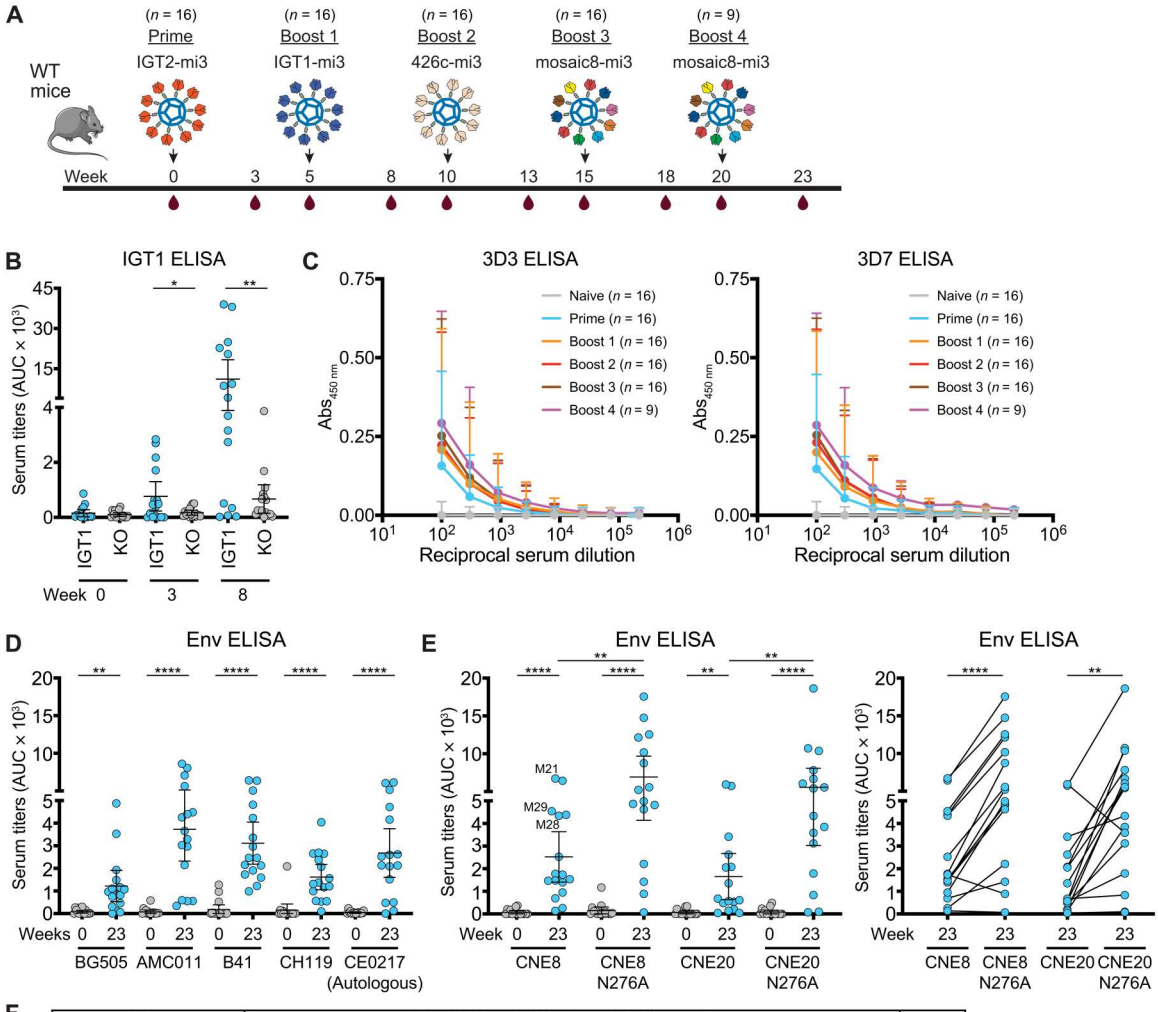

Fig. 4. Sequential immunization with IOMA-targeting immunogens elicits CD4bs-specific responses and heterologous neutralizing serum responses in WT mice. (**A**) Schematic and timeline of immunization regimen for WT mice. (**B**) Serum ELISA binding at the indicated time points to IGT1 or IGT1 CD4bs-KO (KO). RLU, relative light units. (**C** and **D**) Serum ELISA binding to anti-idiotypic monoclonal Abs raised against IOMA iGL (left, 3D3) and IOMA iGL + mature IOMA (right, 3D7). Means ± SEM of 9 to 16 mice per time point are depicted. (**D** and **E**) Serum ELISA binding at the indicated time points to a panel of WT and N276A versions of SOSIP-based Envs. (**F**) Serum neutralization against a panel of 18 viruses and an MLV control at week 23 of WT mice. Animal immunization studies were performed as three independent experiments. Each dot represents results from one mouse. Bars indicate means and 95% confidence interval. Significance was demonstrated using an unpaired (B, D and E, left plot) or paired (E, right plot) *t* test ($P \leq 0.05$).

only after a second boost (*57*). The increase in epitope specificity and serum neutralization titers after boosting with IGT1 suggests that our immunization strategy is well optimized to elicit CD4bs Ab responses.

DISCUSSION

Here, we describe an immunization regimen to elicit Abs to the CD4bs epitope on HIV Env using engineered immunogens targeting IOMA-like CD4bs Ab precursors. The ultimate goal of the germline-targeting approach is the induction of bNAbs at protective concentrations (*1*), but to date, no study has been able to accomplish

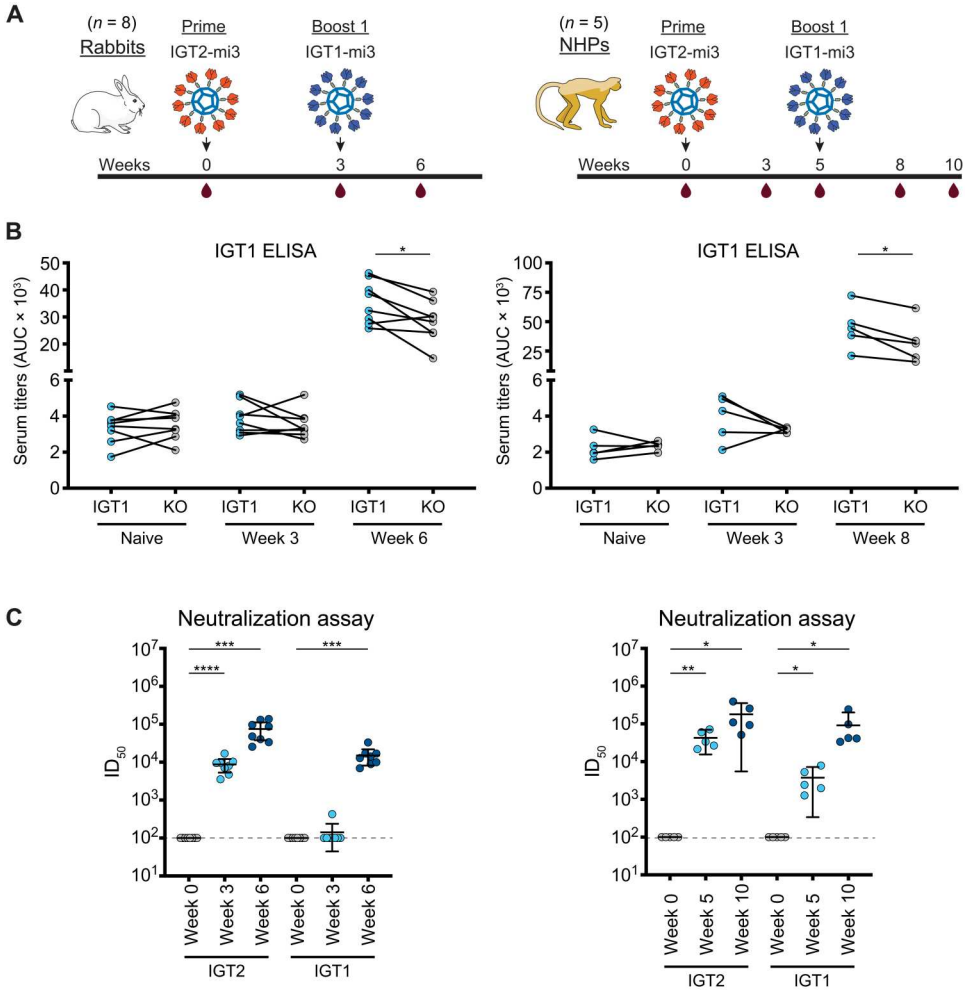

Fig. 5. Prime boost with IGT2-IGT1 elicits CD4bs-specific responses and potent autologous neutralization in rabbits and rhesus macaques. (**A**) Schematic and timeline of immunization regimen for rabbits and rhesus macaques. (**B**) Serum ELISA binding to IGT1 and IGT1 KO for rabbits (left) and rhesus macaques (right). (**C**) Serum neutralization median 50% inhibitory doses (ID_{50} values) of IGT2 and IGT1 pseudo-viruses for rabbits (left) and rhesus macaques (right). The dotted line at $y = 10^2$ indicates the lowest dilution evaluated. Significance was demonstrated using a paired (B) or unpaired (C) *t* test ($P \leq 0.05$).

this feat, although a recent study involving mRNA delivery of HIV-1 Env and gag genes reported reduced risk of SHIV infection in immunized NHPs (*67*). A previous study using a transgenic mouse expressing diverse VRC01 germline precursors demonstrated that priming with eOD-GT8 followed by sequential boosting with more native-like Envs elicited VRC01-like bNAbs (*38*). However, that study required nine immunizations over 81 weeks to elicit VRC01-class Abs with heterologous neutralization. By comparison, our study elicited bNAbs with similar breadth and potency using only four or five immunizations in 18 to 23 weeks. In addition, sequence analysis of the monoclonal Abs elicited in the IOMA iGL transgenic mice revealed that our immunization regimen was much more efficient at eliciting critical mutations required for bNAb development compared with the immunogens used in the attempts to elicit VRC01-class bNAbs (*38*). Last, the neutralization profiles of monoclonal Abs often correlated with serum neutralization from the mouse they were isolated from. For example, IO-010 and IO-017, which neutralized PVO.4 and Q23.17, were isolated from HP3 and HP1, whose sera also demonstrated neutralization activity against these strains (Fig. 2G and fig. S3, A to M).

Accommodation of the $N276_{gp120}$ glycan is considered the major impediment to the elicitation of bNAbs targeting the CD4bs (*32*). To accommodate the N276 $_{gp120}$ glycan, VRC01-class bNAbs require a two- to six-residue deletion or the selection of multiple glycines within CDRL1 (*32*). IOMA requires simpler substitution of four residues in CDRL1 ($S27AR_{LC}$, $S29G_{LC}$, $Y30F_{LC}$, and $N31D_{LC}$) (*34*). These mutations were elicited in our immunization regimen, although no single clone contained all four of these residues. The two most potent monoclonal Abs isolated from immunized iGL mice, IO-010 and IO-017, contained the S31G mutation, suggesting that this residue is most critical for accommodating the $N276_{gp120}$ glycan in IOMA-like Abs and to developing bNAbs capable of potent heterologous neutralization. Although these Abs were cloned from mice after the fourth or fifth immunization, sera from week 8 of our immunization regimen displayed significant binding to 426c Envs containing the $N276_{gp120}$ glycan (Fig. 2D), suggesting that these mutations were elicited after only

two immunizations. In contrast, in the same study noted above (*38*), mutations within CDRL1 of VRC01 required to accommodate the $N276_{gp120}$ glycan occurred only after the ninth immunization at 81 weeks (fig. S8B). Additional mutations known to be important for binding to the CD4bs were also elicited earlier and at higher efficiencies in our immunization regimen compared with previous studies (fig. S8B). No other reported vaccination regimen to elicit CD4bs Abs has elicited all of the required SHMs to accommodate the $N276_{gp120}$ glycan (*23*, *37*, *38*, *68*–*70*), making our results an important achievement in the pursuit to elicit CD4bs bNAbs, although these mutations need to be elicited more efficiently and at higher frequencies in a protective vaccine. Because the CDRL1 of IOMA iGL was already in a helical conformation, the CDRL1 of the IOMA precursor cells selected by priming and boosting with IGT2 and IGT1 might have been in a conformation that allowed it to accommodate the $N276_{gp120}$ glycan and therefore did not require additional SHMs to accommodate the $N276_{gp120}$ glycan introduced in the third immunization using 426c. Thus, boosting with Envs that incorporate only high-mannose glycans at $N276_{gp120}$ followed by boosting with Envs that only incorporate complex-type glycans at $N276_{gp120}$ starting at the second or third immunizations might force IOMA precursor cells to adapt to more diverse and branching glycan moieties and acquire these critical SHMs. Although the vaccine-elicited IOMA-like Abs overall contained fewer SHMs and lower potencies compared with IOMA, our immunization regimen took place over only ~5 months. In contrast, PCIN63, the fastest known VH1-2–derived CD4bs bNAb to arise in a natural infection, first emerged ~40 months after infection and achieved breadth ~64 months after infection and only developed into the fully mature bNAb >70 months after infection (*71*). Thus, our immunization regimen may result in higher levels of SHMs and increased Ab potency if analyzed over longer time courses or if additional boosting immunizations were given at intervals over a longer time period.

Using the strategy that we developed in IOMA iGL knock-in mice, we immunized WT mice with the same immunization regimen (Fig. 4A). A prime-boost sequence with IGT2-mi3 (prime) and IGT1-mi3 (boost) elicited robust CD4bs-specific responses. The Abs elicited by these immunogens resembled IOMA based on binding to an anti-idiotypic Ab raised against IOMA iGL using previously described methods (*72*, *73*). Subsequent immunization with more native-like Envs, 426c degly2 and mosaic8, generated serum responses capable of neutralizing heterologous HIV strains. Serum neutralization correlated with ELISA binding titers, e.g., mice that elicited the highest serum-binding titers against CNE8 (M21, M28, and M29) also elicited heterologous neutralizing activity against CNE8 pseudo-virus. To our knowledge, these results represent CD4bs-specific responses and heterologous neutralization elicited in WT mice, thereby setting a new standard by which to evaluate HIV immunogens in WT mice, although additional work is required to determine whether the Abs targeting the CD4bs were responsible for the neutralizing responses. Because of the success of our immunogens in WT mice, we tested them in additional animals with polyclonal Ab repertoires—rabbits and rhesus macaques. Once again, our priming immunogens elicited CD4bs-specific binding responses in both animal models, representing a germline-targeting immunogen designed to target CD4bs Abs that elicited epitope-specific responses in rabbits and rhesus macaques. These experiments are complicated by the fact that NHPs do not contain the VH1-2 germline gene segment (*74*, *75*), which is required for eliciting VRC01-class bNAbs (*31*) and potentially IOMA-like Abs. In addition, we would not expect bNAb activity in terms of heterologous neutralization ~6 to 10 weeks after a prime immunization because bNAbs require multiple years to arise in a natural infection (*76*). Two previous studies immunizing NHPs with CD4bs-targeting immunogens, eOD-GT8 (*75*) and CH505 M5.G458Y (*77*), did not report heterologous neutralization against WT viruses. Nevertheless, initial reports from a phase 1 clinical trial suggest that a prime with eOD-GT8 can elicit VRC01-class bNAb precursor responses in healthy adult humans (*78*). Thus, a potential lack of heterologous neutralization in these immunization experiments does not suggest that an IOMA targeting strategy involving sequential immunization would not work in humans.

As a final boost, we used a mosaic8 nanoparticle presenting eight different WT Envs on the surface with the intention of more efficiently selecting cross-reactive B cells and increasing neutralization breadth, a strategy that was used to elicit cross-neutralizing responses to influenza or to zoonotic coronaviruses of potential pandemic interest (*79*, *80*). Sera isolated from both WT and transgenic mice after a mosaic8-mi3 boost bound to heterologous Envs in ELISAs and neutralized a panel of heterologous HIV pseudo-viruses, although additional experiments need to be completed to determine whether the cross-neutralization was due to boosting with mosaic8-mi3.

Although a previous study suggested using gp120 cores as an important intermediate immunization step (*38*), our approach resulted in heterologously neutralizing Abs using trimeric SOSIP-based Envs for all immunizations. This is an important distinction, because using trimeric Envs provides the additional benefit of simultaneous targeting of multiple bNAb epitopes. A protective HIV-1 vaccine will most likely require the elicitation of bNAbs to multiple epitopes to prevent escape from the host immune response during early infection to enable clearing of the virus. Thus, our immunogens provide a scaffold upon which to engineer other epitopes to initiate germline targeting of additional bNAb precursors.

IOMA's relatively lower numbers of SHMs and normal-length CDRL3 (*34*) suggest that eliciting IOMA-like bNAbs by vaccination might be easier to achieve compared with eliciting VRC01-class bNAbs. The fact that our IOMA immunogens elicited CD4bs-specific responses in four animal models suggests that germline-targeting immunogens designed to elicit IOMA-like Abs are an attractive route to generate an HIV-1 vaccine, which is supported by our engineered immunogens eliciting epitope-specific responses in WT animals and by a commonality of the mutations that were induced across individual transgenic mice. Furthermore, IOMA-like bNAbs have been isolated from multiple patients (*34*, *81*), suggesting that an immunization regimen targeting this class of bNAbs could be universally effective in a global population. Although IOMA's neutralization breadth is smaller than that of other bNAbs, the fact that some vaccine-elicited IOMA-like Abs neutralized strains that IOMA neutralizes less potently or does not neutralize at all suggests that it is possible to create polyclonal serum responses that include individual Abs with more breadth than IOMA. If elicited at sufficient levels, then such Abs could mediate protection from more strains than predicted by the original IOMA Ab. This is an important property of a potential active vaccine, because clinical trials to evaluate protection from HIV-1 infection by passive administration of VRC01 in humans demonstrated a lack

of protection from infection by HIV-1 strains against which the VRC01 exhibited weak in vitro potencies (*28*). Although polyclonal Abs raised against the CD4bs may be more protective than a single administered monoclonal anti-CD4bs Ab, a successful HIV-1 vaccine will likely require broader and more potent responses to the CD4bs and other epitopes on HIV-1 Env. Our results provide new germline-targeting immunogens to build upon, demonstrate that IOMA-like precursors provide a new starting point to elicit CD4bs bNAbs, and suggest that eliciting this class of bNAbs should be further pursued as a possible strategy to generate a protective HIV-1 vaccine.

MATERIALS AND METHODS

Study design

The objective of this study was to determine whether IOMA-like Abs could be elicited through immunization and whether this process would be easier and more practical than regimens used to elicit other CD4bs Abs. To do this, we established a yeast display platform to screen gp120 libraries and select variants that bind to a germline IOMA precursor. The gp120s were then expressed in mammalian cells and validated biochemically and biophysically by SPR, ELISA, and SEC. The top candidate immunogens were then incorporated into immunization regimens and evaluated to determine whether they select B cells expressing IOMA-like precursors in transgenic and WT animal models. Animal immunizations and serum characterization were conducted by separate laboratories in a blinded manner. Furthermore, different laboratories were responsible for the immunizations of each animal—mice, rabbits, or NHPs. The size of animal cohorts, dosage, and time interval between immunizations were determined from previous experiments so that an optimal regimen could be used without the need for extensive testing. Experimental end points were determined on the basis of serum ELISA binding titers to WT Env proteins. The efficacy of the resulting immunization regimen was evaluated by serum ELISAs and serum neutralization assays. Monoclonal Abs were isolated from transgenic animals demonstrating heterologous serum neutralization activity. These Abs were further characterized in neutralization assays.

Ab, gp120, and Env trimer expression and purification

Env immunogens were expressed as soluble SOSIP.664 native-like gp140 trimers (*33*) as described (*66*). For SpyTagged trimers, either SpyTag (13 residues) (*82*) or SpyTag003 (16 residues) (*83*) was added to the C terminus to allow formation of an irreversible isopeptide bond to SpyCatcher003 moieties. All soluble SOSIP Envs were expressed by transient transfection in human embryonic kidney (HEK) 293-6E cells (National Research Council of Canada) or Expi293 cells (Life Technologies) and purified from transfected cell supernatants by 2G12 affinity chromatography. Soluble Envs were stored at 4°C in 20 mM Tris (pH 8.0) and 150 mM sodium chloride [Tris-buffered saline (TBS)] (untagged and AviTagged versions) or 20 mM sodium phosphate (pH 7.5) and 150 mM NaCl [phosphate-buffered saline (PBS)] (SpyTagged versions). We also expressed untagged gp120 proteins as cores with N/C termini and V1/V2/V3 loop truncations as described (*63*) by transient transfection of suspension-adapted HEK293-S cells. gp120s were purified using Ni–nitrilotriacetic acid affinity chromatography and Superdex 200 16/60 SEC. Proteins were stored in 20 mM Tris (pH 8.0) and 150 mM sodium chloride.

The iGL sequences of IOMA were derived as described in the Results (Design of IOMA-targeting immunogens) section. The iGL sequences of VRC01 and 3BNC60 were derived as described (*27*, *84*). The iGL of BG24, a VRC01-class bNAb with relatively few SHMs (*85*), was derived as described (*86*). IgGs were expressed by transient transfection in Expi293 cells or HEK293-6E cells and purified from cell supernatants using MabSelect SURE (Cytiva) columns followed by SEC purification using a 10/300 or 16/600 Superdex 200 (GE Healthcare) column equilibrated with PBS [20 mM sodium phosphate (pH 7.4) and 150 mM NaCl]. His-tagged Fabs were prepared by transient transfection of truncated HC genes encoding a C-terminal 6x-His tag with a LC expression vector and purified from supernatants using a 5-ml HisTrap colum (GE Healthcare) followed by SEC as described above.

Enzyme-linked immunosorbent assays

Serum ELISAs were performed using randomly biotinylated SOSIP trimers using the EZ-Link NHS-PEG$_4$-Biotin Kit (Thermo Fisher Scientific) according to the manufacturer's guidelines. On the basis of the Pierce Biotin Quantitation Kit (Thermo Fisher Scientific), the number of biotin molecules per protomer was estimated to be about one to four. Biotinylated SOSIP timers were immobilized on streptavidin-coated 96-well plates (Thermo Fisher Scientific) at a concentration of 2 to 5 μg/ml in blocking buffer [1% bovine serum albumin (BSA) in TBS-T: 20 mM Tris (pH 8.0), 150 mM NaCl, and 0.1% Tween 20] for 1 hour at room temperature (RT). After washing the plates in TBS-T, we incubated the plates with a threefold concentration series of mouse, rabbit, or rhesus macaque serum at a top dilution of 1:100 in blocking buffer for 2 to 3 hours at RT. After washing the plates with TBS-T, we added horseradish peroxidase (HRP)–conjugated goat anti-mouse Fc Ab (Southern Biotech, #1033-05), HRP-conjugated goat anti-rabbit IgG Fc Ab (Abcam, ab98467), or HRP-conjugated goat anti-human multispecies IgG Ab (Southern Biotech, #2014-05) at a dilution of 1:8000 in blocking buffer for 1 hour at RT. After washing the plates with TBS-T, we added 1-Step Ultra TMB substrate (Thermo Fisher Scientific) for ~3 min. Reactions were quenched by the addition of 1 N HCl, and absorbance at 450 nm was analyzed using a plate reader (BioTek). ELISAs with gp120s and anti-idiotype monoclonal Abs were performed as above except that these proteins were immobilized directly onto high-binding 96-well assay plates (Costar) in 0.1 M sodium bicarbonate buffer (pH 9.8) at a concentration of 2 to 5 μg/ml in blocking buffer (1% BSA in TBS-T) for 2 hours at RT. ELISAs with IgGs instead of sera were performed as above with a top IgG concentration of 100 μg/ml. All reported values represent the average of at least two independent experiments.

Preparation of SOSIP-mi3 nanoparticles

SpyCatcher003-mi3 particles were prepared by purification from BL21 (DE3)-RIPL *Escherichia coli* (Agilent) transformed with a pET28a SpyCatcher003-mi3 gene (*87*) (including an N-terminal 6x-His tag) as described (*80*, *88*). Briefly, cell pellets from transformed bacteria were lysed with a cell disruptor in the presence of 2.0 mM phenylmethylsulfonyl fluoride (Sigma-Aldrich). Lysates were spun at 21,000*g* for 30 min and filtered with a 0.2-μm filter, and mi3 particles were isolated by ammonium sulfate precipitation,

followed by SEC purification using a HiLoad 16/600 Superdex 200 (GE Healthcare) column equilibrated with 25 mM Tris-HCl (pH 8.0), 150 mM NaCl, and 0.02% NaN_3 (TBS). SpyCatcher003-mi3 particles were stored at 4°C and used for conjugations for up to 1 month after filtering with a 0.2-μm filter and spinning for 30 min at 4°C and 14,000*g*.

Purified SpyCatcher003-mi3 was incubated with a twofold molar excess (SOSIP to mi3 subunit) of purified SpyTagged SOSIP (either a single SOSIP or an equimolar mixture of eight SOSIPs for making mosaic8 particles) overnight at RT in PBS. Conjugated SOSIP-mi3 particles were separated from free SOSIPs by SEC on a Superose 6 10/300 column (GE Healthcare) equilibrated with PBS. Fractions corresponding to conjugated mi3 particles were collected and analyzed by SDS-PAGE. Concentrations of conjugated mi3 particles were determined using the absorbance at 280 nm as measured on a Nanodrop spectrophotometer (Thermo Fisher Scientific).

EM of SOSIP-mi3 nanoparticles

SOSIP-mi3 particles were characterized using negative stain EM to confirm stability and the presence of conjugated SOSIPs on the mi3 surface. Briefly, SOSIP-mi3 particles were diluted to 20 μg/ml in 20 mM Tris (pH 8.0) and 150 mM NaCl, and 3 μl of sample were applied onto freshly glow-discharged 300-mesh copper grids. Sample was incubated on the grid for 40 s, and excess sample was then blotted away with filter paper (Whatman). Uranyl acetate (3 μl) was added for 40 s, and excess stain was then blotted off with filter paper. Prepared grids were imaged on a Talos Arctica (Thermo Fisher Scientific) transmission electron microscope at 200 keV using a Falcon III 4000 × 4000 (Thermo Fisher Scientific) direct electron detector at ×13,500 magnification.

Mice

C57BL/6J and B6(Cg)-Tyrc-2J/J (B6 albino) mice were purchased from the Jackson Laboratory. $Igh^{IOMAiGL}$ and $Igk^{IOMAiGL}$ mice were generated with the Rockefeller University CRISPR and Genome Editing Center and Transgenic and Reproductive Technology Center in CY2.4 albino C57BL/6 J-Tyrc-2J–derived embryonic stem cells. Chimeras were crossed to B6(Cg)-Tyrc-2J/J for germline transmission. $Igh^{IOMAiGL}$ and $Igk^{IOMAiGL}$ mice carry the *IGV(D)J* genes encoding the IOMA iGL HC and LC, respectively. IOMA iGL LC was targeted into the *Igk* locus, deleting the endogenous mouse *Igkj1* to *Igkj5* gene segments. IOMA iGL HC was targeted into the *Igh* locus, deleting the endogenous mouse *Ighd4-1* to *Ighj4* gene segments and thereby minimizing rearrangement of the locus (fig. S2, A and B) (*89*, *90*). The constant regions of *Igh* and *Igk* remain of mouse origin. Mice were only crossed to C57BL/6J or B6(Cg)-Tyrc-2J/J or themselves and maintained at Rockefeller University, and all experiments shown used double homozygous animals for $Igh^{IOMAiGL}$ and $Igk^{IOMAiGL}$-abbreviated IOMAgl mice. These mice are available upon request. Mice were housed at a temperature of 22°C and humidity of 30 to 70% in a 12-hour light/dark cycle with ad libitum access to food and water. Male and female mice aged 6 to 12 weeks at the start of the experiment were used throughout. All experiments were conducted with approval from the Institutional Review Board and the Institutional Animal Care and Use Committee (IACUC) at the Rockefeller University. Sample sizes were not calculated a priori. Given the nature of the comparisons, mice were not randomized into each experimental group, and investigators were not blinded to the group allocation. Instead, experimental groups were age- and sex-matched.

Animal immunizations and sampling

Mice were immunized intraperitoneally with 10 μg of conjugated SOSIP-mi3 in 100 μl of PBS with 1 U of SMNP adjuvant (*59*) [provided by M. Silva, M. B. Melo, and D. J. Irvine, Massachusetts Institute of Technology (MIT)]. Serum samples were collected throughout the experiment by submandibular bleeding, and animals were terminally bled under isoflurane anesthesia first submandibularly, followed by cardiac puncture. The spleens and mesenteric lymph nodes were dissected, mashed though a 70-μm cell strainer, and frozen in fetal bovine serum (FBS) with 10% dimethyl sulfoxide in a gradual-freezing (~1°C/min) container, followed by transfer to liquid N_2 for long-term storage.

Eight 6-month-old New Zealand white rabbits (LabCorp) were used for immunizations. Rabbits were immunized subcutaneously with 50 μg of a SOSIP-mi3 in SMNP adjuvant (375 U per animal) as described (*66*, *91*). Serum samples were collected from rabbits at the time points indicated in Fig. 5A. Procedures in rabbits were approved by the Denver PA IACUC Committee.

Five rhesus macaques (*Macaca mulatta*) of Indian genetic origin were housed in a biosafety level 2 National Institute of Allergy and Infectious Diseases (NIAID) facility and cared for in accordance with the *Guide for Care and Use of Laboratory Animals* report number National Institutes of Health (NIH) 82-53 (Department of Health and Human Services, Bethesda, 1985). All animal procedures and experiments were performed according to protocols approved by the IACUC of NIAID, NIH. The NHPs used in this study did not express the major histocompatibility complex class I Mamu-A*01, Mamu-B*08, and Mamu-B*17 alleles. NHPs were immunized subcutaneously in the medial inner forelegs and hind legs (a total of four sites per animal) with 200 μg of the indicated SOSIP-mi3 adjuvated in SMNP (375 U per animal) as described (*66*). Immunizations and blood samples were obtained from naïve and immunized macaques at the time points indicated in Fig. 5A.

Flow cytometry and cell sorting

Fresh bone marrow was flushed out of one femur and one tibia per mouse. Fresh mouse spleens were forced through a 70-μm mesh into FACS buffer (PBS containing 2% heat-inactivated FBS and 2 mM EDTA), and red blood cells of fresh spleens or bone marrow were lysed in ammonium-chloride-potassium buffer lysing buffer (Gibco) for 3 min. Frozen cells were thawed in a 37°C water bath and immediately transferred to a prewarmed mouse B cell medium consisting of RPMI 1640, supplemented with 10% heat-inactivated FBS, 10 mM Hepes, 1× antibiotic-antimycotic, 1 mM sodium pyruvate, 2 mM L-glutamine, and 53 μM 2-mercaptoethanol (all from Gibco). Bait proteins were randomly conjugated to biotin, and free biotin was removed using the EZ-Link Micro NHS-PEG_4-Biotinylation Kit (Thermo Fisher Scientific, # 21955) according to the manufacturer's instructions.

Fluorophore-conjugated bait and bait-KO antigen tetramers were prepared by mixing a solution (5 μg/ml) of a single randomly biotinylated bait protein with fluorophore-conjugated streptavidin (table S7) at a 1:200 to 1:600 dilution in PBS for 30 min on ice. Conjugates were then mixed equivolumetrically.

RAMOS cells were harvested, washed in FACS buffer, and stained with human Fc-blocking reagent, biotinylated bait antigen–streptavidin tetramers [phycoerythrin (PE), Alexa Fluor 647 (AF647), and sometimes PE-Cy7) and Zombie-NIR (near-infrared) Live/Dead cell marker for 15 min before the addition of anti-human Abs to IgL–allophycocyanin, IgK-BV421, IgM–fluorescein isothiocyanate, and, for some experiments, CD19-PE-Cy7 (table S7).

Mouse cells and controls (see below) were washed and resuspended in a solution of mouse Fc-receptor blocking Ab, fluorophore-conjugated antigen tetramers, and Zombie-NIR Live/Dead cell marker for 15 min on ice. A mastermix of other Abs was then added, and the cells were stained for another 20 min on ice. Abs and reagents are listed in table S7. All cells were analyzed on an LSRFortessa, or cells were sorted on a FACSAria III (both Becton Dickinson) using IOMA-expressing RAMOS cells as an antigen-binding positive control and splenocytes from naïve IOMAgl mice as negative controls (fig. S5). To derive absolute cell numbers, we prepared a master mix of AccuCheck counting beads (Thermo Fisher Scientific, #PCB100) in FACS buffer, and 10^4 beads per sample were added before acquisition. Absolute numbers of cells were calculated as

$$\frac{[\text{Count of acquired beads}]}{[\text{Total beads per sample}]}[\text{Fraction of organ used in stain}] \times [\text{Count of cell population}]$$

IOMA-expressing RAMOS cells were separated from unedited cells by sorting into RAMOS medium and then washed and cultured as described above. Single mouse B cells (1838) from the spleens and mesenteric lymph nodes of three IOMA iGL knock-in mice (ES30, HP1, and HP3) after the final boost (week 18 or 23) were sorted into individual wells of a 96-well plate containing 5 μl of lysis buffer [TCL buffer (QIAGEN, 1031576) with 1% of 2-mercaptoethanol]. Plates were immediately frozen on dry ice and stored at −80°C. Singlet, live Zombie-NIR$^-$CD4$^-$CD8$^-$ F4/80$^-$NK1.1$^-$CD11b$^-$CD11c$^-$B220$^+$ double bait$^+$bait KO$^-$ lymphocytes were sorted unless germinal center B cells were sorted, which were gated as single, live Zombie-NIR$^-$CD4$^-$CD8$^-$F4/80$^-$NK1.1$^-$CD11b$^-$CD11c$^-$B220$^+$CD38$^-$FAS$^+$ lymphocytes (fig. S5).

Mouse germinal center B cells for 10x Genomics single-cell analysis were processed in PBS with 0.5% BSA instead of FACS buffer, and 31,450 cells were sorted into 5 μl of 0.05% BSA in PBS. Cells were spun down to 400*g* for 6 min at 4°C, and volume was adjusted to 22 μl before further processing.

Single-cell Ab cloning

Sequencing and cloning of mouse monoclonal Abs from single-cell sorted B cells were performed as described (*92*) with the modifications detailed in the Supplementary Materials.

Mutation analysis

All HC and LC V(D)J sequences were translated, and the CDR3 region was trimmed. The resulting V region was aligned against the IOMA iGL and IOMA using MAFFT (*93*). Indels were ignored for downstream analysis. All mismatches to IOMA iGL were counted as total mismatches (Fig. 3A). Only mismatches shared with IOMA mature when compared with IOMA iGL were used to assess chemical equivalence and calculate IOMA-like mutations (Fig. 3A). Chemical equivalence was as follows: group 1: G/A/V/L/I; group 2: S/T; group 3: C/M; group 4: D/N/E/Q; group 5: R/K/H; group 6: F/Y/W; and group 7: P. The baseline was calculated using extracted IGHV1-2, IGHJ5 (318,769) and IGLV2-23, IGLJ2 (1,790,961) sequences from healthy, HIV-negative donors generated by Soto *et al.* (*61*) and downloaded from cAb-Rep (*64*), a database of human shared B cell receptor (BCR) clonotypes available at https://cab-rep.c2b2.columbia.edu/.

3D neutralization plot shows the total number of V(D)J amino acid mutations (untrimmed) of each Ab versus the number of these mutations that are chemically equivalent to IOMA (Fig. 3C). Chemical equivalence defined as above.

In vitro neutralization assays

Pseudo-virus neutralization assays were conducted as described (*62*, *94*), either in-house (Figs. 2G, 3A, 4F, and 5B) or at the Collaboration for AIDS Vaccine Discovery (CAVD) core neutralization facility (fig. S1C). Monoclonal Ab IgGs were evaluated in duplicate with an eight-point, threefold dilution series starting at a top concentration of ~100 μg/ml. All pseudo-virus assays using monoclonal Ab IgGs were repeated at least twice for each value reported here. For polyclonal neutralizations, serum samples were heat-inactivated at 56°C for 30 min before being added to the neutralization assays, and then neutralization was evaluated in duplicate with an eight-point, fourfold dilution series starting at a dilution of 1:60. The percentage of neutralization at a 1:100 dilution (% 1:100) is reported for all serum samples. Tiers for viral strains were obtained from (*95*). Ab neutralization score was calculated as

$$[\text{Neutralization score}] = \sum_{v=1}^{n} \frac{5 - \log_{10}(10^3 \times [\text{IC}_{50}]_v)}{n}$$

where n is the number of the different HIV pseudo-viruses v tested for that Ab, and $[\text{IC}_{50}]_v$ is the median inhibitory concentration (IC_{50}) of pseudo-virus v in micrograms per milliliter.

Statistical analysis

Comparisons between groups for ELISAs and neutralization assays were calculated using an unpaired or paired t test in Prism 9.0 (Graphpad). Differences were considered significant when P values were less than 0.05. Exact P values are in the relevant figure at the top of the plot, with asterisks denoting level of significance (* denotes $0.01 < P \leq 0.05$, ** denotes $0.001 < P \leq 0.01$, *** denotes $0.0001 < P \leq 0.001$, and **** denotes $P \leq 0.0001$). Comparisons between total amino acid mutations and IOMA-like mutations in Abs cloned from IOMA iGL mice (Fig. 3) were performed using a Pearson correlation, and R^2 values are presented.

Supplementary Materials

This PDF file includes:
Materials and Methods
Figs. S1 to S8
Tables S1 to S8
References (*96–110*)

Other Supplementary Material for this manuscript includes the following:
MDAR Reproducibility Checklist
Data file S1

View/request a protocol for this paper from *Bio-protocol*.

REFERENCES AND NOTES

1. Z. Mu, B. F. Haynes, D. W. Cain, Strategies for eliciting multiple lineages of broadly neutralizing antibodies to HIV by vaccination. *Curr. Opin. Virol.* **51**, 172–178 (2021).
2. R. P. Smyth, M. P. Davenport, J. Mak, The origin of genetic diversity in HIV-1. *Virus Res.* **169**, 415–429 (2012).
3. T. W. Baba, V. Liska, R. Hofmann-Lehmann, J. Vlasak, W. Xu, S. Ayehunie, L. A. Cavacini, M. R. Posner, H. Katinger, G. Stiegler, B. J. Bernacky, T. A. Rizvi, R. Schmidt, L. R. Hill, M. E. Keeling, Y. Lu, J. E. Wright, T. C. Chou, R. M. Ruprecht, Human neutralizing monoclonal antibodies of the IgG1 subtype protect against mucosal simian-human immunodeficiency virus infection. *Nat. Med.* **6**, 200–206 (2000).
4. A. B. Balazs, J. Chen, C. M. Hong, D. S. Rao, L. Yang, D. Baltimore, Antibody-based protection against HIV infection by vectored immunoprophylaxis. *Nature* **481**, 81–84 (2012).
5. J. W. Eichberg, K. K. Murthy, R. H. Ward, A. M. Prince, Prevention of HIV infection by passive immunization with HIVIG or CD4-IgG. *AIDS Res. Hum. Retroviruses* **8**, 1515 (1992).
6. E. A. Emini, W. A. Schleif, J. H. Nunberg, A. J. Conley, Y. Eda, S. Tokiyoshi, S. D. Putney, S. Matsushrta, K. E. Cobb, C. M. Jett, J. W. Eichberg, K. K. Murthy, Prevention of HIV-1 infection in chimpanzees by gp120 V3 domain-specific monoclonal antibody. *Nature* **355**, 728–730 (1992).
7. A. J. Hessell, E. G. Rakasz, D. M. Tehrani, M. Huber, K. L. Weisgrau, G. Landucci, D. N. Forthal, W. C. Koff, P. Poignard, D. I. Watkins, D. R. Burton, Broadly neutralizing monoclonal antibodies 2F5 and 4E10 directed against the human immunodeficiency virus type 1 gp41 membrane-proximal external region protect against mucosal challenge by simian-human immunodeficiency virus SHIVBa-L. *J. Virol.* **84**, 1302–1313 (2010).
8. A. J. Hessell, P. Poignard, M. Hunter, L. Hangartner, D. M. Tehrani, W. K. Bleeker, P. W. H. I.-Parren, P. A. Marx, D. R. Burton, Effective, low-titer antibody protection against low-dose repeated mucosal SHIV challenge in macaques. *Nat. Med.* **15**, 951–954 (2009).
9. A. J. Hessell, E. G. Rakasz, P. Poignard, L. Hangartner, G. Landucci, D. N. Forthal, W. C. Koff, D. I. Watkins, D. R. Burton, Broadly neutralizing human anti-HIV antibody 2G12 is effective in protection against mucosal SHIV challenge even at low serum neutralizing titers. *PLOS Pathog.* **5**, e1000433 (2009).
10. J. R. Mascola, G. Stiegler, T. C. VanCott, H. Katinger, C. B. Carpenter, C. E. Hanson, H. Beary, D. Hayes, S. S. Frankel, D. L. Birx, M. G. Lewis, Protection of macaques against vaginal transmission of a pathogenic HIV-1/SIV chimeric virus by passive infusion of neutralizing antibodies. *Nat. Med.* **6**, 207–210 (2000).
11. J. R. Mascola, M. G. Lewis, G. Stiegler, D. Harris, T. C. Van Cott, D. Hayes, M. K. Louder, C. R. Brown, C. V. Sapan, S. S. Frankel, Y. Lu, M. L. Robb, H. Katinger, D. L. Birx, Protection of macaques against pathogenic simian/human immunodeficiency virus 89.6PD by passive transfer of neutralizing antibodies. *J. Virol.* **73**, 4009–4018 (1999).
12. B. Moldt, E. G. Rakasz, N. Schultz, P.-Y. Chan-Hui, K. Swiderek, K. L. Weisgrau, S. M. Piaskowski, Z. Bergman, D. I. Watkins, P. Poignard, D. R. Burton, Highly potent HIV-specific antibody neutralization in vitro translates into effective protection against mucosal SHIV challenge in vivo. *Proc. Natl. Acad. Sci. U.S.A.* **109**, 18921–18925 (2012).
13. P. W. Parren, P. A. Marx, A. J. Hessell, A. Luckay, J. Harouse, C. Cheng-Mayer, J. P. Moore, D. R. Burton, Antibody protects macaques against vaginal challenge with a pathogenic R5 simian/human immunodeficiency virus at serum levels giving complete neutralization in vitro. *J. Virol.* **75**, 8340–8347 (2001).
14. J. Pietzsch, H. Gruell, S. Bournazos, B. M. Donovan, F. Klein, R. Diskin, M. S. Seaman, P. J. Bjorkman, J. V. Ravetch, A. Ploss, M. C. Nussenzweig, A mouse model for HIV-1 entry. *Proc. Natl. Acad. Sci. U.S.A.* **109**, 15859–15864 (2012).
15. R. Shibata, T. Igarashi, N. Haigwood, A. Buckler–White, R. Ogert, W. Ross, R. Willey, M. W. Cho, M. A. Martin, Neutralizing antibody directed against the HIV-1 envelope glycoprotein can completely block HIV-1/SIV chimeric virus infections of macaque monkeys. *Nat. Med.* **5**, 204–210 (1999).
16. L. E. McCoy, D. R. Burton, Identification and specificity of broadly neutralizing antibodies against HIV. *Immunol. Rev.* **275**, 11–20 (2017).
17. X. Xiao, W. Chen, Y. Feng, Z. Zhu, P. Prabakaran, Y. Wang, M. Y. Zhang, N. S. Longo, D. S. Dimitrov, Germline-like predecessors of broadly neutralizing antibodies lack measurable binding to HIV-1 envelope glycoproteins: Implications for evasion of immune responses and design of vaccine immunogens. *Biochem. Biophys. Res. Commun.* **390**, 404–409 (2009).
18. M. Bonsignori, K.-K. Hwang, X. Chen, C. Y. Tsao, L. Morris, E. Gray, D. J. Marshall, J. A. Crump, S. H. Kapiga, N. E. Sam, F. Sinangil, M. Pancera, Y. Yongping, B. Zhang, J. Zhu, P. D. Kwong, S. O'Dell, J. R. Mascola, L. Wu, G. J. Nabel, S. Phogat, M. S. Seaman, J. F. Whitesides, M. A. Moody, G. Kelsoe, X. Yang, J. Sodroski, G. M. Shaw, D. C. Montefiori, T. B. Kepler, G. D. Tomaras, S. M. Alam, H.-X. Liao, B. F. Haynes, Analysis of a clonal lineage of HIV-1 envelope V2/V3 conformational epitope-specific broadly neutralizing antibodies and their inferred unmutated common ancestors. *J. Virol.* **85**, 9998–10009 (2011).
19. J. F. Scheid, H. Mouquet, B. Ueberheide, R. Diskin, F. Klein, T. Y. K. Oliveira, J. Pietzsch, D. Fenyo, A. Abadir, K. Velinzon, A. Hurley, S. Myung, F. Boulad, P. Poignard, D. R. Burton, F. Pereyra, D. D. Ho, B. D. Walker, M. S. Seaman, P. J. Bjorkman, B. T. Chait, M. C. Nussenzweig, Sequence and structural convergence of broad and potent HIV antibodies that mimic CD4 binding. *Science* **333**, 1633–1637 (2011).
20. F. Klein, R. Diskin, J. F. Scheid, C. Gaebler, H. Mouquet, I. S. Georgiev, M. Pancera, T. Zhou, R.-B. Incesu, B. Z. Fu, P. N. P. Gnanapragasam, T. Y. Oliveira, M. S. Seaman, P. D. Kwong, P. J. Bjorkman, M. C. Nussenzweig, Somatic mutations of the immunoglobulin framework are generally required for broad and potent HIV-1 neutralization. *Cell* **153**, 126–138 (2013).
21. H. Mouquet, L. Scharf, Z. Euler, Y. Liu, C. Eden, J. F. Scheid, A. Halper-Stromberg, P. N. P. Gnanapragasam, D. I. R. Spencer, M. S. Seaman, H. Schuitemaker, T. Feizi, M. C. Nussenzweig, P. J. Bjorkman, Complex-type *N*-glycan recognition by potent broadly neutralizing HIV antibodies. *Proc. Natl. Acad. Sci. U.S.A.* **109**, E3268–E3277 (2012).
22. T. Zhou, I. Georgiev, X. Wu, Z.-Y. Yang, K. Dai, A. Finzi, Y. do Kwon, J. F. Scheid, W. Shi, L. Xu, Y. Yang, J. Zhu, M. C. Nussenzweig, J. Sodroski, L. Shapiro, G. J. Nabel, J. R. Mascola, P. D. Kwong, Structural basis for broad and potent neutralization of HIV-1 by antibody VRC01. *Science* **329**, 811–817 (2010).
23. P. Dosenovic, L. von Boehmer, A. Escolano, J. Jardine, N. T. Freund, A. D. Gitlin, A. T. McGuire, D. W. Kulp, T. Oliveira, L. Scharf, J. Pietzsch, M. D. Gray, A. Cupo, M. J. van Gils, K.-H. Yao, C. Liu, A. Gazumyan, M. S. Seaman, P. J. Björkman, R. W. Sanders, J. P. Moore, L. Stamatatos, W. R. Schief, M. C. Nussenzweig, Immunization for HIV-1 broadly neutralizing antibodies in human Ig knockin mice. *Cell* **161**, 1505–1515 (2015).
24. N. A. Doria-Rose, C. A. Schramm, J. Gorman, P. L. Moore, J. N. Bhiman, B. J. De Kosky, M. J. Ernandes, I. S. Georgiev, H. J. Kim, M. Pancera, R. P. Staupe, H. R. Altae-Tran, R. T. Bailer, E. T. Crooks, A. Cupo, A. Druz, N. J. Garrett, K. H. Hoi, R. Kong, M. K. Louder, N. S. Longo, K. M. Kee, M. Nonyane, S. O'Dell, R. S. Roark, R. S. Rudicell, S. D. Schmidt, D. J. Sheward, C. Soto, C. K. Wibmer, Y. Yang, Z. Zhang; NISC Comparative Sequencing Program, J. C. Mullikin, J. M. Binley, R. W. Sanders, I. A. Wilson, J. P. Moore, A. B. Ward, G. Georgiou, C. Williamson, S. S. Abdool Karim, L. Morris, P. D. Kwong, L. Shapiro, J. R. Mascola, Developmental pathway for potent V1V2-directed HIV-neutralizing antibodies. *Nature* **509**, 55–62 (2014).
25. A. T. McGuire, S. Hoot, A. M. Dreyer, A. Lippy, A. Stuart, K. W. Cohen, J. Jardine, S. Menis, J. F. Scheid, A. P. West, W. R. Schief, L. Stamatatos, Engineering HIV envelope protein to activate germline B cell receptors of broadly neutralizing anti-CD4 binding site antibodies. *J. Exp. Med.* **210**, 655–663 (2013).
26. S. Hoot, A. T. McGuire, K. W. Cohen, R. K. Strong, L. Hangartner, F. Klein, R. Diskin, J. F. Scheid, D. N. Sather, D. R. Burton, L. Stamatatos, Recombinant HIV envelope proteins fail to engage germline versions of anti-CD4bs bNAbs. *PLOS Pathog.* **9**, e1003106 (2013).
27. J. Jardine, J.-P. Julien, S. Menis, T. Ota, O. Kalyuzhniy, A. McGuire, D. Sok, P. S. Huang, S. MacPherson, M. Jones, T. Nieusma, J. Mathison, D. Baker, A. B. Ward, D. R. Burton, L. Stamatatos, D. Nemazee, I. A. Wilson, W. R. Schief, Rational HIV immunogen design to target specific germline B cell receptors. *Science* **340**, 711–716 (2013).
28. L. Corey, P. B. Gilbert, M. Juraska, D. C. Montefiori, L. Morris, S. T. Karuna, S. Edupuganti, N. M. Mgodi, A. deCamp, E. Rudnicki, Y. Huang, P. Gonzales, R. Cabello, C. Orrell, J. R. Lama, F. Laher, E. M. Lazarus, J. Sanchez, I. Frank, J. Hinojosa, M. E. Sobieszczyk, K. E. Marshall, P. G. Mukwekwerere, J. Makhema, L. R. Baden, J. I. Mullins, C. Williamson, J. Hural, M. McElrath, C. Bentley, S. Takuva, M. M. Gomez Lorenzo, D. N. Burns, N. Espy, A. K. Randhawa, N. Kochar, E. Piwowar-Manning, D. J. Donnell, N. Sista, P. Andrew, J. G. Kublin, G. Gray, J. E. Ledgerwood, J. R. Mascola, M. S. Cohen; HVTN 704/HPTN 085 and HVTN 703/HPTN 081 Study Teams, Two randomized trials of neutralizing antibodies to prevent HIV-1 acquisition. *N. Engl. J. Med.* **384**, 1003–1014 (2021).
29. J. G. Jardine, D. W. Kulp, C. Havenar-Daughton, A. Sarkar, B. Briney, D. Sok, F. Sesterhenn, J. Ereño-Orbea, O. Kalyuzhniy, I. Deresa, X. Hu, S. Spencer, M. Jones, E. Georgeson, Y. Adachi, M. Kubitz, A. C. deCamp, J.-P. Julien, I. A. Wilson, D. R. Burton, S. Crotty, W. R. Schief, HIV-1 broadly neutralizing antibody precursor B cells revealed by germline-targeting immunogen. *Science* **351**, 1458–1463 (2016).
30. A. P. West Jr., L. Scharf, J. F. Scheid, F. Klein, P. J. Bjorkman, M. C. Nussenzweig, Structural insights on the role of antibodies in HIV-1 vaccine and therapy. *Cell* **156**, 633–648 (2014).
31. A. P. West Jr., R. Diskin, M. C. Nussenzweig, P. J. Bjorkman, Structural basis for germline gene usage of a potent class of antibodies targeting the CD4 binding site of HIV-1 gp120. *Proc. Natl. Acad. Sci. USA.* **109**, E2083–E2090 (2012).
32. T. Zhou, J. Zhu, X. Wu, S. Moquin, B. Zhang, P. Acharya, I. S. Georgiev, H. R. Altae-Tran, G.-Y. Chuang, M. G. Joyce, Y. D. Kwon, N. S. Longo, M. K. Louder, T. Luongo, K. McKee, C. A. Schramm, J. Skinner, Y. Yang, Z. Yang, Z. Zhang, A. Zheng, M. Bonsignori, B. F. Haynes, J. F. Scheid, M. C. Nussenzweig, M. Simek, D. R. Burton, W. C. Koff; NISC Comparative Sequencing Program, J. C. Mullikin, M. Connors, L. Shapiro, G. J. Nabel, J. R. Mascola, P. D. Kwong, Multidonor analysis reveals structural elements, genetic determinants, and

maturation pathway for HIV-1 neutralization by VRC01-class antibodies. *Immunity* **39**, 245–258 (2013).

33. R. W. Sanders, R. Derking, A. Cupo, J.-P. Julien, A. Yasmeen, N. de Val, H. J. Kim, C. Blattner, A. Torrents de la Peña, J. Korzun, M. Golabek, K. de Los Reyes, T. J. Ketas, M. J. van Gils, C. Richter King, I. A. Wilson, A. B. Ward, P. J. Klasse, J. P. Moore, A next-generation cleaved, soluble HIV-1 Env trimer, BG505 SOSIP.664 gp140, expresses multiple epitopes for broadly neutralizing but not non-neutralizing antibodies. *PLOS Pathog.* **9**, e1003618 (2013).
34. H. B. Gristick, L. von Boehmer, A. P. West Jr., M. Schamber, A. Gazumyan, J. Golijanin, M. S. Seaman, G. Fätkenheuer, F. Klein, M. C. Nussenzweig, P. J. Bjorkman, Natively glycosylated HIV-1 Env structure reveals new mode for antibody recognition of the CD4-binding site. *Nat. Struct. Mol. Biol.* **23**, 906–915 (2016).
35. X. Wu, Z.-Y. Yang, Y. Li, C.-M. Hogerkorp, W. R. Schief, M. S. Seaman, T. Zhou, S. D. Schmidt, L. Wu, L. Xu, N. S. Longo, K. McKee, S. O'Dell, M. K. Louder, D. L. Wycuff, Y. Feng, M. Nason, N. Doria-Rose, M. Connors, P. D. Kwong, M. Roederer, R. T. Wyatt, G. J. Nabel, J. R. Mascola, Rational design of envelope identifies broadly neutralizing human monoclonal antibodies to HIV-1. *Science* **329**, 856–861 (2010).
36. M. Bonsignori, E. Scott, K. Wiehe, D. Easterhoff, S. M. Alam, K.-K. Hwang, M. Cooper, S.-M. Xia, R. Zhang, D. C. Montefiori, R. Henderson, X. Nie, G. Kelsoe, M. A. Moody, X. Chen, M. G. Joyce, P. D. Kwong, M. Connors, J. R. Mascola, A. T. McGuire, L. Stamatatos, M. Medina-Ramírez, R. W. Sanders, K. O. Saunders, T. B. Kepler, B. F. Haynes, Inference of the HIV-1 VRC01 antibody lineage unmutated common ancestor reveals alternative pathways to overcome a key glycan barrier. *Immunity* **49**, 1162–1174.e8 (2018).
37. M. Tian, C. Cheng, X. Chen, H. Duan, H.-L. Cheng, M. Dao, Z. Sheng, M. Kimble, L. Wang, S. Lin, S. D. Schmidt, Z. Du, M. G. Joyce, Y. Chen, B. J. De Kosky, Y. Chen, E. Normandin, E. Cantor, R. E. Chen, N. A. Doria-Rose, Y. Zhang, W. Shi, W.-P. Kong, M. Choe, A. R. Henry, F. Laboune, I. S. Georgiev, P.-Y. Huang, S. Jain, A. T. McGuire, E. Georgeson, S. Menis, D. C. Douek, W. R. Schief, L. Stamatatos, P. D. Kwong, L. Shapiro, B. F. Haynes, J. R. Mascola, F. W. Alt, Induction of HIV neutralizing antibody lineages in mice with diverse precursor repertoires. *Cell* **166**, 1471–1484.e18 (2016).
38. X. Chen, T. Zhou, S. D. Schmidt, H. Duan, C. Cheng, G.-Y. Chuang, Y. Gu, M. K. Louder, B. C. Lin, C.-H. Shen, Z. Sheng, M. X. Zheng, N. A. Doria-Rose, M. G. Joyce, L. Shapiro, M. Tian, F. W. Alt, P. D. Kwong, J. R. Mascola, Vaccination induces maturation in a mouse model of diverse unmutated VRC01-class precursors to HIV-neutralizing antibodies with >50% breadth. *Immunity* **54**, 324–339.e8 (2021).
39. G. Johnson, T. T. Wu, Kabat database and its applications: 30 years after the first variability plot. *Nucleic Acids Res.* **28**, 214–218 (2000).
40. M. S. Packer, D. R. Liu, Methods for the directed evolution of proteins. *Nat. Rev. Genet.* **16**, 379–394 (2015).
41. G. Chao, W. L. Lau, B. J. Hackel, S. L. Sazinsky, S. M. Lippow, K. D. Wittrup, Isolating and engineering human antibodies using yeast surface display. *Nat. Protoc.* **1**, 755–768 (2006).
42. M. J. Betenbaugh, N. Tomiya, S. Narang, J. T. Hsu, Y. C. Lee, Biosynthesis of human-type N-glycans in heterologous systems. *Curr. Opin. Struct. Biol.* **14**, 601–606 (2004).
43. A. J. Behrens, S. Vasiljevic, L. K. Pritchard, D. J. Harvey, R. S. Andev, S. A. Krumm, W. B. Struwe, A. Cupo, A. Kumar, N. Zitzmann, G. E. Seabright, H. B. Kramer, D. I. R. Spencer, L. Royle, J. H. Lee, P. J. Klasse, D. R. Burton, I. A. Wilson, A. B. Ward, R. W. Sanders, J. P. Moore, K. J. Doores, M. Crispin, Composition and antigenic effects of individual glycan sites of a trimeric HIV-1 envelope glycoprotein. *Cell Rep.* **14**, 2695–2706 (2016).
44. E. P. Go, G. Hewawasam, H. X. Liao, H. Chen, L. H. Ping, J. A. Anderson, D. C. Hua, B. F. Haynes, H. Desaire, Characterization of glycosylation profiles of HIV-1 transmitted/founder envelopes by mass spectrometry. *J. Virol.* **85**, 8270–8284 (2011).
45. C. B. Karsten, G. Alter, The HIV-1 glycan shield: Strategically placed kinks in the armor improve antigen design. *Cell Rep.* **19**, 669–670 (2017).
46. L. Scharf, J. F. Scheid, J. H. Lee, A. P. West Jr., C. Chen, H. Gao, P. N. P. Gnanapragasam, R. Mares, M. S. Seaman, A. B. Ward, M. C. Nussenzweig, P. J. Bjorkman, Antibody 8ANC195 reveals a site of broad vulnerability on the HIV-1 envelope spike. *Cell Rep.* **7**, 785–795 (2014).
47. L. Scharf, H. Wang, H. Gao, S. Chen, A. W. McDowall, P. J. Bjorkman, Broadly neutralizing antibody 8ANC195 recognizes closed and open states of HIV-1 Env. *Cell* **162**, 1379–1390 (2015).
48. A. T. McGuire, A. M. Dreyer, S. Carbonetti, A. Lippy, J. Glenn, J. F. Scheid, H. Mouquet, L. Stamatatos, HIV antibodies. Antigen modification regulates competition of broad and narrow neutralizing HIV antibodies. *Science* **346**, 1380–1383 (2014).
49. A. T. McGuire, M. D. Gray, P. Dosenovic, A. D. Gitlin, N. T. Freund, J. Petersen, C. Correnti, W. Johnsen, R. Kegel, A. B. Stuart, J. Glenn, M. S. Seaman, W. R. Schief, R. K. Strong, M. C. Nussenzweig, L. Stamatatos, Specifically modified Env immunogens activate B-cell precursors of broadly neutralizing HIV-1 antibodies in transgenic mice. *Nat. Commun.* **7**, 10618 (2016).
50. J. G. Jardine, T. Ota, D. Sok, M. Pauthner, D. W. Kulp, O. Kalyuzhniy, P. D. Skog, T. C. Thinnes, D. Bhullar, B. Briney, S. Menis, M. Jones, M. Kubitz, S. Spencer, Y. Adachi, D. R. Burton, W. R. Schief, D. Nemazee, HIV-1 vaccines. Priming a broadly neutralizing antibody response to HIV-1 using a germline-targeting immunogen. *Science* **349**, 156–161 (2015).
51. K. D. Brune, D. B. Leneghan, I. J. Brian, A. S. Ishizuka, M. F. Bachmann, S. J. Draper, S. Biswas, M. Howarth, Plug-and-display: Decoration of virus-like particles via isopeptide bonds for modular immunization. *Sci. Rep.* **6**, 19234 (2016).
52. T. U. J. Bruun, A. C. Andersson, S. J. Draper, M. Howarth, Engineering a rugged nanoscaffold to enhance plug-and-display vaccination. *ACS Nano* **12**, 8855–8866 (2018).
53. J. López-Sagaseta, E. Malito, R. Rappuoli, M. J. Bottomley, Self-assembling protein nanoparticles in the design of vaccines. *Comput. Struct. Biotechnol. J.* **14**, 58–68 (2016).
54. M. K. Slifka, I. J. Amanna, Role of multivalency and antigenic threshold in generating protective antibody responses. *Front. Immunol.* **10**, 956 (2019).
55. M. Bianchi, H. L. Turner, B. Nogal, C. A. Cottrell, D. Oyen, M. Pauthner, R. Bastidas, R. Nedellec, L. E. McCoy, I. A. Wilson, D. R. Burton, A. B. Ward, L. Hangartner, Electron-microscopy-based epitope mapping defines specificities of polyclonal antibodies elicited during HIV-1 BG505 envelope trimer immunization. *Immunity* **49**, 288–300.e8 (2018).
56. L. E. McCoy, M. J. van Gils, G. Ozorowski, T. Messmer, B. Briney, J. E. Voss, D. W. Kulp, M. S. Macauley, D. Sok, M. Pauthner, S. Menis, C. A. Cottrell, J. L. Torres, J. Hsueh, W. R. Schief, I. A. Wilson, A. B. Ward, R. W. Sanders, D. R. Burton, Holes in the glycan shield of the native HIV envelope are a target of trimer-elicited neutralizing antibodies. *Cell Rep.* **16**, 2327–2338 (2016).
57. A. Escolano, H. B. Gristick, R. Gautam, A. T. DeLaitsch, M. E. Abernathy, Z. Yang, H. Wang, M. A. G. Hoffmann, Y. Nishimura, Z. Wang, N. Koranda, L. M. Kakutani, H. Gao, P. N. P. Gnanapragasam, H. Raina, A. Gazumyan, M. Cipolla, T. Y. Oliveira, V. Ramos, D. J. Irvine, M. Silva, A. P. West Jr., J. R. Keeffe, C. O. Barnes, M. S. Seaman, M. C. Nussenzweig, M. A. Martin, P. J. Bjorkman, Sequential immunization of macaques elicits heterologous neutralizing antibodies targeting the V3-glycan patch of HIV-1 Env. *Sci. Transl. Med.* **13**, eabk1533 (2021).
58. T. Amendt, O. E. Ayoubi, A. T. Linder, G. Allies, M. Young, C. S. Setz, H. Jumaa, Primary immune responses and affinity maturation are controlled by IgD. *Front. Immunol.* **12**, 709240 (2021).
59. M. Silva, Y. Kato, M. B. Melo, I. Phung, B. L. Freeman, Z. Li, K. Roh, J. W. Van Wijnbergen, H. Watkins, C. A. Enemuo, B. L. Hartwell, J. Y. H. Chang, S. Xiao, K. A. Rodrigues, K. M. Cirelli, N. Li, S. Haupt, A. Aung, B. Cossette, W. Abraham, S. Kataria, R. Bastidas, J. Bhiman, C. Linde, N. I. Bloom, B. Groschel, E. Georgeson, N. Phelps, A. Thomas, J. Bals, D. G. Carnathan, D. Lingwood, D. R. Burton, G. Alter, T. P. Padera, A. M. Belcher, W. R. Schief, G. Silvestri, R. M. Ruprecht, S. Crotty, D. J. Irvine, A particulate saponin/TLR agonist vaccine adjuvant alters lymph flow and modulates adaptive immunity. *Sci. Immunol.* **6**, eabf1152 (2021).
60. A. deCamp, P. Hraber, R. T. Bailer, M. S. Seaman, C. Ochsenbauer, J. Kappes, R. Gottardo, P. Edlefsen, S. Self, H. Tang, K. Greene, H. Gao, X. Daniell, M. Sarzotti-Kelsoe, M. K. Gorny, S. Zolla-Pazner, C. C. La Branche, J. R. Mascola, B. T. Korber, D. C. Montefiori, Global panel of HIV-1 Env reference strains for standardized assessments of vaccine-elicited neutralizing antibodies. *J. Virol.* **88**, 2489–2507 (2014).
61. C. Soto, R. G. Bombardi, A. Branchizio, N. Kose, P. Matta, A. M. Sevy, R. S. Sinkovits, P. Gilchuk, J. A. Finn, J. E. Crowe Jr., High frequency of shared clonotypes in human B cell receptor repertoires. *Nature* **566**, 398–402 (2019).
62. D. C. Montefiori, Measuring HIV neutralization in a luciferase reporter gene assay. *Methods Mol. Biol.* **485**, 395–405 (2009).
63. P. D. Kwong, R. Wyatt, J. Robinson, R. W. Sweet, J. Sodroski, W. A. Hendrickson, Structure of an HIV gp120 envelope glycoprotein in complex with the CD4 receptor and a neutralizing human antibody. *Nature* **393**, 648–659 (1998).
64. Y. Guo, K. Chen, P. D. Kwong, L. Shapiro, Z. Sheng, cAb-Rep: A database of curated antibody repertoires for exploring antibody diversity and predicting antibody prevalence. *Front. Immunol.* **10**, 2365 (2019).
65. Z. Sheng, C. A. Schramm, R. Kong; NISC Comparative Sequencing Program, J. C. Mullikin, J. R. Mascola, P. D. Kwong, L. Shapiro, Gene-specific substitution profiles describe the types and frequencies of amino acid changes during antibody somatic hypermutation. *Front. Immunol.* **8**, 537 (2017).
66. A. Escolano, H. B. Gristick, M. E. Abernathy, J. Merkenschlager, R. Gautam, T. Y. Oliveira, J. Pai, A. P. West Jr., C. O. Barnes, A. A. Cohen, H. Wang, J. Golijanin, D. Yost, J. R. Keeffe, Z. Wang, P. Zhao, K. H. Yao, J. Bauer, L. Nogueira, H. Gao, A. V. Voll, D. C. Montefiori, M. S. Seaman, A. Gazumyan, M. Silva, A. T. McGuire, L. Stamatatos, D. J. Irvine, L. Wells, M. A. Martin, P. J. Bjorkman, M. C. Nussenzweig, Immunization expands B cells specific to HIV-1 V3 glycan in mice and macaques. *Nature* **570**, 468–473 (2019).
67. P. Zhang, E. Narayanan, Q. Liu, Y. Tsybovsky, K. Boswell, S. Ding, Z. Hu, D. Follmann, Y. Lin, H. Miao, H. Schmeisser, D. Rogers, S. Falcone, S. M. Elbashir, V. Presnyak, K. Bahl, M. Prabhakaran, X. Chen, E. K. Sarfo, D. R. Ambrozak, R. Gautam, M. A. Martin, J. Swerczek, R. Herbert, D. Weiss, J. Misamore, G. Ciaramella, S. Himansu, G. Stewart-Jones, A. McDermott, R. A. Koup, J. R. Mascola, A. Finzi, A. Carfi, A. S. Fauci, P. Lusso, A multiclade

env-gag VLP mRNA vaccine elicits tier-2 HIV-1-neutralizing antibodies and reduces the risk of heterologous SHIV infection in macaques. *Nat. Med.* **27**, 2234–2245 (2021).

68. B. Briney, D. Sok, J. G. Jardine, D. W. Kulp, P. Skog, S. Menis, R. Jacak, O. Kalyuzhniy, N. de Val, F. Sesterhenn, K. M. Le, A. Ramos, M. Jones, K. L. Saye-Francisco, T. R. Blane, S. Spencer, E. Georgeson, X. Hu, G. Ozorowski, Y. Adachi, M. Kubitz, A. Sarkar, I. A. Wilson, A. B. Ward, D. Nemazee, D. R. Burton, W. R. Schief, Tailored immunogens direct affinity maturation toward HIV neutralizing antibodies. *Cell* **166**, 1459–1470.e11 (2016).
69. K. R. Parks, A. J. MacCamy, J. Trichka, M. Gray, C. Weidle, A. J. Borst, A. Khechaduri, B. Takushi, P. Agrawal, J. Guenaga, R. T. Wyatt, R. Coler, M. Seaman, C. L. Branche, D. C. Montefiori, D. Veesler, M. Pancera, A. M. Guire, L. Stamatatos, Overcoming steric restrictions of VRC01 HIV-1 neutralizing antibodies through immunization. *Cell Rep.* **29**, 3060–3072.e7 (2019).
70. H. Duan, X. Chen, J. C. Boyington, C. Cheng, Y. Zhang, A. J. Jafari, T. Stephens, Y. Tsybovsky, O. Kalyuzhniy, P. Zhao, S. Menis, M. C. Nason, E. Normandin, M. Mukhamedova, B. J. De Kosky, L. Wells, W. R. Schief, M. Tian, F. W. Alt, P. D. Kwong, J. R. Mascola, Glycan masking focuses immune responses to the HIV-1 CD4-binding site and enhances elicitation of VRC01-class precursor antibodies. *Immunity* **49**, 301–311.e5 (2018).
71. J. Umotoy, B. S. Bagaya, C. Joyce, T. Schiffner, S. Menis, K. L. Saye-Francisco, T. Biddle, S. Mohan, T. Vollbrecht, O. Kalyuzhniy, S. Madzorera, D. Kitchin, B. Lambson, M. Nonyane, W. Kilembe; IAVI Protocol C Investigators; IAVI African HIV Research Network, P. Poignard, W. R. Schief, D. R. Burton, B. Murrell, P. L. Moore, B. Briney, D. Sok, E. Landais, Rapid and focused maturation of a VRC01-class HIV broadly neutralizing antibody lineage involves both binding and accommodation of the N276-glycan. *Immunity* **51**, 141–154.e6 (2019).
72. E. Seydoux, Y. H. Wan, J. Feng, A. Wall, S. Aljedani, L. J. Homad, A. J. MacCamy, C. Weidle, M. D. Gray, L. Brumage, J. J. Taylor, M. Pancera, L. Stamatatos, A. T. McGuire, Development of a VRC01-class germline targeting immunogen derived from anti-idiotypic antibodies. *Cell Rep.* **35**, 109084 (2021).
73. P. Dosenovic, A. K. Pettersson, A. Wall, E. S. Thientosapol, J. Feng, C. Weidle, K. Bhullar, E. E. Kara, H. Hartweger, J. A. Pai, M. D. Gray, K. R. Parks, J. J. Taylor, M. Pancera, L. Stamatatos, M. C. Nussenzweig, A. T. McGuire, Anti-idiotypic antibodies elicit anti-HIV-1-specific B cell responses. *J. Exp. Med.* **216**, 2316–2330 (2019).
74. M. Navis, K. Tran, S. Bale, G. E. Phad, J. Guenaga, R. Wilson, M. Soldemo, K. McKee, C. Sundling, J. Mascola, Y. Li, R. T. Wyatt, G. B. Karlsson Hedestam, HIV-1 receptor binding site-directed antibodies using a VH1-2 gene segment orthologue are activated by Env trimer immunization. *PLOS Pathog.* **10**, e1004337 (2014).
75. C. Havenar-Daughton, D. G. Carnathan, A. V. Boopathy, A. A. Upadhyay, B. Murrell, S. M. Reiss, C. A. Enemuo, E. H. Gebru, Y. Choe, P. Dhadvai, F. Viviano, K. Kaushik, J. N. Bhiman, B. Briney, D. R. Burton, S. E. Bosinger, W. R. Schief, D. J. Irvine, G. Silvestri, S. Crotty, Rapid germinal center and antibody responses in non-human primates after a single nanoparticle vaccine immunization. *Cell Rep.* **29**, 1756–1766.e8 (2019).
76. S. A. Griffith, L. E. McCoy, To bnAb or not to bnAb: Defining broadly neutralising antibodies against HIV-1. *Front. Immunol.* **12**, 708227 (2021).
77. K. O. Saunders, K. Wiehe, M. Tian, P. Acharya, T. Bradley, S. M. Alam, E. P. Go, R. Scearce, L. Sutherland, R. Henderson, A. L. Hsu, M. J. Borgnia, H. Chen, X. Lu, N. R. Wu, B. Watts, C. Jiang, D. Easterhoff, H. L. Cheng, K. McGovern, P. Waddicor, A. Chapdelaine-Williams, A. Eaton, J. Zhang, W. Rountree, L. Verkoczy, M. Tomai, M. G. Lewis, H. R. Desaire, R. J. Edwards, D. W. Cain, M. Bonsignori, D. Montefiori, F. W. Alt, B. F. Haynes, Targeted selection of HIV-specific antibody mutations by engineering B cell maturation. *Science* **366**, eaay7199 (2019).
78. P. Venkatesan, Preliminary phase 1 results from an HIV vaccine candidate trial. *Lancet Microbe* **2**, e95 (2021).
79. M. Kanekiyo, M. G. Joyce, R. A. Gillespie, J. R. Gallagher, S. F. Andrews, H. M. Yassine, A. K. Wheatley, B. E. Fisher, D. R. Ambrozak, A. Creanga, K. Leung, E. S. Yang, S. Boyoglu-Barnum, I. S. Georgiev, Y. Tsybovsky, M. S. Prabhakaran, H. Andersen, W. P. Kong, U. Baxa, K. L. Zephir, J. E. Ledgerwood, R. A. Koup, P. D. Kwong, A. K. Harris, A. B. McDermott, J. R. Mascola, B. S. Graham, Mosaic nanoparticle display of diverse influenza virus hemagglutinins elicits broad B cell responses. *Nat. Immunol.* **20**, 362–372 (2019).
80. A. A. Cohen, P. N. P. Gnanapragasam, Y. E. Lee, P. R. Hoffman, S. Ou, L. M. Kakutani, J. R. Keeffe, H. J. Wu, M. Howarth, A. P. West, C. O. Barnes, M. C. Nussenzweig, P. J. Bjorkman, Mosaic nanoparticles elicit cross-reactive immune responses to zoonotic coronaviruses in mice. *Science* **371**, 735–741 (2021).
81. J. van Schooten, E. Farokhi, A. Schorcht, T. L. G. M. van den Kerkhof, H. Gao, P. van der Woude, J. A. Burger, T. G. R. Meesters, T. Bijl, R. Ghalaiyini, H. L. Turner, J. Dorning, B. D. C. van Schaik, A. H. C. van Kampen, C. C. Labranche, R. L. Stanfield, D. Sok, D. C. Montefiori, D. R. Burton, M. S. Seaman, G. Ozorowski, I. A. Wilson, R. W. Sanders, A. B. Ward, M. J. van Gils, Identification of IOMA-class neutralizing antibodies targeting the CD4-binding site on the HIV-1 envelope glycoprotein. *Nat. Commun.* **13**, 4515 (2022).
82. B. Zakeri, J. O. Fierer, E. Celik, E. C. Chittock, U. Schwarz-Linek, V. T. Moy, M. Howarth, Peptide tag forming a rapid covalent bond to a protein, through engineering a bacterial adhesin. *Proc. Natl. Acad. Sci. U.S.A.* **109**, E690–E697 (2012).
83. A. H. Keeble, P. Turkki, S. Stokes, I. N. A. Khairil Anuar, R. Rahikainen, V. P. Hytönen, M. Howarth, Approaching infinite affinity through engineering of peptide–protein interaction. *Proc. Natl. Acad. Sci. U.S.A.* **116**, 26523–26533 (2019).
84. L. Scharf, A. P. West Jr., S. A. Sievers, C. Chen, S. Jiang, H. Gao, M. D. Gray, A. T. McGuire, J. F. Scheid, M. C. Nussenzweig, L. Stamatatos, P. J. Bjorkman, Structural basis for germline antibody recognition of HIV-1 immunogens. *eLife* **5**, e13783 (2016).
85. C. O. Barnes, T. Schoofs, P. N. P. Gnanapragasam, J. Golijanin, K. E. Huey-Tubman, H. Gruell, P. Schommers, N. Suh-Toma, Y. E. Lee, J. C. C. Lorenzi, A. Piechocka-Trocha, J. F. Scheid, A. P. West Jr., B. D. Walker, M. S. Seaman, F. Klein, M. C. Nussenzweig, P. J. Bjorkman, A naturally arising broad and potent CD4-binding site antibody with low somatic mutation. *Sci. Adv.* **8**, eabp8155 (2022).
86. K.-M. A. Dam, C. O. Barnes, H. B. Gristick, T. Schoofs, M. C. Nussenzweig, P. J. Bjorkman, HIV-1 CD4-binding site germline antibody–Env structures inform vaccine design. bioRxiv: 2022.03.25.485873 [Preprint]. 26 March 2022. https://doi.org/10.1101/2022.03.25.485873.
87. R. Rahikainen, P. Rijal, T. K. Tan, H. J. Wu, A. M. C. Andersson, J. R. Barrett, T. A. Bowden, S. J. Draper, A. R. Townsend, M. Howarth, Overcoming symmetry mismatch in vaccine nanoassembly through spontaneous amidation. *Angew. Chem. Int. Ed. Engl.* **60**, 321–330 (2021).
88. A. A. Cohen, Z. Yang, P. N. P. Gnanapragasam, S. Ou, K. M. A. Dam, H. Wang, P. J. Bjorkman, Construction, characterization, and immunization of nanoparticles that display a diverse array of influenza HA trimers. *PLOS ONE* **16**, e0247963 (2021).
89. R. Pelanda, S. Schwers, E. Sonoda, R. M. Torres, D. Nemazee, K. Rajewsky, Receptor editing in a transgenic mouse model: Site, efficiency, and role in B cell tolerance and antibody diversification. *Immunity* **7**, 765–775 (1997).
90. T. A. Shih, M. Roederer, M. C. Nussenzweig, Role of antigen receptor affinity in T cell-independent antibody responses in vivo. *Nat. Immunol.* **3**, 399–406 (2002).
91. K. Lövgren-Bengtsson, B. Morein, in *Vaccine Adjuvants: Preparation Methods and Research Protocols*, D. T. O'Hagan, Ed. (Humana, 2000), pp. 239–258.
92. C. Viant, A. Escolano, S. T. Chen, M. C. Nussenzweig, Sequencing, cloning, and antigen binding analysis of monoclonal antibodies isolated from single mouse B cells. *STAR Protoc.* **2**, 100389 (2021).
93. K. Katoh, D. M. Standley, MAFFT multiple sequence alignment software version 7: Improvements in performance and usability. *Mol. Biol. Evol.* **30**, 772–780 (2013).
94. D. C. Montefiori, Evaluating neutralizing antibodies against HIV, SIV, and SHIV in luciferase reporter gene assays. *Curr. Protoc. Immunol.* **Chapter 12**, 12.11.1–12.11.17 (2005).
95. M. M. Sajadi, A. Dashti, Z. R. Tehrani, W. D. Tolbert, M. S. Seaman, X. Ouyang, N. Gohain, M. Pazgier, D. Kim, G. Cavet, J. Yared, R. R. Redfield, G. K. Lewis, A. L. De Vico, Identification of near-pan-neutralizing antibodies against HIV-1 by deconvolution of plasma humoral responses. *Cell* **173**, 1783–1795.e14 (2018).
96. Z. Wang, F. Muecksch, D. Schaefer-Babajew, S. Finkin, C. Viant, C. Gaebler, H. H. Hoffmann, C. O. Barnes, M. Cipolla, V. Ramos, T. Y. Oliveira, A. Cho, F. Schmidt, J. da Silva, E. Bednarski, L. Aguado, J. Yee, M. Daga, M. Turroja, K. G. Millard, M. Jankovic, A. Gazumyan, Z. Zhao, C. M. Rice, P. D. Bieniasz, M. Caskey, T. Hatziioannou, M. C. Nussenzweig, Naturally enhanced neutralizing breadth against SARS-CoV-2 one year after infection. *Nature* **595**, 426–431 (2021).
97. Z. Wang, J. C. C. Lorenzi, F. Muecksch, S. Finkin, C. Viant, C. Gaebler, M. Cipolla, H. H. Hoffmann, T. Y. Oliveira, D. A. Oren, V. Ramos, L. Nogueira, E. Michailidis, D. F. Robbiani, A. Gazumyan, C. M. Rice, T. Hatziioannou, P. D. Bieniasz, M. Caskey, M. C. Nussenzweig, Enhanced SARS-CoV-2 neutralization by dimeric IgA. *Sci. Transl. Med.* **13**, eabf1555 (2021).
98. R. W. Siegel, Antibody affinity optimization using yeast cell surface display. *Methods Mol. Biol.* **504**, 351–383 (2009).
99. J. Snijder, M. S. Ortego, C. Weidle, A. B. Stuart, M. D. Gray, M. J. McElrath, M. Pancera, D. Veesler, A. T. McGuire, An antibody targeting the fusion machinery neutralizes dual-tropic infection and defines a site of vulnerability on Epstein-Barr virus. *Immunity* **48**, 799–811.e9 (2018).
100. P. D. Adams, P. V. Afonine, G. Bunkóczi, V. B. Chen, I. W. Davis, N. Echols, J. J. Headd, L. W. Hung, G. J. Kapral, R. W. Grosse-Kunstleve, A. J. McCoy, N. W. Moriarty, R. Oeffner, R. J. Read, D. C. Richardson, J. S. Richardson, T. C. Terwilliger, P. H. Zwart, PHENIX: A comprehensive Python-based system for macromolecular structure solution. *Acta Crystallogr. D Biol. Crystallogr.* **66**, 213–221 (2010).
101. P. Emsley, B. Lohkamp, W. G. Scott, K. CoWTan, Features and development of Coot. *Acta Crystallogr. D Biol. Crystallogr.* **66**, 486–501 (2010).
102. S. A. Gai, K. D. Wittrup, Yeast surface display for protein engineering and characterization. *Curr. Opin. Struct. Biol.* **17**, 467–473 (2007).
103. S. Tian, R. Das, Primerize-2D: Automated primer design for RNA multidimensional chemical mapping. *Bioinformatics* **33**, 1405–1406 (2017).

104. J. Staal, K. Alci, W. De Schamphelaire, M. Vanhoucke, R. Beyaert, Engineering a minimal cloning vector from a pUC18 plasmid backbone with an extended multiple cloning site. *Biotechniques* **66**, 254–259 (2019).
105. M. L. L. Donnelly, G. Luke, A. Mehrotra, X. Li, L. E. Hughes, D. Gani, M. D. Ryan, Analysis of the aphthovirus 2A/2B polyprotein 'cleavage' mechanism indicates not a proteolytic reaction, but a novel translational effect: A putative ribosomal 'skip'. *J. Gen. Virol.* **82**, 1013–1025 (2001).
106. H. Hartweger, A. T. McGuire, M. Horning, J. J. Taylor, P. Dosenovic, D. Yost, A. Gazumyan, M. S. Seaman, L. Stamatatos, M. Jankovic, M. C. Nussenzweig, HIV-specific humoral immune responses by CRISPR/Cas9-edited B cells. *J. Exp. Med.* **216**, 1301–1310 (2019).
107. J. Ye, N. Ma, T. L. Madden, J. M. Ostell, IgBLAST: An immunoglobulin variable domain sequence analysis tool. *Nucleic Acids Res.* **41**, W34–W40 (2013).
108. X. Brochet, M. P. Lefranc, V. Giudicelli, IMGT/V-QUEST: The highly customized and integrated system for IG and TR standardized V-J and V-D-J sequence analysis. *Nucleic Acids Res.* **36**, W503–W508 (2008).
109. T. D. Goddard, C. C. Huang, E. C. Meng, E. F. Pettersen, G. S. Couch, J. H. Morris, T. E. Ferrin, UCSF ChimeraX: Meeting modern challenges in visualization and analysis. *Protein Sci.* **27**, 14–25 (2018).
110. F. Sievers, A. Wilm, D. Dineen, T. J. Gibson, K. Karplus, W. Li, R. Lopez, H. McWilliam, M. Remmert, J. Söding, J. D. Thompson, D. G. Higgins, Fast, scalable generation of high-quality protein multiple sequence alignments using Clustal Omega. *Mol. Syst. Biol.* **7**, 539 (2011).

Acknowledgments: We thank J. Moore (Weill Cornell Medical College), R.W. Sanders, and M.J. van Gils (Amsterdam UMC) for SOSIP expression plasmids; M. Silva, M. B. Melo, and D. J. Irvine (MIT) for providing the SMNP adjuvant; L. von Boehmer (Stanford University) for discussion; J. Vielmetter, P. Hoffman, and the Protein Expression Center in the Beckman Institute at Caltech for expression assistance; T. Eisenreich and S. Tittley for animal husbandry; and K. Gordon and K. Chosphel for FACS at Rockefeller University. EM was performed in the Caltech Cryo-EM Center with assistance from S. Chen and A. Malyutin. **Funding:** This work was supported by the NIAID grants HIVRAD P01 AI100148 (to P.J.B. and M.C.N.), HIVRAD P01 AI138212 (to L.S., A.T.M., and M.C.N.), and R21 AI127249 (to A.T.M.); the Bill and Melinda Gates Foundation CAVD grant INV-002143 (to P.J.B., M.C.N., and M.A.M.); a Bill and Melinda Gates Foundation grant # OPP1146996 (to M.S.S.); the Intramural Research Program of the NIAID (to M.A.M. and Y.N.); and NIH P50 AI150464 (to P.J.B.). M.E.A. was supported by a NSF Graduate Research Fellowship. **Author contributions:** H.B.G., H.H., A.P.W., M.C.N., M.A.M., and P.J.B. conceived the experiments. H.B.G. and H.H. designed and performed all experiments with assistance from other authors. M.L. assisted with Ab cloning. J.v.S. set up the yeast libraries and helped develop the original IGT variants, and M.E.A. and A.J.P.-B. assisted in developing the later IGT variants. V.R. and T.Y.O. performed computational analysis of the Ab sequencing data. Y.N. performed the rhesus macaque experiments. N.S.K. and H.G. performed cloning and purification of antigens and Abs. A.W., A.T.M., and L.S. generated the anti-idiotypic Abs. K.-H.Y. assisted with the mouse experiments, D.P. assisted with IOMAgl mouse generation, A.G. helped with the recombinant Ab production, and M.W. and M. Horning assisted with mouse experiments and cell sorting. J.R.K. provided project administration, M.A.G.H., P.N.P.G., and L.M.K. performed neutralization assays, Z.Y. performed the EM experiments, and K.-M.A.D. helped in understanding IOMA-like Ab clones isolated from transgenic mice. M.S.S. helped with recombinant Ab neutralization assays. M. Howarth assisted with nanoparticle conjugations. The paper was written by H.B.G., H.H., P.J.B., M.C.N., and M.A.M. with assistance from other authors. **Competing interests:** M.C.N. is an HHMI investigator. H.B.G., P.J.B., H.H., and M.C.N. are coinventors on a patent (CIT 8845-P) covering IGT immunogens. P.J.B. is on the Scientific Advisory Board of Vir Biotechnology. M.C.N is on the Scientific Advisory Board of Celdex, Fronteir Bio, Areium Therapeutics, and Apriori Bio. M. Howarth is an inventor on patents on spontaneous amide bond formation (EP2534484) and SpyTag003:SpyCatcher003 (WO/2020/183198) and is a cofounder, shareholder, and former consultant of SpyBiotech. All other authors declare that they have no competing interests. **Data and materials availability:** The structure of IOMA iGL Fab is available in the Protein Data Bank under accession code 7TQG. 10x Genomics V(D)J sequencing data are available from Gene Expression Omnibus accession number GSE197951. All other data, mice, and reagents used in this study are available from the corresponding authors upon reasonable request. Ab HC and LC genes were analyzed using our previously described IgPipeline (*96*, *97*). The code for the IgPipeline is available at https://github.com/stratust/igpipeline/tree/igpipeline2_timepoint_v2.
 Further information and reasonable requests for reagents and resources should be directed to P.J.B. (bjorkman@caltech.edu).

Submitted 29 August 2022
Accepted 20 January 2023
Published 10 February 2023
10.1126/sciimmunol.ade6364

Science Immunology

CD4 binding site immunogens elicit heterologous anti–HIV-1 neutralizing antibodies in transgenic and wild-type animals

Harry B. Gristick, Harald Hartweger, Maximilian Loewe, Jelle van Schooten, Victor Ramos, Thiago Y. Oliveira, Yoshiaki Nishimura, Nicholas S. Koranda, Abigail Wall, Kai-Hui Yao, Daniel Poston, Anna Gazumyan, Marie Wiatr, Marcel Horning, Jennifer R. Keeffe, Magnus A.G. Hoffmann, Zhi Yang, Morgan E. Abernathy, Kim-Marie A. Dam, Han Gao, Priyanthi N.P. Gnanapragasam, Leesa M. Kakutani, Ana Jimena Pavlovitch-Bedzyk, Michael S. Seaman, Mark Howarth, Andrew T. McGuire, Leonidas Stamatatos, Malcolm A. Martin, Anthony P. West, Jr., Michel C. Nussenzweig, and Pamela J. Bjorkman

Sci. Immunol., **8** (80), eade6364.
DOI: 10.1126/sciimmunol.ade6364

Reverse engineering HIV-1 neutralizing antibodies
Reverse Engineering HIV-1 Neutralizing AntibodiesEfforts to develop HIV-1 vaccines have included the identification of HIV-1 Env epitopes that can induce broadly neutralizing antibodies (bNAbs) targeting the CD4 binding site (CD4bs). The CD4bs bNAb IOMA is considered a good candidate for guiding development of Env immunogens because it is known to have low somatic mutation rates, a normal length CDRL3, and can accommodate the N276gp120 N-glycan on Env. Gristick/Hartweger *et al*. used a yeast display library screen and structure-based sequential immunization to evaluate Env immunogens in transgenic mice expressing germline-reverted IOMA. CD4bs-specific antibody responses with heterologous neutralization capacity were induced by vaccination in both transgenic mice and in animals with polyclonal antibody repertoires. These findings highlight the potential of immunogens that can induce IOMA-class bNAbs as a potential HIV-1 vaccine strategy. —CNF

Science Immunology
AAAS

Supplementary Materials for

CD4 binding site immunogens elicit heterologous anti–HIV-1 neutralizing antibodies in transgenic and wild-type animals

Harry B. Gristick *et al.*

Corresponding author: Pamela J. Bjorkman, bjorkman@caltech.edu;
Michel C. Nussenzweig, nussen@rockefeller.edu

Sci. Immunol. **8**, eade6364 (2023)
DOI: 10.1126/sciimmunol.ade6364

The PDF file includes:

Materials and Methods
Figs. S1 to S8
Tables S1 to S8
References (*96–110*)

Other Supplementary Material for this manuscript includes the following:

MDAR Reproducibility Checklist

Supplementary Materials and Methods

Generation of anti-idiotypic monoclonal antibodies

Mice were injected three times with purified IOMA iGL. 3 days after the final injection spleens were harvested and used to generate hybridomas at the Fred Hutchinson Antibody Technology Center. Hybridoma supernatants were initially screened against IOMA iGL to identify antigen-specific hybridomas. Supernatants from positive wells were then screened against a panel of monoclonal antibodies that included IOMA, IOMA iGL, and inferred germlines of other anti-HIV-1 antibodies that served as isotype controls using a high throughput bead array. We identified two hybridomas of interest; 3D3, which bound specifically to IOMA iGL, and 3D7, which bound to IOMA and IOMA iGL, which were subcloned from single cells. To produce recombinant anti-idiotypes, RNA was extracted from 1×10^6 cells using the RNeasy kit (Qiagen), and the heavy and light chain sequences of the murine hybridomas were by obtained using the mouse Ig-primer set (69831; EMD Millipore) as described (*98*). Sequences were codon optimized, cloned into pTT3-based IgG expression vectors with human constant regions (*99*) using In-Fusion cloning (Clontech), expressed in 293 cells, and purified using Protein A chromatography.

X-ray crystallography

Crystallization screens for IOMA iGL Fab were performed using the sitting drop vapor diffusion method at room temperature (RT) by mixing 0.2 µL Fabs with 0.2 µL of reservoir solution (Hampton Research) using a TTP Labtech Mosquito automatic microliter pipetting robot. IOMA iGL Fab crystals were obtained in 20% (v/v) PEG 2000, 0.1 M Sodium Acetate (pH 4.6). Crystals were looped and cryopreserved in reservoir solution supplemented with 20% glycerol and flash frozen in liquid nitrogen.

The crystal structure of IOMA iGL Fab was solved with data sets. A 1.9 Å-resolution structure of IOMA – 10-1074 – BG505 was solved with a single data set collected at 100 K and 1 Å resolution on Beamline 12-2 at the Stanford Synchrotron Radiation Lightsource (SSRL) with a Pilatus 6M pixel detector (Dectris) that was indexed and integrated with iMosflm v7.4, and then merged with AIMLESS in the CCP4 software package v7.1.018. The structure was determined by molecular replacement using Phaser with one copy of IOMA Fab (PDB 5T3Z). Coordinates were refined with PHENIX v1.19.2-4158 (*100*) with group B factor and TLS restraints. Manual rebuilding was performed iteratively with Coot v1.0.0 (*101*). Data refinement statistics are shown in Table S2, with > 98% of the residues in the favored region of the Ramachandran plot and < 1% in the disallowed regions.

Cloning yeast libraries

Crystal structures of IOMA in complex with BG505 SOSIP.664 (PDB ID 5T3X and 5T3Z) were analyzed to determine mutations on gp120 that potentially could be beneficial for IOMA iGL binding. In addition, we modeled the crystal structure of IOMA iGL (PDB ID 7TQG) onto 426c.TM4ΔV1-3 (426c.TM4) gp120 (PDB ID 5FEC) and selected positions within gp120 that we predicted to be favorable for IOMA iGL binding. We chose 426c.TM4ΔV1-3 (426c TM4), an engineered clade C Env previously shown to activate B cell precursors of HIV-1 bNAbs targeting the CD4bs (*25*) as the starting point for our library design.

Yeast libraries were generated as described (*102*). Specifically, to generate the libraries of 426c gp120 variants we used degenerate oligos in conjunction with an overlap assembly polymerase chain reaction (PCR) method. Overlapping primers for the PCR assembly reactions were designed using Primerize (*103*) and shown in Table S6. NNK codons (where N = A/C/G/T and K = G/T) were utilized that encode for all 20 amino acids but decrease the chances of introducing a premature stop codon. Two different DNA fragments (426c library fragment 1 and 2) were synthesized first and then linearized in a final PCR step to generate the full-length 426c gp120 library used in yeast transformation. To obtain the full-length 426c gp120, a final PCR reaction was performed in which the PCR products of the 426c Library Fragment 1 and 2 were used as a template. Primers were used with overhangs complementary to the yeast display vector pCTCON-2 necessary for the homologous recombination in yeast. Library 2 was cloned in a similar manner as Library 1, but using a different set of primers as shown in Table S6 based on results from Library 1.

Yeast transformation

The yeast display vector pCTCON-2 was used for cell surface display of the 426c gp120 proteins in *Saccharomyces cerevisiae* (*S. cerevisiae*) strain EBY100. A primary culture of 5 mL 2x YPD (40 g/L glucose, 20 g/L peptone, 20 g/L yeast extract) media was inoculated with a single *S. cerevisiae* EBY100 colony (freshly streaked on a YPD plate) and incubated overnight in a shaker at 30 °C and 250 rpm. 100 µL of the overnight yeast *S. cerevisiae* EBY100 cultures was transferred into 5 mL 2x YPD media and incubated overnight at 30 °C, 250 rpm. The following day, 300 mL 2x YPD media was inoculated with the overnight precultures to an OD_{600} ~0.3 and was grown until an OD_{600} ~1.6. 3 mL of sterile filtered Tris/DTT (0.462 g 1,4-dithiothreitol in 3 mL 1 M Tris, pH 8.0) and 15 mL sterile filtered 2 M LiAc/TE (1.98 g LiAc in 10 mL of TE (10 mM Tris, 1 mM EDTA) was added and the culture incubated for 15 min at 30 °C and 250 rpm. Yeast cells were then pelleted at 3,500 g for 3 min and washed with 50 mL ice-cold sterile filtered NewE buffer (0.6 g Tris base, 91.09 g Sorbitol (1 M), 73.50 mg $CaCl_2$ in

ddH_2O to a final volume of 500 mL, pH 7.5). After two additional wash steps, the pellet was re-suspended in 3 mL NewE buffer and 50 µg 426c library DNA insert and 10 µg pCTCON-2 vector (digested with NheI and BamHI) was added. 200 µL of this transformation mix was then aliquoted into pre-chilled 2 mm electroporation cuvettes (Bio-Rad) and electroporated at 1500 V with an average time constant of ~4.5 ms using a Gene Pulser Xcell Electroporation System (Bio-Rad), which was repeated for the entire transformation mix. After electroporation, yeast cells were directly recovered with 2 mL 2x YPD media and transferred into 50 mL cold 2x YPD media (final volume up to 200 mL 2x YPD media) and grown for 1 h at 30 °C and 250 rpm. Serial dilutions of the freshly transformed yeast culture were plated on SDCAA (20 g/L glucose, 6.7 g/L Difco yeast nitrogen base, 1.4 g/L Yeast Synthetic Drop-out Medium Supplements without histidine, leucine, tryptophan and uracil, 20 mg/L uracil, 50 mg/L histidine, 100 mg/L leucine) agarose plates to test the viability and size of the library. After 1 h, the culture was removed and the cells were pelleted and resuspended in 500 mL SDCAA media + carbenicillin (100 µg/mL final concentration) and grown for two days at 30 °C and 250 rpm. To confirm the genetic diversity of the library, a yeast colony PCR was performed on the liquid culture and the PCR product was sequenced. Sequencing reactions were performed at Laragen Inc (Culver City, CA). The sequence data was analyzed using SeqMan Pro (DNASTAR, v13.02). After two days, cells were pelleted and glycerol stocks were made by suspending ~10^9 yeast cells in 1 mL of freezing buffer (0.335 g Yeast Nitrogen Base, 1 mL glycerol in 50 mL H_2O, sterilized by filtration). Aliquots were flash frozen in liquid nitrogen and stored at -80 °C.

Magnetic-activated cell sorting

Magnetic-activated cell sorting (MACS) was used to remove transformants containing stop codons. After growing up the freshly transformed cells for two days in SDCAA, cells were pelleted and induced at an OD_{600} ~1.0 in 100 mL SGCAA-carb (SDCAA prepared with 20 g/L galactose instead of glucose and supplemented with 100 µg/mL carbenicillin final concentration) for 20 h at 20 °C and 250 rpm. Yeast cells were washed 5 times with PBSF (PBS + 0.1% bovine serum albumin (BSA)) and 10^8 cells were incubated with 400 µL PBSF and 100 µL µMACS™ anti-c-Myc MicroBeads (Miltenyi Biotec) for 45 min on a rotator at 4 °C. Cells were then pelleted and resuspended in 5 mL PBSF and sorted using a MidiMACS Separator magnet (Miltenyi Biotec) in combination with an LS column (Miltenyi Biotec) equilibrated in PBSF. Isolated cells were then grown for 2 days in 100 mL SDCAA-carb at 30 °C and 250 rpm and then induced again with SGCAA-carb for 20 h at 20 °C and 250 rpm.

Yeast flow cytometry and cell sorting

To prepare the yeast library for FACS analysis, cells were pelleted at 3000 rpm for 2 min and washed 5 times with PBSF. Cells were then stained at a density of 10^7 cells/mL with 1:500 anti-c-Myc antibody conjugated to AlexaFluor488 (Abcam, ab190026) and 1 μM IOMA iGL and incubated for 1 – 2 h on a rotator at 4 °C. Cells were then washed twice with PBSF and resuspended in 200 μL PBSF with 1:1000 goat anti-human antibody conjugated to AlexaFluor647 (Abcam, ab190560, RRID:AB_2876372) and incubated for 30 min at 4 °C. Cells were then analyzed on a MACSQuant Analyzer (Miltenyi Biotec) or sorted using an SY3200 cell sorter system (Sony). In either case, non-transformed yeast cells and single-stained transformed samples stained with either anti-c-Myc or IOMA iGL IgG were used to set the gates for analysis and collection. Cells that stained double-positive for both c-Myc and IOMA iGL were collected and grown in 5 mL SDCAA-carb for 1 - 2 days at 30 °C and 250 rpm and then transferred to 100 mL SDCAA-carb for an additional 1 - 2 days at 30 °C and 250 rpm. Cells were then pelleted and resuspended in H_2O and plated onto SDCAA-carb for 2 - 3 days at 30 °C. After multiple iterative rounds of sorting (three rounds for Library 1 and seven rounds for Library 2), sequences were recovered by colony PCR and sequence confirmed (Laragen). Primers were used with specific complementary regions to enable ligation of the linear product into the expression vector pTT5 using the Gibson assembly method for protein production. After construction, plasmids were isolated from *E.coli* using the QIAprep Miniprep kit (Qiagen) and confirmed by Sanger sequencing (Laragen).

Generation of IOMA-expressing RAMOS cells by CRISPR/Cas9 gene editing

A targeting vector was constructed using the NEB Hifi DNA assembly kit to clone a gBlock (IDT) into pUCmu (*104*). The gBlock (IDT) contained ~0.5 kb homology arms to the human IgH locus which flanked an expression cassette consisting of the C_μ splice acceptor, the entire IOMA LC gene, a furin-GSG-P2A sequence (*105*) followed by the IOMA HC Leader-VDJ and the J_H4 splice donor based on previously-described designs (*106*) (Figure S5C). Vectors were maxi-prepped (Machery-Nagle) for transfection.

RAMOS (RA 1) cells were purchased from ATCC (CRL-1596) and maintained in RPMI-1640 supplemented with 10 FCS, 1x antibiotic/antimycotic, 2 mM glutamine, 1 mM sodium pyruvate, 10 mM HEPES and 55 μM β-mercaptoethanol. Before transfection, cells were harvested, washed once in PBS and resuspended at $6x10^7$ cells/mL in Neon kit buffer T (ThermoFisher). Three ribonucleoprotein complexes (RNPs) were prepared using 3 different sgRNAs. AGGCATCGGAAAATCCACAG was used to target the IgH locus in the intron 3' of *IGHJ6* to integrate the sequence flanked by the appropriate homology arms from the targeting vector; CTGGGAGTTACCCGATTGGA was used to ablate the human *IGKC* exon and CACGCATGAAGGGAGCACCG was used to ablate all functional *IGLC* genes

(*IgLC1, IGL2, IGLC3* and *IGLC7*). Complexes were prepared by mixing 1.875 µL of 100 µM sgRNA with 1 µL of 61 µM Cas9 (all IDT) for a molar ratio of ~3:1 followed by incubation for 20 min at RT. *IGH:IGK:IGL* RNPs were then mixed at a 2:1:1 v/v/v ratio. 2.6 µg targeting vector (at 4 mg/mL) were mixed with 1.5 µL *IGH:IGK:IGL* RNP mix and 11 µL RAMOS cells in buffer T. 10 µL of the final mix were transfected in a 10 µL Neon tip in a Neon device at 1350 V 30 ms 1 pulse. Cells were immediately transferred into 50 µL RAMOS medium without 1x antibiotic/antimycotic in a 48-well plate and 2 h later 450 µL full RAMOS medium was added. Cells were then cultured as before. Edited IOMA-expressing cells were bulk sorted by flow cytometry as live, singlet, $CD19^+$, RC1 $antigen^{hi}$, IgL^+, IgK^+ IgM^+ (Table S7) and cultured as before. IOMA-expression was further verified by staining with 426c-, CNE8- and CNE20-derived SOSIPs and 426c-CD4bs-KO proteins to show specificity.

10x Genomics single cell processing and next generation V(D)J sequencing

Cells were counted in the final injection volume, and 18,000 cells loaded onto a Chromium Controller (10x Genomics). Single-cell RNA-seq libraries were prepared using the Chromium Single Cell 5 v2 Reagent Kit (PN-1000265) according to manufacturer's protocol. Chromium Single Cell Mouse BCR Amplification Kit (PN-1000255) was used for VDJ cDNA amplification. After QC, 5' expression and VDJ Libraries were pooled 1:1 and sequenced on an Illumina NOVAseq S1 flowcell at the Rockefeller University Genomics Core.

Computational Analyses of V(D)J sequences derived from IOMAgl mice by next generation sequencing

The single-cell V(D)J assembly was carried out by Cell Ranger 6.0.1. A customized reference was created by adding the knocked-in IOMA iGL V(D)J genes to the mouse GRCm38 V(D)J reference so Cell Ranger could recognize and assemble the human/mouse chimera transcripts. Contigs associated with a valid cell barcode according to Cell Ranger were selected for downstream processing using seqtk version 1.3-r106 (https://github.com/lh3/seqtk).

IgBlast standalone version 1.14 (*107*) was used to annotate the immunoglobulin sequences based on a custom database with mouse and human V(D)J genes. Productive IG sequences with more than 20 reads of coverage and with any identified isotype were selected for downstream processing. Unexpectedly, although the IgBlast algorithm identified the V and J genes for 8010 LC sequences, it failed to annotate the CDR3, and consequently, the information regarding their functionality was missing. We extracted and submitted 7782 (97.15%) sequences corresponding to the knock-in LC to

IMGT/V-QUEST (*108*), which successfully identified the CDR3 and provided the productivity information.

Cell barcodes associated with sequences coded by different V genes for either HC or LC were considered doublets and were subsequently removed from downstream analysis. HCs and LCs derived from the same cell were paired, and clones were assigned using our previously-described IgPipeline (*96, 97*) (https://github.com/stratust/igpipeline/tree/igpipeline2_timepoint_v2).

Single cell antibody cloning

The following modifications were applied to the described protocol from reference (*92*) Briefly, single cell RNA in 96-well plates was purified using magnetic beads (RNAClean XP, Beckman Coulter, Cat # A63987). RNA was eluted from the magnetic beads with 11 µL of a solution containing 14.5 ng/µL of random primers (Invitrogen, Cat # 48190011), 0.5% of Igepal Ca-630 (type NP-40, 10% in dH_2O, MP Biomedicals, Cat # 198596) and 0.6 U/µL of RNase inhibitor (Promega, Cat# N2615) in nuclease-free water (Qiagen, Cat # 129117), and incubated at 65 °C for 3 min. cDNA was synthesized by reverse transcription (SuperScript™ III Reverse Transcriptase 10,000 U, Invitrogen, Cat# 18080-044). cDNA was stored at −80 °C or used for antibody gene amplification by nested polymerase chain reaction (PCR) after addition of 10 µL of nuclease-free water.

Mouse antibody genes were amplified using HotstarTaq DNA polymerase (Qiagen Cat # 203209) with the primer sets specific for the $Igh^{IOMAiGL}$ and $Igk^{IOMAiGL}$ transgenes. Primer sequences and reaction mixes are provided in Table S8. Thermocycler conditions were as follows for annealing (°C)/elongation (s)/number of cycles: PCR1 (IgG, IgM and IgK): 51/55/50; PCR2 (IgG and IgM): 54/55/50; PCR2 (IgK): 50/55/50.

PCR products of antibody HC and LC genes were purified and Sanger-sequenced (Genewiz) and *ab1 files analyzed using our previously described IgPipeline (https://github.com/stratust/igpipeline/tree/igpipeline2_timepoint_v2) (*96, 97*). V(D)J sequences were ordered as eBlocks (IDT) with short homologies for Gibson assembly and cloned into human IgG1 or human IgL2 expression vectors using the NEB Hifi DNA Assembly mix (NEB, Cat#E2621L). Plasmid sequences were verified by Sanger sequencing (Genewiz).

SPR binding studies

All SPR measurements were performed on a Biacore T200 (GE Healthcare) at 20 °C in HBS-EP+ (GE Healthcare) running buffer. IgGs were directly immobilized onto a CM5 chip (GE Healthcare) to ~3000 resonance units (RUs) using primary amine chemistry. A concentration series of monomeric gp120 core constructs (IGT2, IGT1, 426c TM4) were injected over the flow cells at increasing concentrations (top concentrations ranging from 600 μM to 10 μM) at a flow rate of 60 μL/min for 60 s and allowed to dissociate for 300 s. Regeneration of flow cells was achieved by injecting one pulse each of 10 mM glycine pH 2.0 at a flow rate of 90 μL/min. Kinetic analyses were used after subtraction of reference curves to derive on/off rates (k_a/k_d) and binding constants (K_Ds) using a 1:1 binding model with or without bulk refractive index change (RI) correction as appropriate (Biacore T200 Evaluation software v3.0). Reported affinities represent the average of two independent experiments. SPR experiments that were not used to derive binding affinities or kinetic constants were done using a single high concentration (1 μM) to qualitatively determine binding versus no binding.

Analysis Software

Unless stated otherwise, Geneious Prime 2021.2.2, MacVector 18.2.0 and DNAStar SeqMan Pro 17.1.1 were used for sequence analysis and graphs were created using R language. Flow cytometry data were processed using Mac versions of FlowJo 10.7.2. and GraphPad Prism 9.3 and Microsoft Excel for Mac 16.54 were used for data analysis. Structural figures were made using PyMOL (Schrödinger, LLC) or ChimeraX (*109*). V(D)J gene assignments of NHP and murine antibodies were done using IMGT/V-QUEST (*108*). Sequence alignments were done using Clustal Omega (*110*).

Figs. S1 to S8

A **HC**

```
                 ————————————FR1————————— —CDRH1— ——FR2—— ———CDRH2——— ——————————————FR3——————————— ————CDRH3———— ——FR4——
                    5   10   15   20   25   30   35   40   45   50   55   60   65   70   75        80   85   90   95        100  105  110
                    •    •    •    •    •    •    •    •    •    •    •    •    •    •    •         •    •    •    •         •    •    •
VH1-2*02        QVQLVQSGAEVKKPGASVKVSCKASGYTF-TGYYMHWVRQAPGQGLEWMGWINPNSGGTNY-AQKFQGRVTMTRDTSI----STAYMELSRLRSDDTAVYYCAR-----------------------------
IOMA            E....E...Q.......T...T....K.....H........R..........FR.AVK..P.N.R...S......M....EIF.......T...........EMFDS..SADWSPWRGMVAWGQGTLVTVSS
VRC01           ........GQM....E.MRI..R....E..IDCTLN.I.L...KRP.....LK.RG.AV....RPL.........VYS....D..FL..RS.TV......F.T.GKNCD.......YNWDFEHWGRGTPVIVSS
```

LC

```
                 ————————————FR1———————— —CDRL1— ——FR2—— ———CDRL2——— ————————FR3————————— ——CDRL3—— ——FR4———
                    5   10   15   20   25   30        35   40   45   50   55   60   65   70   75   80   85   90   95   100  105  110
                    •    •    •    •    •    •         •    •    •    •    •    •    •    •    •    •    •    •    •    •    •    •
VL2-23*02       QSALTQ-PASVSGSPGQSITISCTGTSSDVGSYNLVSWYQQHPGKAPKLMIYEVSKRPSGVSNRFSGSKSGNTASLTISGLQAEDEADYYCCSYAGS---STF---------------
IOMA            ......-................A.S.R...GFD...............I....N.....I.S...A...............E....H...Y...DG---VA.GGGTKLT-VLGQPKA

VK3-20*01       EIVLTQSPGTLSLSPGERATLSCRASQSVSSSYLAWYQQKPGQAPRLLIYGASSRATGIPDRFSGSGSGTDFTLTISRLEPEDFAVYYCQQYG---SS------------------
VRC01           ................T.II...T..Y---GS......R.......V..SG.T..A.........RW.P.YN....N..SG..G.......E------FFGQGTKVQVDIKR---
```

B

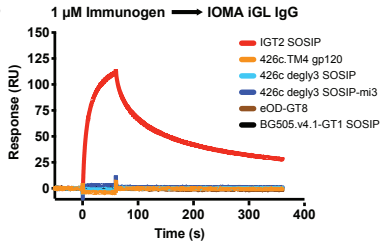

C

Virus	Clade	Tier	IC_{50} (μg/mL) IOMA	IC_{50} (μg/mL) IOMA iGL
QH0692.42	B	2	12.9	>100
SC422661.8	B	2	17.3	>100
PVO.4	B	3	0.5	>100
TRO.11	B	2	0.5	>100
RHPA4259.7	B	2	9.6	>100
THRO4156.18	B	2	29.7	>100
TRJO4551.58	B	3	11.7	>100
CAAN5342.A2	B	2	1.7	>100
WEAU_d15_410_787	B (T/F)	NC	3.0	>100
1006_11_C3_1601	B (T/F)	2	0.3	>100
1054_07_TC4_1499	B (T/F)	2	2.2	>100
1056_10_TA11_1826	B (T/F)	1	2.1	>100
1012_11_TC21_3257	B (T/F)	1	0.3	>100
6240_08_TA5_4622	B (T/F)	2	4.0	>100
6244_13_B5_4576	B (T/F)	2	0.6	>100
62357_14_D3_4589	B (T/F)	2	11.2	>100
SC05_8C11_2344	B (T/F)	2	1.5	>100
ZM214M.PL15	C	2	1.7	>100
Ce1086_B2	C (T/F)	2	0.6	>100
Ce1176_A3	C (T/F)	2	3.0	>100
Ce2010_F5	C (T/F)	3	20.4	>100
Ce0682_E4	C (T/F)	2	1.2	>100
7030102001ES(Rev-)	C (T/F)	2	13.3	>100
Ce704809221_1B3	C (T/F)	2	2.5	>100
CNE30	BC	NC	8.3	>100
CNE53	BC	NC	0.1	>100
0260.v5.c36	A	NC	1.6	>100
3415.v1.c1	A	2	0.7	>100
3365.v2.c2	A	2	5.0	>100
R1166.c01	CRF01_AE	NC	8.4	>100
C2101.c01	CRF01_AE	NC	1.5	>100
C3347.c11	CRF01_AE	NC	0.1	>100
BJOX025000.01.1	CRF01_AE (T/F)	NC	1.5	>100
BJOX028000.10.3	CRF01_AE (T/F)	NC	20.5	>100
P0402_c2_11	G	NC	16.0	>100
X1632_S2_B10	G	NC	0.6	>100
A07412M1.vrc12	D	NC	8.4	>100
3817.v2.c59	CD	NC	14.2	>100
3301.v1.c24	AC	NC	34.9	>100
MLV	–	–	>50	>50

<0.1 μg/mL | 0.1-0.99 μg/mL | 1-9.99 μg/mL | 10-50 μg/mL | >50 μg/mL

D 2.07Å IOMA iGL crystal structure

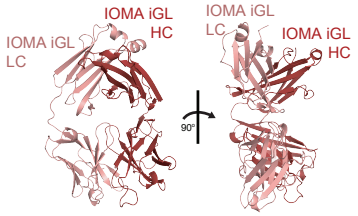

E Overlay of IOMA iGL & IOMA (PDB 5T3Z) RMSD – 0.64Å

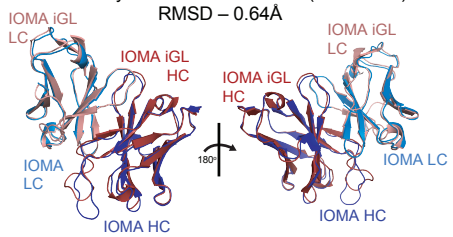

F

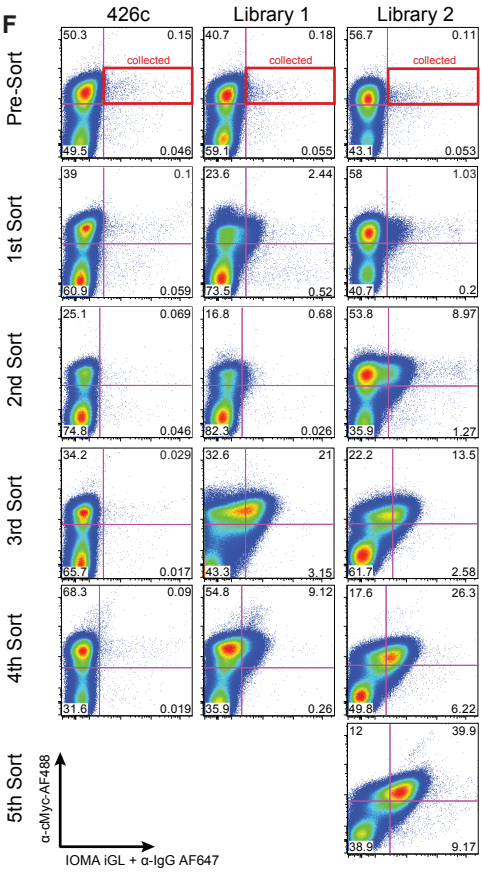

G

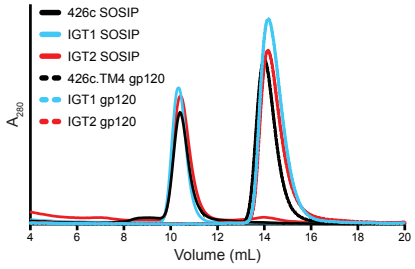

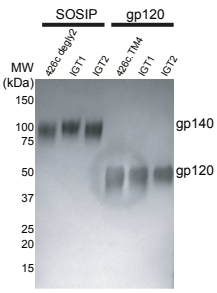

H

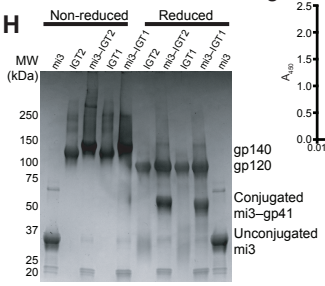

I

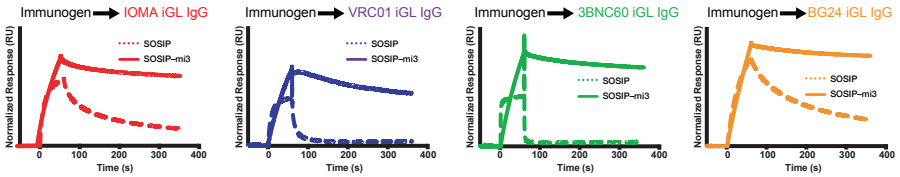

J

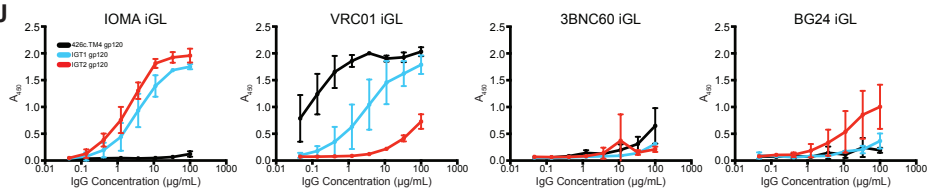

Figure S1. Development and characterization of IGT1 and IGT2 immunogens. (A) Amino acid alignment of IOMA and VRC01 to their respective germline V genes. **(B)** Representative SPR sensorgrams demonstrating no detectable binding of IOMA iGL to previously described immunogens (eOD-GT8, 426c.TM4, BG505.v4.1-GT1). This experiment was performed to qualitatively evaluate binding of IGT2 and previously described CD4bs immunogens to IOMA iGL rather than to derive affinity or kinetic constants. **(C)** Neutralization titers (IC_{50}s) of IOMA and IOMA iGL against a panel of 38 viruses and an MLV control. **(D)** 2.07 Å crystal structure of IOMA iGL Fab shown in two views. **(E)** Structural overlay of IOMA iGL Fab and IOMA Fab from BG505-bound structure (PDB 5T3Z).**(F)** Flow cytometric analysis of yeast cells expressing 426c.TM4 starting protein (left), Library 1 (middle), or Library 2 (right) stained with IOMA iGL IgG/anti-IgG AF647 (x-axis) and anti-cMyc AF488 (y-axis). **(G)** Representative size exclusion chromatography profiles and Coomassie-stained SDS-PAGE analysis for 426c.TM4 gp120, IGT1 gp120, and IGT2 gp120, 426c SOSIP, IGT1 SOSIP, and IGT2 SOSIP demonstrating that all of these proteins are monodispersed samples and that the selected mutations do not alter the stability or behavior of the immunogens compared to the starting proteins. **(H)** Coomassie-stained SDS–PAGE analysis for mi3, IGT2, IGT2-mi3, IGT1, and IGT1-mi3 under non-reducing and reducing conditions. **(I)** SPR sensorgrams demonstrating binding of IGT2 (dashed line) and IGT2-mi3 (solid line) to IOMA iGL IgG (red), VRC01 iGL IgG (purple), 3BNC60 iGL IgG (green), and BG24 iGL IgG (orange). IgG was immobilized to the CM5 chip and 1 μM SOSIP or 1 μM SOSIP-mi3 was flowed over the chip surface. **(J)** Representative ELISA binding curves measuring binding of 426c.TM4 gp120, IGT1 gp120, and IGT2 gp120 to the same iGL IgGs as in (I). Dots indicate mean and error bars indicate 95% confidence interval.

Figure S2

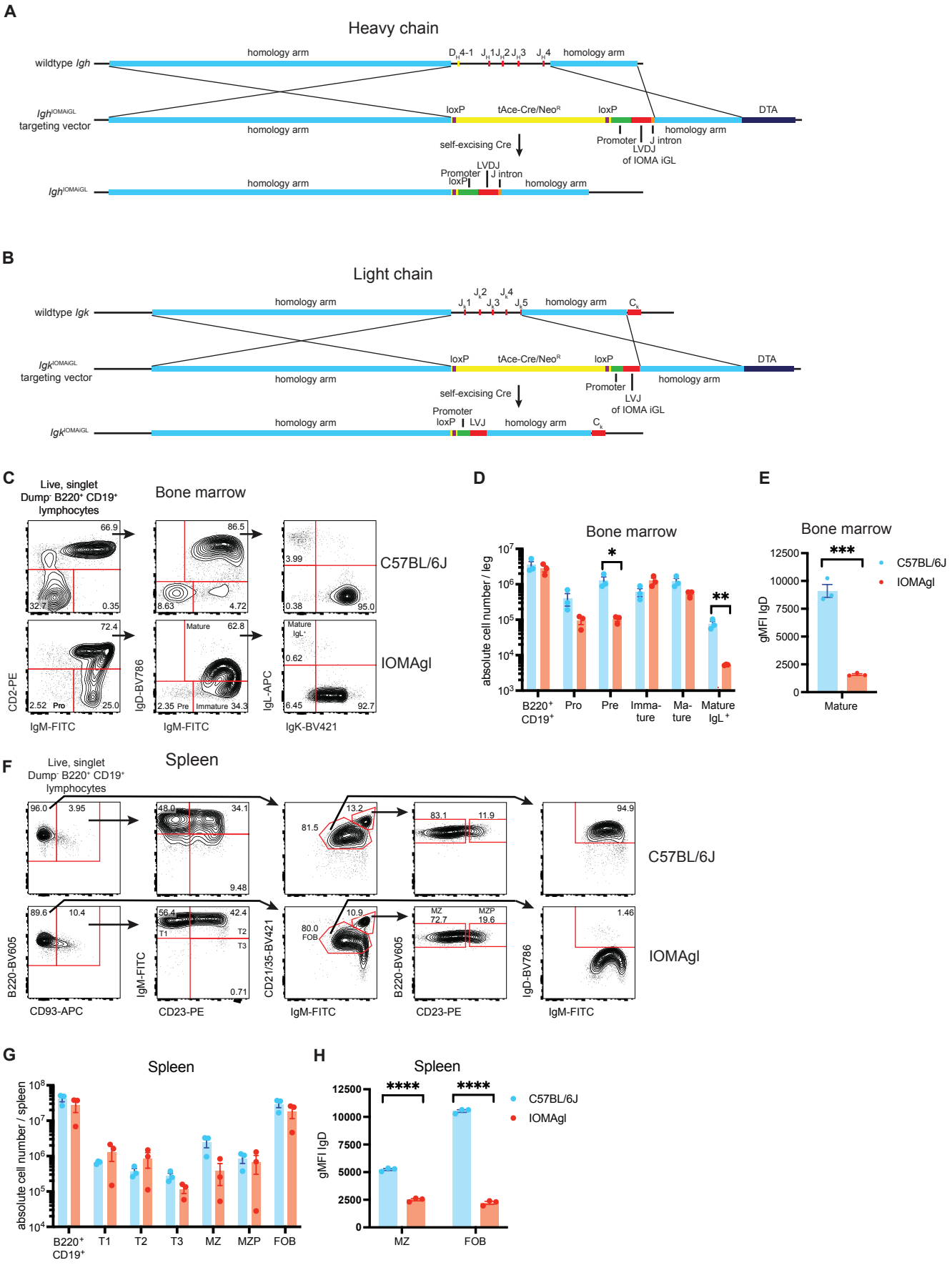
A
Heavy chain
wildtype Igh
homology arm
DH4-1 JH1 JH2 JH3 JH4
homology arm
IghIOMAiGL targeting vector
loxP
tAce-Cre/NeoR
loxP
DTA
homology arm
homology arm
Promoter
J intron
LVDJ of IOMA iGL
self-excising Cre
Promoter
LVDJ
J intron
loxP
IghIOMAiGL
homology arm
homology arm
B
Light chain
wildtype Igk
homology arm
Jk1 Jk2 Jk3 Jk4 Jk5
homology arm
Ck
IgkIOMAiGL targeting vector
loxP
tAce-Cre/NeoR
loxP
DTA
homology arm
homology arm
Promoter
LVJ of IOMA iGL
self-excising Cre
Promoter
loxP
LVJ
homology arm
homology arm
Ck
IgkIOMAiGL
C
Live, singlet Dump- B220+ CD19+ lymphocytes
Bone marrow
66.9
32.7
0.35
86.5
8.63
4.72
3.99
0.38
95.0
C57BL/6J
72.4
2.52 Pro
25.0
Mature
62.8
2.35 Pre
Immature 34.3
Mature IgL+
0.62
6.45
92.7
IOMAgl
CD2-PE
IgM-FITC
IgD-BV786
IgM-FITC
IgL-APC
IgK-BV421
D
Bone marrow
absolute cell number / leg
B220+ CD19+
Pro
Pre
Imma-ture
Ma-ture
Mature IgL+
*
**
E
Bone marrow
gMFI IgD
Mature
***
C57BL/6J
IOMAgl
F
Live, singlet Dump- B220+ CD19+ lymphocytes
Spleen
96.0
3.95
48.0
34.1
9.48
81.5
13.2
83.1
11.9
94.9
C57BL/6J
89.6
10.4
56.4
42.4
T1
T2
T3
0.71
80.0 FOB
10.9
MZ 72.7
MZP 19.6
1.46
IOMAgl
B220-BV605
CD93-APC
IgM-FITC
CD23-PE
CD21/35-BV421
IgM-FITC
B220-BV605
CD23-PE
IgD-BV786
IgM-FITC
G
Spleen
absolute cell number / spleen
B220+ CD19+
T1
T2
T3
MZ
MZP
FOB
H
Spleen
gMFI IgD
****
****
C57BL/6J
IOMAgl
MZ
FOB

Figure S2. Targeting strategy and characterization of IOMAgl mice. (A) In *Igh*^{IOMAiGL} mice *Ighd4-1* to *Ighj4* are replaced by a self-excising Neomycin cassette followed by the mouse *Ighv9-4* promoter, a leader sequence (L) followed by the iGL version of the IOMA HC VDJ sequence and a *Ighj1* splice donor sequence. **(B)** In *Igk*^{IOMAiGL} mice *Igkj1* to *Igkj5* are replaced by a self-excising Neomycin cassette followed by a mouse *Igkv3-12* promoter, a leader sequence followed by the iGL version of the IOMA lambda LC VDJ sequence and a *Igkj5* splice donor sequence. DTA, diphtheria toxin A **(C)** Flow cytometric analysis of B cell development in the bone marrow of control (C57BL/6J) or IOMAgl (*Igh*$^{IOMAiGL/IOMAiGL}$ *Igk*$^{IOMAiGL/IOMAiGL}$) mice. **(D)** Absolute cell number quantification from (C). **(E)** Geometric mean fluorescence intensity (gMFI) of IgD in mature recirculating B cells from the bone marrow. **(F)** Flow cytometric analysis of peripheral B cell development in the spleens of control (C57BL/6J) or IOMAgl mice. **(G)** Absolute cell number quantification from (F). **(H)** gMFI of IgD in marginal zone and follicular B cell. MZ, marginal zone B cells; MZP, marginal zone precursors; FOB, follicular B cells. Data from 1 of 2 independent experiments, each dot represents a data from 1 mouse. Bars represent mean ± SEM. Statistical analysis used unpaired t test.

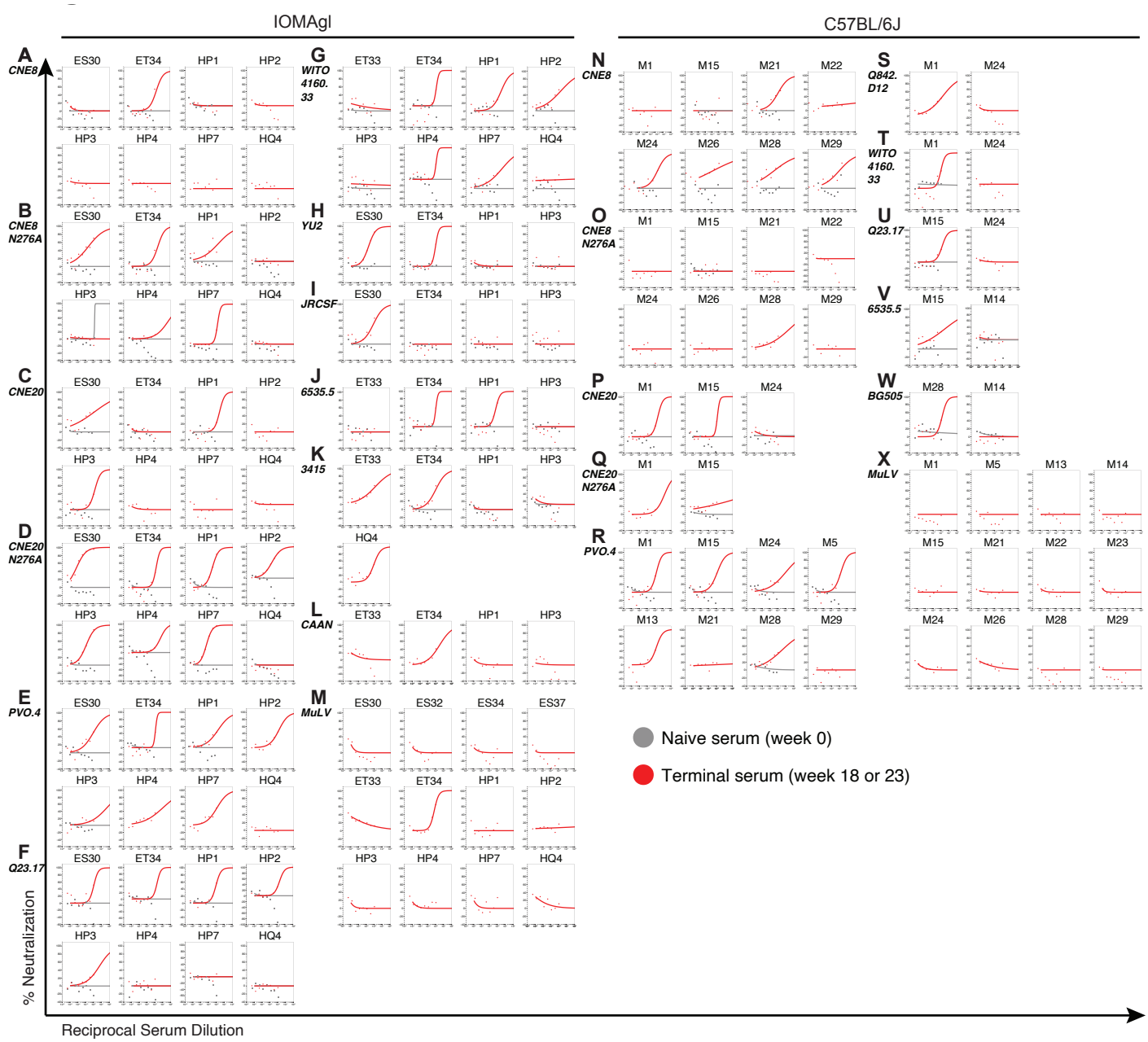

Figure S3. Serum neutralization from immunized mice. Neutralization curves of serum isolated from IOMA iGL transgenic mice (**A-M**) or C57BL/6J wildtype mice (**N-X**) against the following HIV strains or control MuLV: **(A,N)** CNE8, **(B,O)** CNE8 N276A, **(C,P)** CNE20, **(D,Q)** CNE20 N276A, **(E,R)** PVO.4, **(F,U)** Q23.17, **(G,T)** WITO4160.33, **(H)** YU2, **(I)** JRCSF, **(J, V)** 6535.5, **(K)** 3415_V1_C1, **(L)** CAAN5342.A2, **(M,X)** MuLV, (**S**) Q842.D12 and (**W**) BG505. Naïve serum was also tested against the same strains when available. Note that sera which showed neutralization activity of < 40% as listed in Table S3 are presented in Figure 2G as white rectangles; several of these sera neutralized strains above background including ET33 against PVO.4; ET34 against CNE20 N276A and Q23.17; HP1 against CNE8 N276A, CNE20, and WITO4160.33; HP2 against Q23.17; HP3 against Q23.17 and PVO.4; HP4 against CNE8 N276A, CNE20 N276A, and PVO.4.

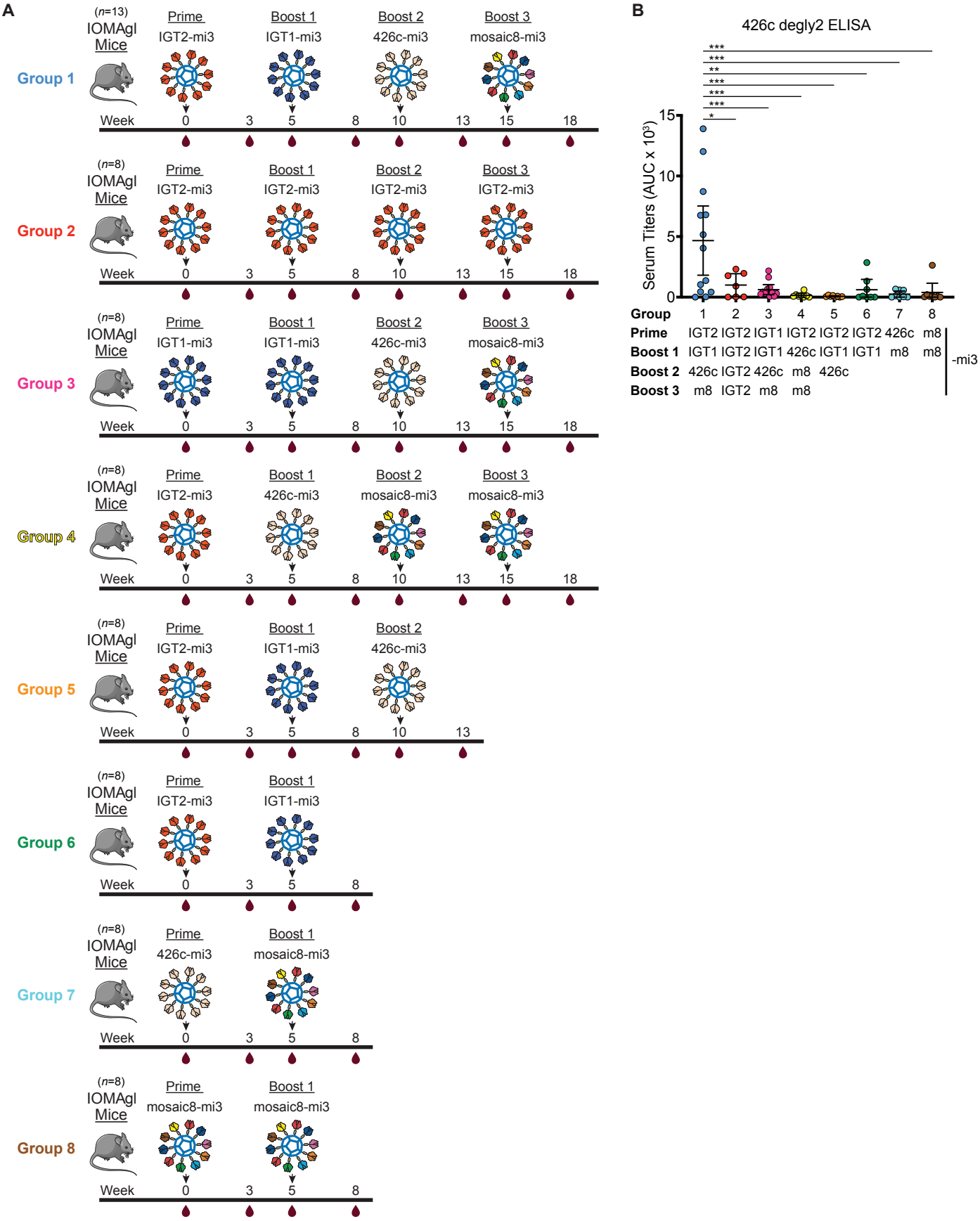
A
(n=13)
IOMAgI Mice
Group 1
Prime IGT2-mi3
Boost 1 IGT1-mi3
Boost 2 426c-mi3
Boost 3 mosaic8-mi3
Week 0 3 5 8 10 13 15 18
(n=8)
IOMAgI Mice
Group 2
Prime IGT2-mi3
Boost 1 IGT2-mi3
Boost 2 IGT2-mi3
Boost 3 IGT2-mi3
Week 0 3 5 8 10 13 15 18
(n=8)
IOMAgI Mice
Group 3
Prime IGT1-mi3
Boost 1 IGT1-mi3
Boost 2 426c-mi3
Boost 3 mosaic8-mi3
Week 0 3 5 8 10 13 15 18
(n=8)
IOMAgI Mice
Group 4
Prime IGT2-mi3
Boost 1 426c-mi3
Boost 2 mosaic8-mi3
Boost 3 mosaic8-mi3
Week 0 3 5 8 10 13 15 18
(n=8)
IOMAgI Mice
Group 5
Prime IGT2-mi3
Boost 1 IGT1-mi3
Boost 2 426c-mi3
Week 0 3 5 8 10 13
(n=8)
IOMAgI Mice
Group 6
Prime IGT2-mi3
Boost 1 IGT1-mi3
Week 0 3 5 8
(n=8)
IOMAgI Mice
Group 7
Prime 426c-mi3
Boost 1 mosaic8-mi3
Week 0 3 5 8
(n=8)
IOMAgI Mice
Group 8
Prime mosaic8-mi3
Boost 1 mosaic8-mi3
Week 0 3 5 8
B
426c degly2 ELISA
Serum Titers (AUC x 10³)
15
10
5
0
***
***
**
***
***
***
*
Group 1 2 3 4 5 6 7 8
Prime IGT2 IGT2 IGT1 IGT2 IGT2 IGT2 426c m8
Boost 1 IGT1 IGT2 IGT1 426c IGT1 IGT1 m8 m8
Boost 2 426c IGT2 426c m8 426c
Boost 3 m8 IGT2 m8 m8
-mi3

Figure S4. Screening immunization regimens to determine the optimal boosting strategy. (A) Schematic and timeline of immunization strategies to determine the optimal regimen to elicit IOMA-like bNAbs. **(B)** Serum ELISA binding to 426c degly2 represented as AUC using serum samples isolated from mice at the end of the regimen. m8, mosaic8.

Figure S5

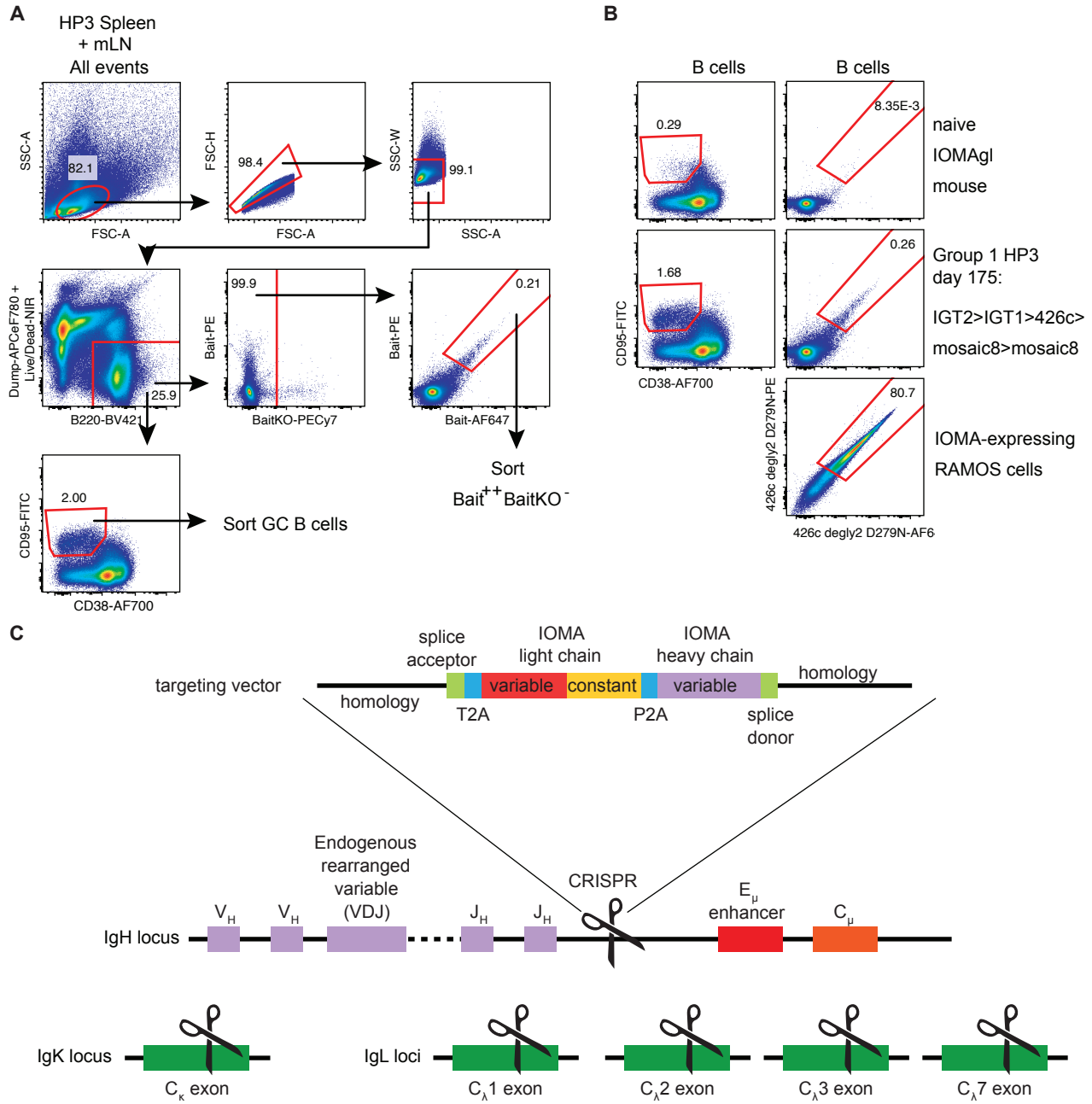

Figure S5. Cell sorting strategies and sorting controls. (A) Representative full gating of cell sorts for single cell Bait++ BaitKO^{-} B cell cloning and 10x Genomics next generation VDJ sequencing of bulk-sorted GC B cells from splenic and mesenteric lymph nodes. Baits used were 426c degly2 D279N or CNE8 N276A with 426c degly2 D279N-CD4bs KO, the former is shown. **(B)** Induction of germinal center response and wt SOSIP-binding cells by immunization regimen (group 1). Naïve IOMAgl mouse splenocytes and IOMA-expressing RAMOS cells served as negative and positive control, respectively. (**C**) Gene editing strategy to generate IOMA-expressing RAMOS cells.

Simultaneous targeting of IgH, IgK and IgL loci with CRISPR/Cas9 to delete endogenous LCs and edit a promoterless tricistronic expression cassette into the IgH locus to express IOMA on the surface of RAMOS cells. A polycistronic mRNA was created using T2A and P2A sequences to induce ribosomal skipping (*96*).


A
Color code
Identity
100 %
<100 - 30 %
<30 %
Kabat #
Mouse
Sorted Population
Identity [%]
Antibody ID
IOMA
IOMA IGL
Domains
CDRH1
CDRH2
CDRH3
Structurally important residues

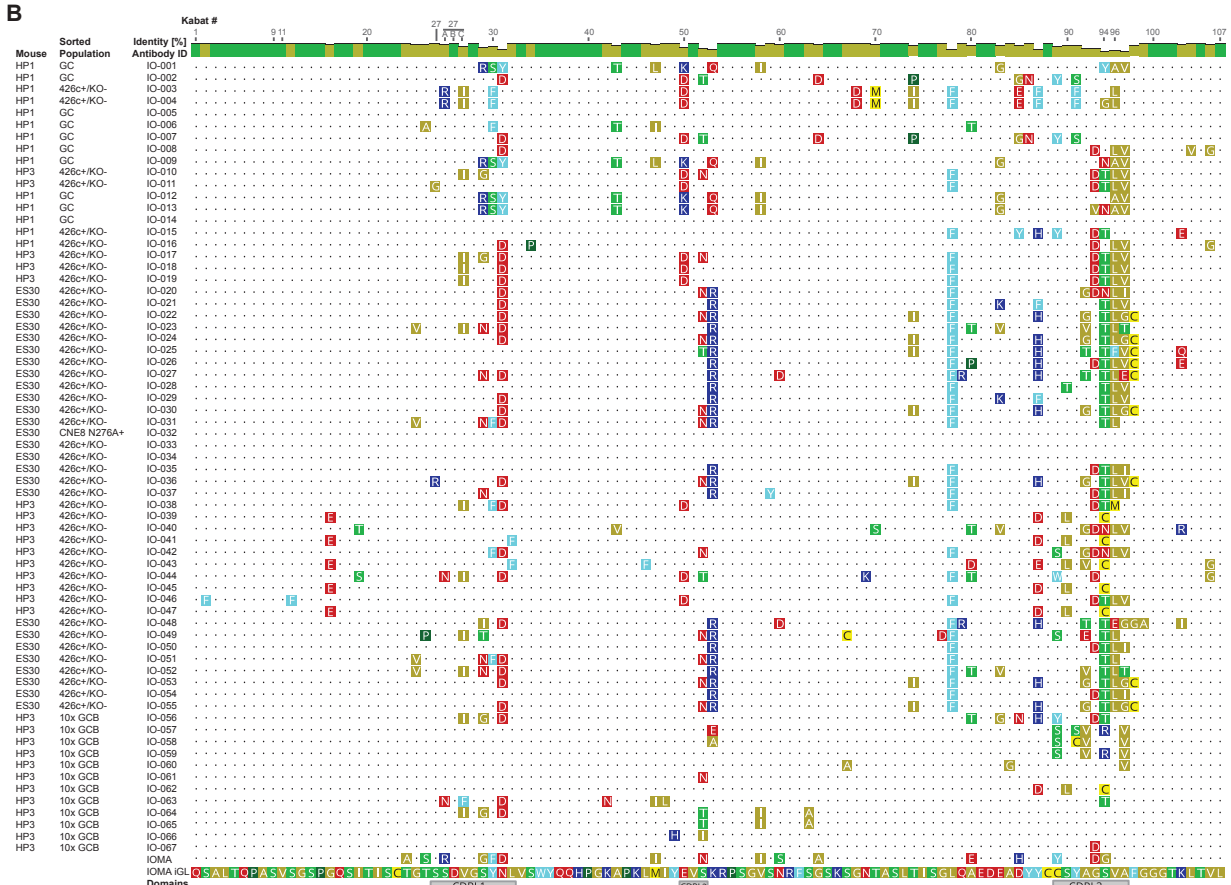
B
Kabat #
Mouse
Sorted Population
Identity [%]
Antibody ID
IOMA
IOMA IGL
Domains
CDRL1
CDRL2
CDRL3
Structurally important residues

Figure S6. Amino acid alignments of selected IOMAgl mouse-derived antibodies. (A) V_H alignment of cloned antibodies IO-001 to IO-067 that were expressed and tested for Env binding. IOMA iGL and IOMA sequence at the bottom as reference. Mouse ID and population sorted are indicated. Differences to IOMA iGL are highlighted using chemically similar color coding; dots indicate identical residues to IOMA iGL. Kabat numbering and percent identity of residues are indicated on top. Domains and residues of structural importance are annotated below. **(B)** as above but corresponding V_L alignment.

Figure S7

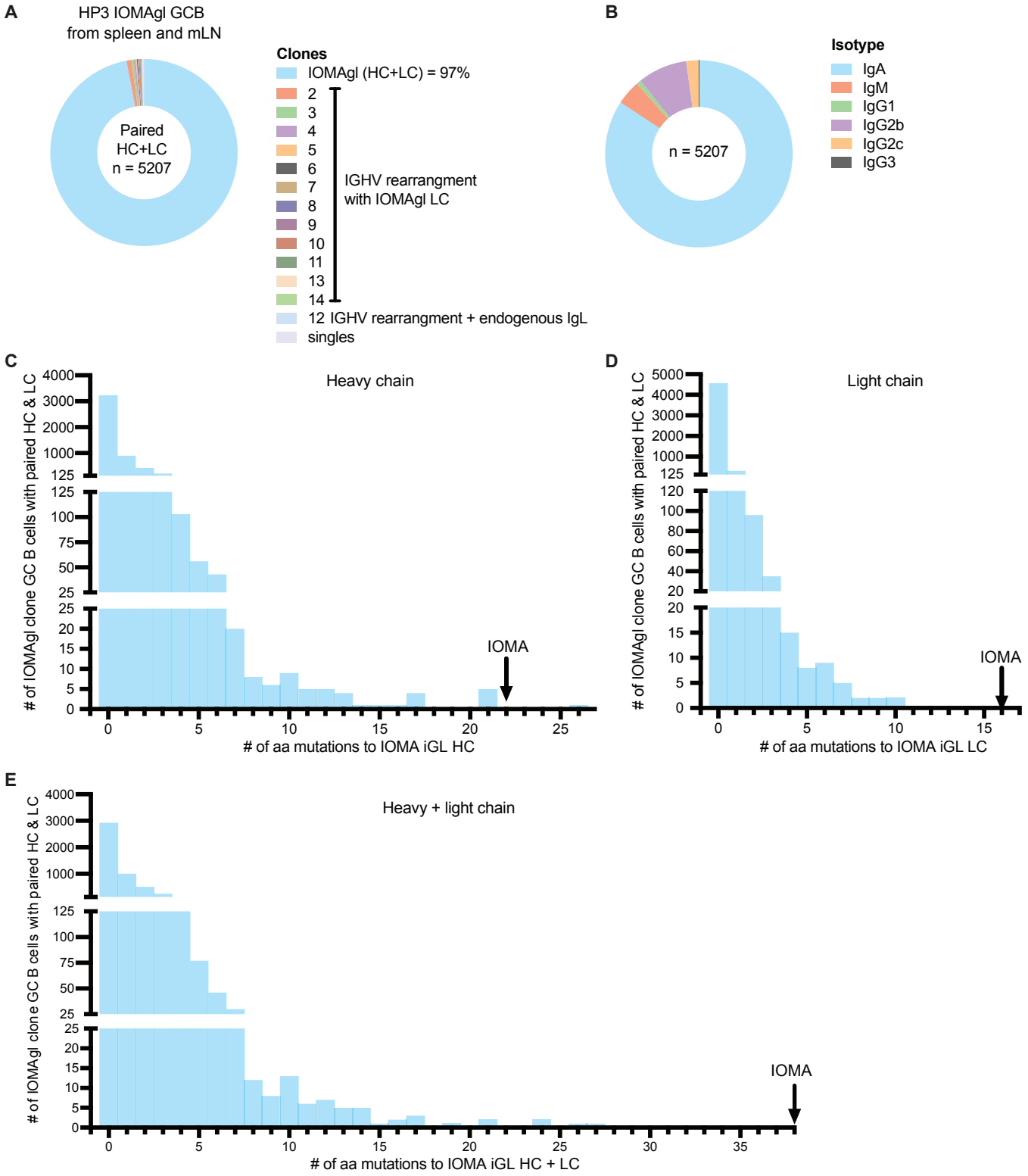

Figure S7. Next generation single cell VDJ analysis determines the extent of mutations in germinal centers of IOMAgl mice. (A) Clonal analysis of paired HC and LC sequences from splenic and mesenteric lymph node germinal center B cells of IOMAgl mouse HP3. **(B)** Isotype distribution among these cells. **(C)** Frequency distribution of the number of amino acid mutations to IOMA iGL in

the HC sequences of these cells. **(D)** Frequency distribution of the number of amino acid mutations to IOMA iGL in the LC sequences of these cells. **(E)** Frequency distribution of the number of amino acid mutations to IOMA iGL in the paired HC and LC sequences of these cells.

A

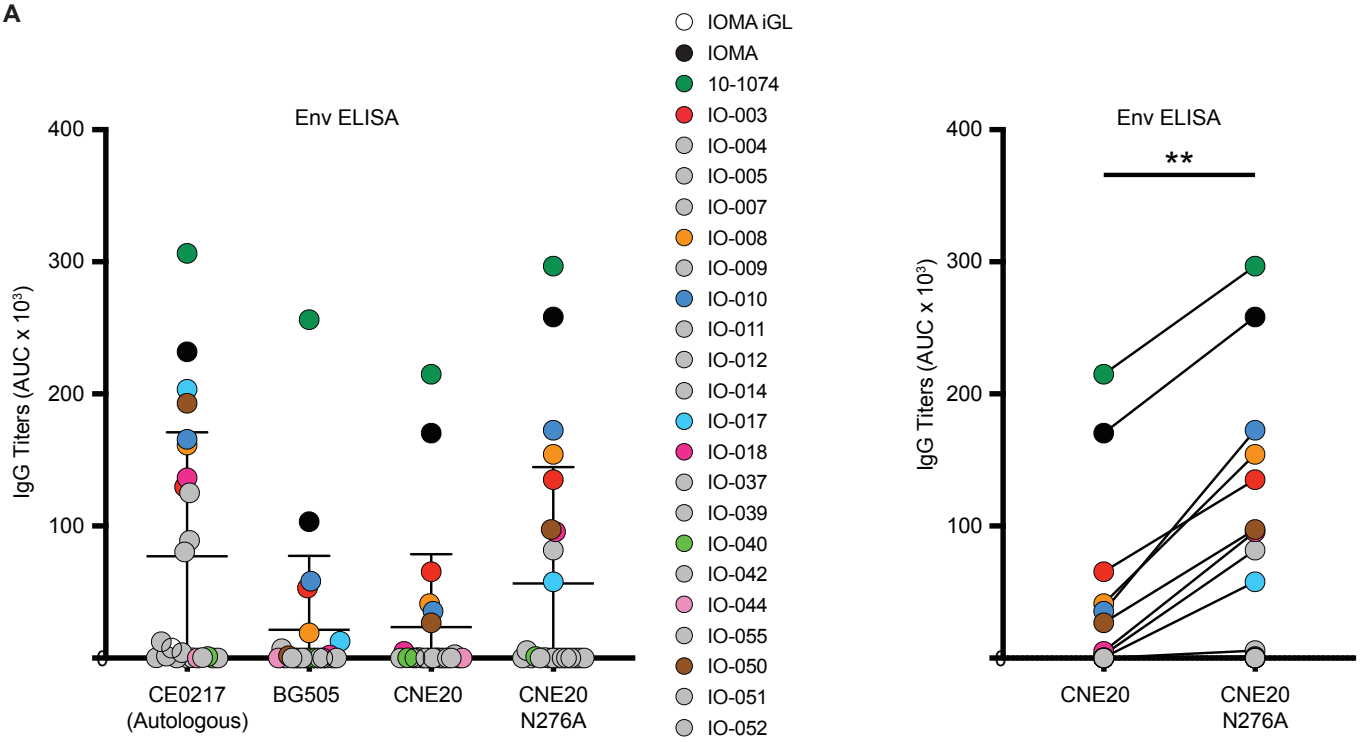

B

Reference		This Study	Chen et al, *Immunity* 2021			
Immunogen		IGT2-mi3	eOD-GT6 60mer		eOD-GT8 60mer	
Immunizations		4 or 5	6	9	4	9
Residue	SHM					
Heavy Chain						
K19	T/R	67	N/A	N/A	N/A	N/A
Y33	H/D/E/F (V/F/L/I)	58	7.5	56	25	85
V37	(M/L/I)	N/A	3.7	23	7.50	52
N52	(K/R)	N/A	0	9.3	4.3	23
N53	F/Y/K/R/T (Y/K/R/T/V/L)	73	31	56	20	65
S54	R/F/N/T (R/F/N/T/Y/W/H/G)	82	41	65	46	88
G56	A (A)	30	1.5	40	2.2	54
T57	V/I/P/R (V/I/P/R)	66	13	67	12	88
N58	K/E/D	58	N/A	N/A	N/A	N/A
Q61	(R/H/K/W)	N/A	13	40	37	58
V89	(L/I/M/T)	N/A	4.5	26	5.9	77
Light Chain						
CDR L1	(deletion)	N/A	2.6	21	0	15
CDR L1	(G/S)	N/A	11.8	47	0	69
Q27	(Y/F/H)	N/A	0	5.3	7.2	17
S27A	R/N (F/Y)	5.9	0	18	0	17
S31	G	6.0	N/A	N/A	N/A	N/A
Y32	F	10	N/A	N/A	N/A	N/A
N33	D	42	N/A	N/A	N/A	N/A
G93	D	33	N/A	N/A	N/A	N/A
Average # Key SHMs per HC		4.3	1.6	3.8	1.6	6.5

Figure S8. Monoclonal antibodies cloned from IOMA iGL transgenic mice bind to heterologous Envs. (A) AUC of ELISA binding curves of selected monoclonal antibodies isolated from IOMA iGL knock-in mice to BG505, CE0217, CNE20 and CNE20 N276A SOSIPs. **(B)** Comparison of the occurrence frequency of key mutations among IOMA-like antibody sequences selected for cloning and VRC01-class antibody sequences from reference 37 at different time points throughout the respective sequential immunization regimen. Mutations essential for IOMA-class antibody binding to gp120 are listed first, while mutations essential for VRC01-class antibody binding to gp120 are listed second in brackets. Values for each residue represent the percentage of antibodies containing one of the essential mutations at that position.

Tables S1 to S8

Table S1: Amino acid sequences for HIV Envs and antibodies used in this study.

Protein Name	Sequence
IGT2 gp120	VWKEAKTTLFCASDAKAYEKECHNVWATHACVPTDPNPQEVVLENVTENFNMWKNDMVDQMQEDVISIWDQ CLKPCVKLTNTSTLTQACPKVTFDPIPIHYCAPAGYAILKCNNKTFNGKGPCNNVSTVQCTHGIKPVVSTQ LLLNGSLAEEEIVIRSKNLRNNAKIIIVQLNKSVEIVCTRPNNGGSGSGGDIRQAYCNISGRNWSEAVNQV KKKLKEHFPHKNISFQSSSGGDLEITTHSFNCGGEFFYCNTSGLFNDTISNATIMLPCRIKQIINMWQEPG KAIYAPPIKGNITCKSDITGLLLLRDGGNALRPTEIFRPSGGDMRDNWRSELYKYKVVEIKPLHHHHHH
IGT1 gp120	VWKEAKTTLFCASDAKAYEKECHNVWATHACVPTDPNPQEVVLENVTENFNMWKNDMVDQMQEDVISIWDQ CLKPCVKLTNTSTLTQACPKVTFDPIPIHYCAPAGYAILKCNNKTFNGKGPCNNVSTVQCTHGIKPVVSTQ LLLNGSLAEEEIVIRSKNLRNNAKIIIVQLNKSVEIVCTRPNNGGSGSGGDIRQAYCNISGRNWSEAVNQV KKKLKEHFPHKNISFQSSSGGDLEITTHSFNCGGEFFYCNTSGLFNDTISNATIMLPCRIKQIINMWQEPG KAIYAPPIKGNITCKSDITGLLLLRDGGNSQRETEIFRPSGGDMRDNWRSELYKYKVVEIKPLHHHHHH
426c.TM4 gp120	VWKEAKTTLFCASDAKAYEKECHNVWATHACVPTDPNPQEVVLENVTENFNMWKNDMVDQMQEDVISIWDQ CLKPCVKLTNTSTLTQACPKVTFDPIPIHYCAPAGYAILKCNNKTFNGKGPCNNVSTVQCTHGIKPVVSTQ LLLNGSLAEEEIVIRSKNLRDNAKIIIVQLNKSVEIVCTRPNNGGSGSGGDIRQAYCNISGRNWSEAVNQV KKKLKEHFPHKNISFQSSSGGDLEITTHSFNCGGEFFYCNTSGLFNDTISNATIMLPCRIKQIINMWQEVG KAIYAPPIKGNITCKSDITGLLLLRDGGDTTDNTEIFRPSGGDMRDNWRSELYKYKVVEIKPLHHHHHH
IGT2 SOSIP	GSNLWVTVYYGVPVWKEAKTTLFCASDAKAYEKEVHNVWATHACVPTDPNPQEVVLENVTENFNMWKNDMV DQMQEDVISIWDQSLKPCVKLTPLCVTLNCTNVNVTSNSTNVNSSSTDNTTLGEIKNCSFDITTEIRDKTR KEYALFYRLDIVPLDNSSNPNSSNTYRLINCNTSTCTQACPKVTFDPIPIHYCAPAGYAILKCNNKTFNGK GPCNNVSTVQCTHGIKPVVSTQLLLNGSLAEEEIVIRSKNLRNNAKIIIVQLNKSVEIVCTRPNNNTRRSI RIGPGQTFYATDIIGDIRQAYCNISGRNWSEAVNQVKKKLKEHFPHKNISFQSSSGGDLEITTHSFNCGGE FFYCNTSGLFNDTISNATIMLPCRIKQIINMWQEVGKCIYAPPIKGNITCKSDITGLLLLRDGGNALRPTE IFRPSGGDMRDNWRSELYKYKVVKIEPLGVAPTRCKRRVVGRRRRRRAVGIGAVFLGFLGAAGSTMGAASM TLTVQARNLLSGIVQQQSNLLRAPEAQQHLLKLTVWGIKQLQARVLAVERYLRDQQLLGIWGCSGKLICCT NVPWNSSWSNRNLSEIWDNMTWLQWDKEISNYTQIIYGLLEESQNQQEKNEQDLLALD
IGT1 SOSIP	GSNLWVTVYYGVPVWKEAKTTLFCASDAKAYEKEVHNVWATHACVPTDPNPQEVVLENVTENFNMWKNDMV DQMQEDVISIWDQSLKPCVKLTPLCVTLNCTNVNVTSNSTNVNSSSTDNTTLGEIKNCSFDITTEIRDKTR KEYALFYRLDIVPLDNSSNPNSSNTYRLINCNTSTCTQACPKVTFDPIPIHYCAPAGYAILKCNNKTFNGK GPCNNVSTVQCTHGIKPVVSTQLLLNGSLAEEEIVIRSKNLRNNAKIIIVQLNKSVEIVCTRPNNNTRRSI RIGPGQTFYATDIIGDIRQAYCNISGRNWSEAVNQVKKKLKEHFPHKNISFQSSSGGDLEITTHSFNCGGE FFYCNTSGLFNDTISNATIMLPCRIKQIINMWQEVGKCIYAPPIKGNITCKSDITGLLLLRDGGNSQRETE IFRPSGGDMRDNWRSELYKYKVVKIEPLGVAPTRCKRRVVGRRRRRRAVGIGAVFLGFLGAAGSTMGAASM TLTVQARNLLSGIVQQQSNLLRAPEAQQHLLKLTVWGIKQLQARVLAVERYLRDQQLLGIWGCSGKLICCT NVPWNSSWSNRNLSEIWDNMTWLQWDKEISNYTQIIYGLLEESQNQQEKNEQDLLALD
426c SOSIP	AENLWVTVYYGVPVWKEAKTTLFCASDAKAYEKEVHNVWATHACVPTDPNPQEVVLENVTENFNMWKNDMV DQMQEDVISIWDQSLKPCVKLTPLCVTLNCTNVNVTSNSTNVNSSSTDNTTLGEIKNCSFDITTEIRDKTR KEYALFYRLDIVPLDNSSNPNSSNTYRLINCNTSTCTQACPKVTFDPIPIHYCAPAGYAILKCNNKTFNGK GPCNNVSTVQCTHGIKPVVSTQLLLNGSLAEEEIVIRSKNLSDNAKIIIVQLNKSVEIVCTRPNNNTRRSI RIGPGQTFYATDIIGDIRQAYCNISGRNWSEAVNQVKKKLKEHFPHKNISFQSSSGGDLEITTHSFNCGGE FFYCNTSGLFNDTISNATIMLPCRIKQIINMWQEVGKCIYAPPIKGNITCKSDITGLLLLRDGGNTTNNTE IFRPGGGDMRDNWRSELYKYKVVKIEPLGVAPTRCKRRVVGRRRRRRAVGIGAVFLGFLGAAGSTMGAASM TLTVQARNLLSGIVQQQSNLLRAPEAQQHLLKLTVWGIKQLQARVLAVERYLRDQQLLGIWGCSGKLICCT NVPWNSSWSNRNLSEIWDNMTWLQWDKEISNYTQIIYGLLEESQNQQEKNEQDLLALD
426c D279N SOSIP	AENLWVTVYYGVPVWKEAKTTLFCASDAKAYEKEVHNVWATHACVPTDPNPQEVVLENVTENFNMWKNDMV DQMQEDVISIWDQSLKPCVKLTPLCVTLNCTNVNVTSNSTNVNSSSTDNTTLGEIKNCSFDITTEIRDKTR KEYALFYRLDIVPLDNSSNPNSSNTYRLINCNTSTCTQACPKVTFDPIPIHYCAPAGYAILKCNNKTFNGK GPCNNVSTVQCTHGIKPVVSTQLLLNGSLAEEEIVIRSKNLSNNAKIIIVQLNKSVEIVCTRPNNNTRRSI RIGPGQTFYATDIIGDIRQAYCNISGRNWSEAVNQVKKKLKEHFPHKNISFQSSSGGDLEITTHSFNCGGE FFYCNTSGLFNDTISNATIMLPCRIKQIINMWQEVGKCIYAPPIKGNITCKSDITGLLLLRDGGNTTNNTE IFRPGGGDMRDNWRSELYKYKVVKIEPLGVAPTRCKRRVVGRRRRRRAVGIGAVFLGFLGAAGSTMGAASM TLTVQARNLLSGIVQQQSNLLRAPEAQQHLLKLTVWGIKQLQARVLAVERYLRDQQLLGIWGCSGKLICCT NVPWNSSWSNRNLSEIWDNMTWLQWDKEISNYTQIIYGLLEESQNQQEKNEQDLLALD

426c degly2 SOSIP	AENLWVTVYYGVPVWKEAKTTLFCASDAKAYEKEVHNVWATHACVPTDPNPQEVVLENVTENFNMWKNDMV DQMQEDVISIWDQSLKPCVKLTPLCVTLNCTNVNVTSNSTNVNSSSTDNTTLGEIKNCSFDITTEIRDKTR KEYALFYRLDIVPLDNSSNPNSSNTYRLINCNTSTCTQACPKVTFDPIPIHYCAPAGYAILKCNNKTFNGK GPCNNVSTVQCTHGIKPVVSTQLLLNGSLAEEEIVIRSKNLTDNAKIIIVQLNKSVEIVCTRPNNNTRRSI RIGPGQTFYATDIIGDIRQAYCNISGRNWSEAVNQVKKKLKEHFPHKNISFQSSSGGDLEITTHSFNCGGE FFYCNTSGLFNDTISNATIMLPCRIKQIINMWQEVGKCIYAPPIKGNITCKSDITGLLLLRDGGNTANNAE IFRPGGGDMRDNWRSELYKYKVVKIEPLGVAPTRCKRRVVGRRRRRRAVGIGAVFLGFLGAAGSTMGAASM TLTVQARNLLSGIVQQQSNLLRAPEAQQHLLKLTVWGIKQLQARVLAVERYLRDQQLLGIWGCSGKLICCT NVPWNSSWSNRNLSEIWDNMTWLQWDKEISNYTQIIYGLLEESQNQQEKNEQDLLALD
426c degly2 D279N SOSIP	AENLWVTVYYGVPVWKEAKTTLFCASDAKAYEKEVHNVWATHACVPTDPNPQEVVLENVTENFNMWKNDMV DQMQEDVISIWDQSLKPCVKLTPLCVTLNCTNVNVTSNSTNVNSSSTDNTTLGEIKNCSFDITTEIRDKTR KEYALFYRLDIVPLDNSSNPNSSNTYRLINCNTSTCTQACPKVTFDPIPIHYCAPAGYAILKCNNKTFNGK GPCNNVSTVQCTHGIKPVVSTQLLLNGSLAEEEIVIRSKNLTNNAKIIIVQLNKSVEIVCTRPNNNTRRSI RIGPGQTFYATDIIGDIRQAYCNISGRNWSEAVNQVKKKLKEHFPHKNISFQSSSGGDLEITTHSFNCGGE FFYCNTSGLFNDTISNATIMLPCRIKQIINMWQEVGKCIYAPPIKGNITCKSDITGLLLLRDGGNTANNAE IFRPGGGDMRDNWRSELYKYKVVKIEPLGVAPTRCKRRVVGRRRRRRAVGIGAVFLGFLGAAGSTMGAASM TLTVQARNLLSGIVQQQSNLLRAPEAQQHLLKLTVWGIKQLQARVLAVERYLRDQQLLGIWGCSGKLICCT NVPWNSSWSNRNLSEIWDNMTWLQWDKEISNYTQIIYGLLEESQNQQEKNEQDLLALD
426c degly3 SOSIP	AENLWVTVYYGVPVWKEAKTTLFCASDAKAYEKEVHNVWATHACVPTDPNPQEVVLENVTENFNMWKNDMV DQMQEDVISIWDQSLKPCVKLTPLCVTLNCTNVNVTSNSTNVNSSSTDNTTLGEIKNCSFDITTEIRDKTR KEYALFYRLDIVPLDNSSNPNSSNTYRLINCNTSTCTQACPKVTFDPIPIHYCAPAGYAILKCNNKTFNGK GPCNNVSTVQCTHGIKPVVSTQLLLNGSLAEEEIVIRSKALTDNAKIIIVQLNKSVEIVCTRPNNNTRRSI RIGPGQTFYATDIIGDIRQAYCNISGRNWSEAVNQVKKKLKEHFPHKNISFQSSSGGDLEITTHSFNCGGE FFYCNTSGLFNDTISNATIMLPCRIKQIINMWQEVGKCIYAPPIKGNITCKSDITGLLLLRDGGNTANNAE IFRPGGGDMRDNWRSELYKYKVVKIEPLGVAPTRCKRRVVGRRRRRRAVGIGAVFLGFLGAAGSTMGAASM TLTVQARNLLSGIVQQQSNLLRAPEAQQHLLKLTVWGIKQLQARVLAVERYLRDQQLLGIWGCSGKLICCT NVPWNSSWSNRNLSEIWDNMTWLQWDKEISNYTQIIYGLLEESQNQQEKNEQDLLALD
BG505.v4.1-GT1 SOSIP	AENLWVTVYYGVPVWKDAETTLFCASDAKAYETKKHNVWATHACVPTDPNPQEIHLENVTEEFNMWKNNMV EQMHTDIISLWDQSLKPCVKLTPLCVTLQCTNVTNAITDDMRGELKNCSFNMTTELRDKRQKVHALFYKLD IVPINENQNTSYRLINCNTAAITQACPKVSFEPIPIHYCAPAGFAILKCKDKKFNGTGPCPSVSTVQCTHG IKPVVSTQLLLNGSLAEEEVMIRSEDIRNNAKNILVQFNTPVQINCTRPNNNTRKSIRIGPGQWFYATGDI IGDIRQAHCNVSKATWNETLGKVVKQLRKHFGNNTIIRFANSSGGDLEVTTHSFNCGGEFFYCDTSGLFNS TWISNTSVQGSNSTGSNDSITLPCRIKQIINMWQRIGQAMYAPPIQGVIRCVSNITGLILTRDGGSTDSTT ETFRPSGGDMRDNWRSELYKYKVVKIEPLGVAPTRCKRRVVGRRRRRRAVGIGAVFLGFLGAAGSTMGAAS MTLTVQARNLLSGIVQQQSNLLRAPEAQQHLLKLTVWGIKQLQARVLAVERYLRDQQLLGIWGCSGKLICC TNVPWNSSWSNRNLSEIWDNMTWLQWDKEISNYTQIIYGLLEESQNQQEKNEQDLLALD
eOD-GT8	DTITLPCRPAPPPHCSSNITGLILTRQGGYSNANTVIFRPSGGDWRDIARCQIAGTVVSTQLFLNGSLAEE EVVIRSEDWRDNAKSICVQLATSVEIACTGAGHCAISRAKWANTLKQIASKLREQYGAKTIIFKPSSGGDP EFVNHSFNCGGEFFYCASTQLFASTWFASTGTGTK
IGT2 SOSIP SpyTag	GSNLWVTVYYGVPVWKEAKTTLFCASDAKAYEKEVHNVWATHACVPTDPNPQEVVLENVTENFNMWKNDMV DQMQEDVISIWDQSLKPCVKLTPLCVTLNCTNVNVTSNSTNVNSSSTDNTTLGEIKNCSFDITTEIRDKTR KEYALFYRLDIVPLDNSSNPNSSNTYRLINCNTSTCTQACPKVTFDPIPIHYCAPAGYAILKCNNKTFNGK GPCNNVSTVQCTHGIKPVVSTQLLLNGSLAEEEIVIRSKNLRNNAKIIIVQLNKSVEIVCTRPNNNTRRSI RIGPGQTFYATDIIGDIRQAYCNISGRNWSEAVNQVKKKLKEHFPHKNISFQSSSGGDLEITTHSFNCGGE FFYCNTSGLFNDTISNATIMLPCRIKQIINMWQEVGKCIYAPPIKGNITCKSDITGLLLLRDGGNALRPTE IFRPSGGDMRDNWRSELYKYKVVKIEPLGVAPTRCKRRVVGRRRRRRAVGIGAVFLGFLGAAGSTMGAASM TLTVQARNLLSGIVQQQSNLLRAPEAQQHLLKLTVWGIKQLQARVLAVERYLRDQQLLGIWGCSGKLICCT NVPWNSSWSNRNLSEIWDNMTWLQWDKEISNYTQIIYGLLEESQNQQEKNEQDLLALDGGGGSGGGSGGGS GSGAHIVMVDAYKPTK
IGT1 SOSIP SpyTag	GSNLWVTVYYGVPVWKEAKTTLFCASDAKAYEKEVHNVWATHACVPTDPNPQEVVLENVTENFNMWKNDMV DQMQEDVISIWDQSLKPCVKLTPLCVTLNCTNVNVTSNSTNVNSSSTDNTTLGEIKNCSFDITTEIRDKTR KEYALFYRLDIVPLDNSSNPNSSNTYRLINCNTSTCTQACPKVTFDPIPIHYCAPAGYAILKCNNKTFNGK GPCNNVSTVQCTHGIKPVVSTQLLLNGSLAEEEIVIRSKNLRNNAKIIIVQLNKSVEIVCTRPNNNTRRSI RIGPGQTFYATDIIGDIRQAYCNISGRNWSEAVNQVKKKLKEHFPHKNISFQSSSGGDLEITTHSFNCGGE FFYCNTSGLFNDTISNATIMLPCRIKQIINMWQEVGKCIYAPPIKGNITCKSDITGLLLLRDGGNSQRETE IFRPSGGDMRDNWRSELYKYKVVKIEPLGVAPTRCKRRVVGRRRRRRAVGIGAVFLGFLGAAGSTMGAASM TLTVQARNLLSGIVQQQSNLLRAPEAQQHLLKLTVWGIKQLQARVLAVERYLRDQQLLGIWGCSGKLICCT NVPWNSSWSNRNLSEIWDNMTWLQWDKEISNYTQIIYGLLEESQNQQEKNEQDLLALDGGGGSGGGSGGGS GSGAHIVMVDAYKPTK

426c degly2 D279N SOSIP SpyTag	AENLWVTVYYGVPVWKEAKTTLFCASDAKAYEKEVHNVWATHACVPTDPNPQEVVLENVTENFNMWKNDMV DQMQEDVISIWDQSLKPCVKLTPLCVTLNCTNVNVTSNSTNVNSSSTDNTTLGEIKNCSFDITTEIRDKTR KEYALFYRLDIVPLDNSSNPNSSNTYRLINCNTSTCTQACPKVTFDPIPIHYCAPAGYAILKCNNKTFNGK GPCNNVSTVQCTHGIKPVVSTQLLLNGSLAEEEIVIRSKNLTNNAKIIIVQLNKSVEIVCTRPNNNTRRSI RIGPGQTFYATDIIGDIRQAYCNISGRNWSEAVNQVKKKLKEHFPHKNISFQSSSGGDLEITTHSFNCGGE FFYCNTSGLFNDTISNATIMLPCRIKQIINMWQEVGKCIYAPPIKGNITCKSDITGLLLLRDGGNTANNAE IFRPGGGDMRDNWRSELYKYKVVKIEPLGVAPTRCKRRVVGRRRRRRAVGIGAVFLGFLGAAGSTMGAASM TLTVQARNLLSGIVQQQSNLLRAPEAQQHLLKLTVWGIKQLQARVLAVERYLRDQQLLGIWGCSGKLICCT NVPWNSSWSNRNLSEIWDNMTWLQWDKEISNYTQIIYGLLEESQNQQEKNEQDLLALDGGGGSGGGSGGGS GSGRGVPHIVMVDAYKRYK
398F1 SOSIP SpyTag	AENLWVTVYYGVPVWKDAETTLFCASDAKAYHTEVHNVWATHACVPTDPNPQEINLENVTEEFNMWKNKMV EQMHTDIISLWDQSLKPCVQLTPLCVTLDCQYNVTNINSTSDMAREINNCSYNITTELRDREQKVYSLFYR SDIVQMNSDNSSKYRLINCNTSACKQACPKVTFEPIPIHYCAPAGFAILKCKDKEFNGTGPCKNVSTVQCT HGIKPVVSTQLLLNGSLAEEKVMIRSENITDNAKNIIVQFKEPVKINCTRPNNNTRKSVRIGPGQTFYATG EIIGDIRQAHCNVSKAHWENTLQEVANQLKLMIHSNKTIIFANSSGGDLEITTHSFNCGGEFFYCYTSGLF NYTFNDTSTNSTESKSNDTITLQCRIKQIINMWQRAGQCVYAPPIPGIIRCESNITGLILTRDGGNNNSNT NETFRPGGGDMRDNWRSELYRYKVVKIEPLGVAPTRCKRRVVGRRRRRRAVGIGAVSLGFLGAAGSTMGAA SMTLTVQARNLLSGIVQQQSNLLRAPEPQQHLLKDTHWGIKQLQARVLAVEHYLRDQQLLGIWGCSGKLIC CTNVPWNSSWSNRNLSEIWDNMTWLQWDKEISNYTQIIYGLLEESQNQQEKNEQDLLALDGGGGSGGGSGG GSGSGAHIVMVDAYKPTK
BJOX2000 SOSIP SpyTag	AENLWVTVYYGVPVWKEATTTLFCASDAKAYDTEVHNVWATHACVPTDPDPQEMFLENVTENFNMWKNNMV DQMHEDVISLWDQSLKPCVKLTPLCVTLECKNVNSSSSDTKNGTDPEMKNCSFNATTELRDRKQKVYALFY KLDIVPLNEKNSSEYRLINCNTSTCTQACPKVTFDPIPIHYCTPAGYAILKCNDEKFNGTGPCSNVSTVQC THGIKPVVSTQLLLNGSLAEKGIVIRSENLTNNVKTIIVHLNQSVEILCIRPNNNTRKSIRIGPGQTFYAT GEIIGDIRQAHCNISGKVWNETLQRVGEKLAEYFPNKTIKFNSSSGGDLEITTHSFNCGGEFFYCNTSKLF NGTFNGTYMPNVTEGNSTISIPCRIKQIINMWQKVGRCMYAPPIEGNITCKSKITGLLLERDGGPENDTEI FRPGGGDMRNNWRSELYKYKVVEIKPLGVAPTRCKRRVVGRRRRRRAVGIGAVSLGFLGAAGSTMGAASMT LTVQARNLLSGIVQQQSNLLRAPEPQQHLLKDTHWGIKQLQARVLAVEHYLRDQQLLGIWGCSGKLICCTN VPWNSSWSNRNLSEIWDNMTWLQWDKEISNYTQIIYGLLEESQNQQEKNEQDLLALDGGGGSGGGSGGGSG SGAHIVMVDAYKPTK
CE1176 SOSIP SpyTag	AENLWVTVYYGVPVWKEAKTTLFCASDAKAYEKEVHNVWATHACVPTDPNPQEMVLENVTENFNMWKNDMV DQMHEDVISLWDQSLKPCVKLTPLCVTLTCTNTTVSNGSSNSNANFEEMKNCSFNATTEIKDKKKNEYALF YKLDIVPLNNSSGKYRLINCNTSACAQACPKVTFEPIPIHYCAPAGYAILKCNNKTFNGTGPCNNVSTVQC THGIKPVVSTQLLLNGSLAEKEIIIRSENLTNNAKTIIIHFNESVGIVCTRPSNNTRKSIRIGPGQTFYAT GDIIGDIRQAHCNVSKQNWNRTLQQVGRKLAEHFPNRNITFNHSSGGDLEITTHSFNCRGEFFYCNTSGLF NGTYHPNGTYNETAVNSSDTITLQCRIKQIINMWQEVGRCMYAPPIAGNITCNSTITGLLLTRDGGINQTG EEIFRPGGGDMRDNWRNELYKYKVVEIKPLGVAPTRCKRRVVGRRRRRRAVGIGAVSLGFLGAAGSTMGAA SMTLTVQARNLLSGIVQQQSNLLRAPEPQQHLLKDTHWGIKQLQARVLAVEHYLRDQQLLGIWGCSGKLIC CTNVPWNSSWSNRNLSEIWDNMTWLQWDKEISNYTQIIYGLLEESQNQQEKNEQDLLALDGGGGSGGGSGG GSGSGAHIVMVDAYKPTK
CE0217 SOSIP SpyTag	AENLWVTVYYGVPVWREAKTTLFCASDAKAYEREVHNVWATHACVPTDPNPQERVLENVTENFNMWKNNMV DQMHEDIISLWDESLKPCIKLTPLCVTLNCGNAIVNESTIEGMKNCSFNVTTELKDKKKKEYALFYKLDVV PLNGENNNSNSKNFSEYRLINCNTSTCTQACPKVSFDPIPIHYCAPAGFAILKCNNETFNGTGPCNNVSTV QCTHGIKPVVSTQLLLNGSLAEKEIIIRSENLTNNAKIIIVHLNNPVKIICTRPGNNTRKSMRIGPGQTFY ATGDIIGDIRRAYCNISEKTWYDTLKNVSDKFQEHFPNASIEFKPSAGGDLEITTHSFNCRGEFFYCDTSE LFNGTYNNSTYNSSNNITLQCKIKQIINMWQGVGRCMYAPPIAGNITCESNITGLLLTRDGGNNKSTPETF RPGGGDMRDNWRSELYKYKVVEIKPLGVAPTRCKRRVVGRRRRRRAVGIGAVSLGFLGAAGSTMGAASMTL TVQARNLLSGIVQQQSNLLRAPEPQQHLLKDTHWGIKQLQARVLAVEHYLRDQQLLGIWGCSGKLICCTNV PWNSSWSNRNLSEIWDNMTWLQWDKEISNYTQIIYGLLEESQNQQEKNEQDLLALDGGGGSGGGSGGGSGS GAHIVMVDAYKPTK
CNE55 SOSIP SpyTag	AENLWVTVYYGVPVWRDADTTLFCASDAKAHETEVHNVWATHACVPTDPNPQEIHLVNVTENFNMWKNKMV EQMQEDVISLWDESLKPCVKLTPLCVTLNCTTANTNETKNNTTDDNIKDEMKNCTFNMTTEIRDKKQRVSA LFYKLDIVPIDDSKNNSEYRLINCNTSVCKQACPKVSFDPIPIHYCTPAGYVILKCNDKNFNGTGPCKNVS SVQCTHGIKPVVSTQLLLNGSLAEEEIIIRSENLTDNAKNIIVHLNKSVEINCTRPSNNTRTSVRIGPGQV FYRTGDITGDIRKAYCNISGTEWNKTLTQVAEKLKEHFNKTIVYQPPSGGDLEITMHHFNCRGEFFYCNTT QLFNNSVGNSTIKLPCRIKQIINMWQGVGQCMYAPPISGAINCLSNITGILLTRDGGGNNRSNETFRPGGG NIKDNWRSELYKYKVVEIEPLGVAPTRCKRRVVGRRRRRRAVGIGAVSLGFLGAAGSTMGAASMTLTVQAR NLLSGIVQQQSNLLRAPEPQQHLLKDTHWGIKQLQARVLAVEHYLRDQQLLGIWGCSGKLICCTNVPWNSS WSNRNLSEIWDNMTWLQWDKEISNYTQIIYGLLEESQNQQEKNEQDLLALDGGGGSGGGSGGGSGSGAHIV MVDAYKPTK

Tro11 SOSIP SpyTag	AENLWVTVYYGVPVWKDASTTLFCASDAKAYDTEVHNVWATHACVPTDPNPQEVVLGNVTENFNMWKNNMV DQMHEDIISLWDQSLKPCVKLTPLCVTLNCTDNITNTNTNSSKNSSTHSYNNSLEGEMKNCSFNITAGIRD KVKKEYALFYKLDVVPIEEDKDTNKTTYRLRSCNTSVCTQACPKVTFEPIPIHYCAPAGFAILKCNDKKFN GTGPCTNVSTVQCTHGIRPVVSTQLLLNGSLAEEEVVIRSENFTNNAKTIIVQLNESIAINCTRPNNNTRR SIHIGPGRAFYATGDIIGDIRQAHCNISRTEWNSTLRQIVTKLREQLGDPNKTIIFNQSSGGDTEITMHSF NCGGEFFYCNTTKLFNSTWNGNNTTESDSTGENITLPCRIKQIINLWQEVGKCMYAPPIKGQISCSSNITG LLLTRDGGNNNSSGPETFRPGGGNMKDNWRSELYKYKVIKIEPLGVAPTRCKRRVVGRRRRRRAVGIGAVS LGFLGAAGSTMGAASMTLTVQARNLLSGIVQQQSNLLRAPEPQQHLLKDTHWGIKQLQARVLAVEHYLRDQ QLLGIWGCSGKLICCTNVPWNSSWSNRNLSEIWDNMTWLQWDKEISNYTQIIYGLLEESQNQQEKNEQDLL ALDGGGGSGGGSGGGSGSGAHIVMVDAYKPTK
X1632 SOSIP SpyTag	AENLWVTVYYGVPVWEDADTTLFCASDAKAYSTESHNVWATHACVPTDPNPQEIYLENVTEDFNMWENNMV EQMQEDIISLWDESLKPCVKLTPLCVTLTCTNVTNVTDSVGTNSRLKGYKEELKNCSFNTTTEIRDKKKQE YALFYKLDIVPINDNSNNSNGYRLINCNVSTCKQACPKVSFDPIPIHYCAPAGFAILKCRDKEFNGTGTCR NVSTVQCTHGIKPVVSTQLLLNGSLAEGDIVIRSENITDNAKTIIVHLNKTVSITCTRPNNNTRKSIRIGP GQALYATGAIIGDTRQAHCNISGSEWYEMIQNVKNKLNETFKKNITFNPSSGGDLEITTHSFNCRGEFFYC NTSELFNSSHLFNGSTLSTNGTITLPCRIKQIVRMWQRVGQCMYAPPIAGNITCRSNITGLLLTRDGGTNK DTNEAETFRPGGGDMRDNWRSELYKYKVVKIKPLGVAPTRCKRRVVGRRRRRRAVGIGAVSLGFLGAAGST MGAASMTLTVQARNLLSGIVQQQSNLLRAPEPQQHLLKDTHWGIKQLQARVLAVEHYLRDQQLLGIWGCSG KLICCTNVPWNSSWSNRNLSEIWDNMTWLQWDKEISNYTQIIYGLLEESQNQQEKNEQDLLALDGGGGSGG GSGGGSGSGAHIVMVDAYKPTK
X2278 SOSIP SpyTag	AENLWVTVYYGVPVWKEATTTLFCASEAKAYDTEVHNIWATHACVPTDPNPQEMELKNVTENFNMWKNNMV EQMHQDIISLWDQSLKPCVKLTPLCVTLDCTNINSTNSTNNTSSNSKMEETIGVIKNCSFNVTTNIRDKVK KENALFYSLDLVSIGNSNTSYRLISCNTSICTQACPKVSFDPIPIHYCAPAGFAILKCRDKKFNGTGPCRN VSSVQCTHGIRPVVSTQLLLNGSLAEEEIVIRSANLTDNAKTIIIQLNETIQINCTRPNNNTRRSIPIGPG RTFYATGDIIGDIRKAYCNISATKWNNTLRQIAEKLREKFNKTIIFNQSSGGDPEVVRHTFNCGGEFFYCN SSQLFNSTWYSNGTSNGGLNNSANITLPCRIKQIINLWQEVGKCMYAPPIKGVINCLSNITGIILTRDGGE NNGTTETFRPGGGDMRDNWRSELYKYKVVKIEPLGVAPTRCKRRVVGRRRRRRAVGIGAVSLGFLGAAGST MGAASMTLTVQARNLLSGIVQQQSNLLRAPEPQQHLLKDTHWGIKQLQARVLAVEHYLRDQQLLGIWGCSG KLICCTNVPWNSSWSNRNLSEIWDNMTWLQWDKEISNYTQIIYGLLEESQNQQEKNEQDLLALDGGGGSGG GSGGGSGSGAHIVMVDAYKPTK
BG505 SOSIP	NLWVTVYYGVPVWKDAETTLFCASDAKAYETEKHNVWATHACVPTDPNPQEIHLENVTEEFNMWKNNMVEQ MHTDIISLWDQSLKPCVKLTPLCVTLQCTNVTNNITDDMRGELKNCSFNMTTELRDKKQKVYSLFYRLDVV QINENQGNRSNNSNKEYRLINCNTSAITQACPKVSFEPIPIHYCAPAGFAILKCKDKKFNGTGPCPSVSTV QCTHGIKPVVSTQLLLNGSLAEEEVMIRSENITNNAKNILVQFNTPVQINCTRPNNNTRKSIRIGPGQAFY ATGDIIGDIRQAHCNVSKATWNETLGKVVKQLRKHFGNNTIIRFANSSGGDLEVTTHSFNCGGEFFYCNTS GLFNSTWISNTSVQGSNSTGSNDSITLPCRIKQIINMWQRIGQAMYAPPIQGVIRCVSNITGLILTRDGGS TNSTTETFRPGGGDMRDNWRSELYKYKVVKIEPLGVAPTRCKRRVVGRRRRRRAVGIGAVSLGFLGAAGST MGAASMTLTVQARNLLSGIVQQQSNLLRAPEPQQHLLKDTHWGIKQLQARVLAVEHYLRDQQLLGIWGCSG KLICCTNVPWNSSWSNRNLSEIWDNMTWLQWDKEISNYTQIIYGLLEESQNQQEKNEQDLLALD
AMC011 SOSIP	AEQLWVTVYYGVPVWKEATTTLFCASDARAYDTEVRNVWATHCCVPTDPNPQEVVLENVTENFNMWKNNMV EQMHEDIISLWDQSLKPCVKLTPLCVTLNCTDLRNATNTNATNTTSSSRGTMEGGEIKNCSFNITTSMRDK VQKEYALFYKLDVVPIKNDNTSYRLISCNTSVITQACPKVSFEPIPIHYCAPAGFAILKCNNKTFNGTGPC TNVSTVQCTHGIRPVVSTQLLLNGSLAEEEVVIRSANFTDNAKIIIVQLNKSVEINCTRPNNNTRKSIHIG PGRWFYTTGEIIGDIRQAHCNISGTKWNDTLKQIVVKLKEQFGNKTIVFNHSSGGDPEIVMHSFNCGGEFF YCNSTQLFNSTWNDTTGSNYTGTIVLPCRIKQIVNMWQEVGKAMYAPPIKGQIRCSSNITGLILIRDGGKN RSENTEIFRPGGGDMRDNWRSELYKYKVVKIEPLGIAPTKCKRRVVQRRRRRRAVGIGAVFLGFLGAAGST MGAASMTLTVQARQLLSGIVQQQNNLLRAPECQQHLLKLTVWGIKQLQARVLAVERYLKDQQLLGIWGCSG KLICCTAVPWNTSWSNKSYNQIWNNMTWMEWEREIDNYTSLIYTLIEDSQNQQEKNEQELLELD
B41 SOSIP	AAKKWVTVYYGVPVWKEATTTLFCASDAKAYDTEVHNVWATHACVPTDPNPQEIVLGNVTENFNMWKNNMV EQMHEDIISLWDQSLKPCVKLTPLCVTLNCNNVNTNNTNNSTNATISDWEKMETGEMKNCSFNVTTSIRDK IKKEYALFYKLDVVPLENKNNINNTNITNYRLINCNTSVITQACPKVSFEPIPIHYCAPAGFAILKCNSKT FNGSGPCTNVSTVQCTHGIRPVVSTQLLLNGSLAEEEIVIRSENITDNAKTIIVQLNEAVEINCTRPNNNT RKSIHIGPGRWFYATGDIIGNIRQAHCNISKARWNETLGQIVAKLEEQFPNKTIIFNHSSGGDPEIVTHSF NCGGEFFYCNTTPLFNSTWNNTRTDDYPTGGEQNITLQCRIKQIINMWQGVGKAMYAPPIRGQIRCSSNIT GLLLTRDGGRDQNGTETFRPGGGNMRDNWRSELYKYKVVKIEPLGIAPTACKRRVVQRRRRRRAVGLGAFI LGFLGAAGSTMGAASMALTVQARLLLSGIVQQQNNLLRAPEAQQHMLQLTVWGIKQLQARVLAVERYLRDQ QLLGIWGCSGKIICCTNVPWNDSWSNKTINEIWDNMTWMQWEKEIDNYTQHIYTLLEVSQIQQEKNEQELL ELD

CH119 SOSIP	AENLWVTVYYGVPVWKEATTTLFCASDAKAYDTEVHNVWATHACVPTDPSPQELVLENVTENFNMWKNEMV NQMHEDVISLWDQSLKPCVKLTPLCVTLECSKVSNNETDKYNGTEEMKNCSFNATTVVRDRQQKVYALFYR LDIVPLTEKNSSENSSKYYRLINCNTSACTQACPKVSFEPIPIHYCTPAGYAILKCNDKTFNGTGPCHNVS TVQCTHGIKPVVSTQLLLNGSLAEGEIIIRSENLTNNVKTILVHLNQSVEIVCTRPNNNTRKSIRIGPGQT FYATGDIIGDIRQAHCNISKWHETLKRVSEKLAEHFPNKTINFTSSSGGDLEITTHSFTCRGEFFYCNTSG LFNSTYMPNGTYLHGDTNSNSSITIPCRIKQIINMWQEVGRCMYAPPIEGNITCKSNITGLLLVRDGGTES NNTETNNTEIFRPGGGDMRDNWRSELYKYKVVEIKPLGVAPTRCKRRVVGRRRRRRAVGIGAVSLGFLGAA GSTMGAASMTLTVQARNLLSGIVQQQSNLLRAPEPQQHLLKDTHWGIKQLQARVLAVEHYLRDQQLLGIWG CSGKLICCTNVPWNSSWSNRNLSEIWDNMTWLQWDKEISNYTQIIYGLLEESQNQQEKNEQDLLALD
CE0217 SOSIP	AENLWVTVYYGVPVWREAKTTLFCASDAKAYEREVHNVWATHACVPTDPNPQERVLENVTENFNMWKNNMV DQMHEDIISLWDESLKPCIKLTPLCVTLNCGNAIVNESTIEGMKNCSFNVTTELKDKKKKEYALFYKLDVV PLNGENNNSNSKNFSEYRLINCNTSTCTQACPKVSFDPIPIHYCAPAGFAILKCNNETFNGTGPCNNVSTV QCTHGIKPVVSTQLLLNGSLAEKEIIIRSENLTNNAKIIIVHLNNPVKIICTRPGNNTRKSMRIGPGQTFY ATGDIIGDIRRAYCNISEKTWYDTLKNVSDKFQEHFPNASIEFKPSAGGDLEITTHSFNCRGEFFYCDTSE LFNGTYNNSTYNSSNNITLQCKIKQIINMWQGVGRCMYAPPIAGNITCESNITGLLLTRDGGNNKSTPETF RPGGGDMRDNWRSELYKYKVVEIKPLGVAPTRCKRRVVGRRRRRRAVGIGAVSLGFLGAAGSTMGAASMTL TVQARNLLSGIVQQQSNLLRAPEPQQHLLKDTHWGIKQLQARVLAVEHYLRDQQLLGIWGCSGKLICCTNV PWNSSWSNRNLSEIWDNMTWLQWDKEISNYTQIIYGLLEESQNQQEKNEQDLLALD
CNE8 SOSIP	AENLWVTVYYGVPVWRDADTTLFCASDAKAYDTEVHNVWATHACVPTDPNPQEIHLENVTENFNMWKNKMA EQMQEDVISLWDESLKPCVQLTPLCVTLNCTNANLNATVNASTTIGNITDEVRNCSFNTTTELRDKKQNVY ALFYKLDIVPINNNSEYRLINCNTSVCKQACPKVSFDPIPIHYCAPAGYAILRCNDKNFNGTGPCKNVSSV QCTHGIKPVVSTQLLLNGSLAEDEIIIRSENLTDNVKTIIVHLNKSVEINCTRPSNNTRTSVRIGPGQVFY RTGDIIGDIRKAYCNISRTKWHETLKQVATKLREHFNKTIIFQPPSGGDIEITMHHFNCRGEFFYCNTTKL FNSTWGENTTMEGHNDTIVLPCRIKQIVNMWQGVGQCMYAPPIRGSINCVSNITGILLTRDGGTNMSNETF RPGGGNIKDNWRSELYKYKVVEIEPLGVAPTRCKRRVVGRRRRRRAVGIGAVSLGFLGAAGSTMGAASMTL TVQARNLLSGIVQQQSNLLRAPEPQQHLLKDTHWGIKQLQARVLAVEHYLRDQQLLGIWGCSGKLICCTNV PWNSSWSNRNLSEIWDNMTWLQWDKEISNYTQIIYGLLEESQNQQEKNEQDLLALD
CNE8 N276A SOSIP	AENLWVTVYYGVPVWRDADTTLFCASDAKAYDTEVHNVWATHACVPTDPNPQEIHLENVTENFNMWKNKMA EQMQEDVISLWDESLKPCVQLTPLCVTLNCTNANLNATVNASTTIGNITDEVRNCSFNTTTELRDKKQNVY ALFYKLDIVPINNNSEYRLINCNTSVCKQACPKVSFDPIPIHYCAPAGYAILRCNDKNFNGTGPCKNVSSV QCTHGIKPVVSTQLLLNGSLAEDEIIIRSEALTDNVKTIIVHLNKSVEINCTRPSNNTRTSVRIGPGQVFY RTGDIIGDIRKAYCNISRTKWHETLKQVATKLREHFNKTIIFQPPSGGDIEITMHHFNCRGEFFYCNTTKL FNSTWGENTTMEGHNDTIVLPCRIKQIVNMWQGVGQCMYAPPIRGSINCVSNITGILLTRDGGTNMSNETF RPGGGNIKDNWRSELYKYKVVEIEPLGVAPTRCKRRVVGRRRRRRAVGIGAVSLGFLGAAGSTMGAASMTL TVQARNLLSGIVQQQSNLLRAPEPQQHLLKDTHWGIKQLQARVLAVEHYLRDQQLLGIWGCSGKLICCTNV PWNSSWSNRNLSEIWDNMTWLQWDKEISNYTQIIYGLLEESQNQQEKNEQDLLALD
CNE20 SOSIP	NLWVTVYYGVPVWKEATTTLFCASDAKAYDTEVHNVWATHACVPTDPNPHELVLENVTENFNMWKNEMVNQ MHEDVISLWDQSLKPCVKLTPLCVTLECGNITTRKESMTEMKNCSFNATTVVKDRKQTVYALFYKLDIVPL SGKNSSGYYRLINCNTSACTQACPKVNFDPIPIHYCTPAGYAILKCNDKTFNGTGPCHNVSTVQCTHGIKP VISTQLLLNGSLAEGEIVIRSENLTNNAKIIIVHLNQTVEIVCTRPGNNTRKSIRIGPGQTFYATGEIIGN IRQAHCNISENQWHKTLQNVSKKLAEHFQNKTITFASSSGGDLEITTHSFNCRGEFFYCNTSGLFNGTYMS NNTEGNSSSIITIPCRIKQIINMWQEVGRCIYAPPIEGNITCKSNITGLLLERDGGTESNDTEIFRPGGGD MRNNWRSELYKYKVVEIKPLGVAPTRCKRRVVGRRRRRRAVGIGAVSLGFLGAAGSTMGAASMTLTVQARN LLSGIVQQQSNLLRAPEPQQHLLKDTHWGIKQLQARVLAVEHYLRDQQLLGIWGCSGKLICCTNVPWNSSW SNRNLSEIWDNMTWLQWDKEISNYTQIIYGLLEESQNQQEKNEQDLLALD
CNE20 N276A SOSIP	NLWVTVYYGVPVWKEATTTLFCASDAKAYDTEVHNVWATHACVPTDPNPHELVLENVTENFNMWKNEMVNQ MHEDVISLWDQSLKPCVKLTPLCVTLECGNITTRKESMTEMKNCSFNATTVVKDRKQTVYALFYKLDIVPL SGKNSSGYYRLINCNTSACTQACPKVNFDPIPIHYCTPAGYAILKCNDKTFNGTGPCHNVSTVQCTHGIKP VISTQLLLNGSLAEGEIVIRSEALTNNAKIIIVHLNQTVEIVCTRPGNNTRKSIRIGPGQTFYATGEIIGN IRQAHCNISENQWHKTLQNVSKKLAEHFQNKTITFASSSGGDLEITTHSFNCRGEFFYCNTSGLFNGTYMS NNTEGNSSSIITIPCRIKQIINMWQEVGRCIYAPPIEGNITCKSNITGLLLERDGGTESNDTEIFRPGGGD MRNNWRSELYKYKVVEIKPLGVAPTRCKRRVVGRRRRRRAVGIGAVSLGFLGAAGSTMGAASMTLTVQARN LLSGIVQQQSNLLRAPEPQQHLLKDTHWGIKQLQARVLAVEHYLRDQQLLGIWGCSGKLICCTNVPWNSSW SNRNLSEIWDNMTWLQWDKEISNYTQIIYGLLEESQNQQEKNEQDLLALD
IOMA HC Fab	EVQLVESGAQVKKPGASVTVSCTASGYKFTGYHMHWVRQAPGRGLEWMGWINPFRGAVKYPQNFRGRVSMT RDTSMEIFYMELSRLTSDDTAVYYCAREMFDSSADWSPWRGMVAWGQGTLVTVSSASTKGPSVFPLAPSSK STSGGTAALGCLVKDYFPEPVTVSWNSGALTSGVHTFPAVLQSSGLYSLSSVVTVPSSSLGTQTYICNVNH KPSNTKVDKRVEPKSCDKT

IOMA HC	EVQLVESGAQVKKPGASVTVSCTASGYKFTGYHMHWVRQAPGRGLEWMGWINPFRGAVKYPQNFRGRVSMT RDTSMEIFYMELSRLTSDDTAVYYCAREMFDSSADWSPWRGMVAWGQGTLVTVSSASTKGPSVFPLAPSSK STSGGTAALGCLVKDYFPEPVTVSWNSGALTSGVHTFPAVLQSSGLYSLSSVVTVPSSSLGTQTYICNVNH KPSNTKVDKRVEPKSCDKTHTCPPCPAPELLGGPSVFLFPPKPKDTLMISRTPEVTCVVVDVSHEDPEVKF NWYVDGVEVHNAKTKPREEQYNSTYRVVSVLTVLHQDWLNGKEYKCKVSNKALPAPIEKTISKAKGQPREP QVYTLPPSREEMTKNQVSLTCLVKGFYPSDIAVEWESNGQPENNYKTTPPVLDSDGSFFLYSKLTVDKSRW QQGNVFSCSVMHEALHNHYTQKSLSLSPGK
IOMA LC	QSALTQPASVSGSPGQSITISCAGSSRDVGGFDLVSWYQQHPGKAPKLIIYEVNKRPSGISSRFSASKSGN TASLTISGLQEEDEAHYYCYSYADGVAFGGGTKLTVLGQPKAAPSVTLFPPSSEELQANKATLVCLISDFY PGAVTVAWKADSSPVKAGVETTTPSKQSNNKYAASSYLSLTPEQWKSHRSYSCQVTHEGSTVEKTVAPTEC S
IOMA iGL HC Fab	QVQLVQSGAEVKKPGASVKVSCKASGYTFTGYYMHWVRQAPGQGLEWMGWINPNSGGTNYAQKFQGRVTMT RDTSISTAYMELSRLRSDDTAVYYCARDFTSSYDSSGYYHEGYWGQGTLVTVSSASTKGPSVFPLAPSSKS TSGGTAALGCLVKDYFPEPVTVSWNSGALTSGVHTFPAVLQSSGLYSLSSVVTVPSSSLGTQTYICNVNHK PSNTKVDKRVEPKSCDKT
IOMA iGL HC	QVQLVQSGAEVKKPGASVKVSCKASGYTFTGYYMHWVRQAPGQGLEWMGWINPNSGGTNYAQKFQGRVTMT RDTSISTAYMELSRLRSDDTAVYYCARDFTSSYDSSGYYHEGYWGQGTLVTVSSASTKGPSVFPLAPSSKS TSGGTAALGCLVKDYFPEPVTVSWNSGALTSGVHTFPAVLQSSGLYSLSSVVTVPSSSLGTQTYICNVNHK PSNTKVDKRVEPKSCDKTHTCPPCPAPELLGGPSVFLFPPKPKDTLMISRTPEVTCVVVDVSHEDPEVKFN WYVDGVEVHNAKTKPREEQYNSTYRVVSVLTVLHQDWLNGKEYKCKVSNKALPAPIEKTISKAKGQPREPQ VYTLPPSREEMTKNQVSLTCLVKGFYPSDIAVEWESNGQPENNYKTTPPVLDSDGSFFLYSKLTVDKSRWQ QGNVFSCSVMHEALHNHYTQKSLSLSPGK
IOMA iGL LC	QSALTQPASVSGSPGQSITISCTGTSSDVGSYNLVSWYQQHPGKAPKLMIYEVSKRPSGVSNRFSGSKSGN TASLTISGLQAEDEADYYCCSYAGSVAFGGGTKLTVLGQPKAAPSVTLFPPSSEELQANKATLVCLISDFY PGAVTVAWKADSSPVKAGVETTTPSKQSNNKYAASSYLSLTPEQWKSHRSYSCQVTHEGSTVEKTVAPTEC S
VRC01 iGL HC	QVQLVQSGAEVKKPGASVKVSCKASGYTFTGYYMHWVRQAPGQGLEWMGWINPNSGGTNYAQKFQGRVTMT RDTSISTAYMELSRLRSDDTAVYYCARGKNSDYNWDFQHWGQGTLVTVSSASTKGPSVFPLAPSSKSTSGG TAALGCLVKDYFPEPVTVSWNSGALTSGVHTFPAVLQSSGLYSLSSVVTVPSSSLGTQTYICNVNHKPSNT KVDKRVEPKSCDKTHTCPPCPAPELLGGPSVFLFPPKPKDTLMISRTPEVTCVVVDVSHEDPEVKFNWYVD GVEVHNAKTKPREEQYNSTYRVVSVLTVLHQDWLNGKEYKCKVSNKALPAPIEKTISKAKGQPREPQVYTL PPSREEMTKNQVSLTCLVKGFYPSDIAVEWESNGQPENNYKTTPPVLDSDGSFFLYSKLTVDKSRWQQGNV FSCSVMHEALHNHYTQKSLSLSPGK
VRC01 iGL LC	EIVLTQSPATLSLSPGERATLSCRASQSVSSYLAWYQQKPGQAPRLLIYDASNRATGIPARFSGSGSGTDF TLTISSLEPEDFAVYYCQQYEFFGQGTKLEIKRTVAAPSVFIFPPSDEQLKSGTASVVCLLNNFYPREAKV QWKVDNALQSGNSQESVTEQDSKDSTYSLSSTLTLSKADYEKHKVYACEVTHQGLSSPVTKSFNRGEC
3BNC60 iGL HC	QVQLVQSGAEVKKPGASVKVSCKASGYTFTGYYMHWVRQAPGQGLEWMGWINPNSGGTNYAQKFQGRVTMT RDTSISTAYMELSRLRSDDTAVYYCARERSDFWDFDLWGRGTLVTVSSASTKGPSVFPLAPSSKSTSGGTA ALGCLVKDYFPEPVTVSWNSGALTSGVHTFPAVLQSSGLYSLSSVVTVPSSSLGTQTYICNVNHKPSNTKV DKRVEPKSCDKTHTCPPCPAPELLGGPSVFLFPPKPKDTLMISRTPEVTCVVVDVSHEDPEVKFNWYVDGV EVHNAKTKPREEQYNSTYRVVSVLTVLHQDWLNGKEYKCKVSNKALPAPIEKTISKAKGQPREPQVYTLPP SREEMTKNQVSLTCLVKGFYPSDIAVEWESNGQPENNYKTTPPVLDSDGSFFLYSKLTVDKSRWQQGNVFS CSVMHEALHNHYTQKSLSLSPGK
3BNC60 iGL LC	DIQMTQSPSSLSASVGDRVTITCQASQDISNYLNWYQQKPGKAPKLLIYDASNLETGVPSRFSGSGSGTDF TFTISSLQPEDIATYYCQQYEFIGPGTKVDIKRTVAAPSVFIFPPSDEQLKSGTASVVCLLNNFYPREAKV QWKVDNALQSGNSQESVTEQDSKDSTYSLSSTLTLSKADYEKHKVYACEVTHQGLSSPVTKSFNRGEC
BG24 iGL HC	QVQLVQSGAEVKKPGASVKVSCKASGYTFTGYYMHWVRQAPGQGLEWMGWINPNSGGTNYAQKFQGRVTMT RDTSISTAYMELSRLRSDDTAVYYCATQLELDSSAGYAFDIWGQGTMVTVSSASTKGPSVFPLAPSSKSTS GGTAALGCLVKDYFPEPVTVSWNSGALTSGVHTFPAVLQSSGLYSLSSVVTVPSSSLGTQTYICNVNHKPS NTKVDKRVEPKSCDKTHTCPPCPAPELLGGPSVFLFPPKPKDTLMISRTPEVTCVVVDVSHEDPEVKFNWY VDGVEVHNAKTKPREEQYNSTYRVVSVLTVLHQDWLNGKEYKCKVSNKALPAPIEKTISKAKGQPREPQVY TLPPSREEMTKNQVSLTCLVKGFYPSDIAVEWESNGQPENNYKTTPPVLDSDGSFFLYSKLTVDKSRWQQG NVFSCSVMHEALHNHYTQKSLSLSPGK

BG24 iGL LC	QSALTQPRSVSGSPGQSVTISCTGTSSDVGGYNYVSWYQQHPGKAPKLMIYDVSKRPSGVPDRFSGSKSGN TASLTISGLQAEDEADYYCSSYEYFGGGTKLTVLSQPKAAPSVTLFPPSSEELQANKATLVCLISDFYPGA VTVAWKADSSPVKAGVETTTPSKQSNNKYAASSYLSLTPEQWKSHRSYSCQVTHEGSTVEKTVAPTECS

Table S2: X-ray data collection for IOMA iGL Fab crystals

Space group	P 2_1 2_1 2_1
Cell dimensions	
a, *b*, *c* (Å)	57.7, 66.7, 166.3
α, *β*, *γ* (°)	90, 90, 90
Resolution (Å)	38.6–2.07 (2.15–2.07)[a]
R_{merge}	0.08 (0.58)
R_{pim}	0.05 (0.36)
$I/\sigma(I)$	9.7 (2.5)
$CC_{1/2}$	0.99 (0.92)
Completeness (%)	99 (99)
Redundancy	6.3 (6.6)
Refinement	
Resolution (Å)	38.6–2.07
No. reflections	39,372
R_{work} / R_{free}	0.224 / 0.257
No. atoms	
Protein	3,241
Ligand/ion	N/A
B factors (Å^2)	
Protein	46.7
Ligand/ion	N/A
R.m.s. deviations	
Bond lengths (Å)	0.008
Bond angles (°)	1.00

[a] Values in parentheses are for the highest-resolution shell.

Table S3: Serum neutralization data for IOMA iGL transgenic mice

			ES30		ES32		ES34		ES37		ET33		ET34	
			B3 (week 18)		B3 (week 18)		B3 (week 18)		B3 (week 18)		B3 (week 18)		B3 (week 18)	
Virus	Clade	Tier	ID_{50}	% 1:100	ID_{50}	% 1:100	ID_{50}	% 1:100	ID_{50}	% 1:100	ID_{50}	% 1:100	ID_{50}	% 1:100
426c	C	2	–	–	–	–	–	–	–	–	<100	0	<100	0
25710	B	2	–	–	–	–	–	–	–	–	<100	0	<100	0
CNE8	AE	1	<100	0	<100	0	<100	0	<100	0	<100	0	104	54
CNE8 N276A	AE	1	463	71	<100	0	<100	0	<100	0	<100	0	<100	40
CNE20	BC	2	<100	49	<100	0	<100	0	<100	0	<100	0	<100	0
CNE20 N276A	BC	2	14,922	95	<100	0	<100	0	<100	0	<100	0	<100	36
JRCSF	B	2	136	65	<100	0	<100	0	<100	0	<100	0	<100	0
Q23.17	A	1	100	51	<100	0	<100	0	<100	0	<100	0	<100	26
YU2	B	2	571	86	<100	0	<100	0	<100	0	<100	0	112	56
BG505 T332N	A	2	–	–	–	–	–	–	–	–	<100	0	<100	0
6535.5	B	1	–	–	–	–	–	–	–	–	<100	0	104	53
3415_V1_C1	A	2	–	–	–	–	–	–	–	–	154	53	102	59
CAAN5342.A2	B	2	–	–	–	–	–	–	–	–	<100	0	<100	41
PVO.4	B	3	113	52	<100	0	<100	0	<100	0	<100	22	<100	57
Q842.D12	A	2	–	–	–	–	–	–	–	–	<100	0	<100	0
RHPA4259.7	B	2	–	–	–	–	–	–	–	–	<100	0	<100	43
WITO4160.33	B	2	<100	0	<100	0	<100	0	<100	0	<100	0	<100	45
ZM214M.PL15	C	2	–	–	–	–	–	–	–	–	<100	0	<100	0
MuLV			<100	0	<100	0	<100	0	<100	0	<100	0	162	65

			HP1		HP2		HP3		HP4		HP6		HP7		HQ4	
			B4 (week 23)		B4 (week 23)		B4 (week 23)		B4 (week 23)		B4 (week 23)		B4 (week 23)		B4 (week 23)	
Virus	Clade	Tier	ID_{50}	% 1:100	ID_{50}	% 1:100	ID_{50}	% 1:100	ID_{50}	% 1:100	ID_{50}	% 1:100	ID_{50}	% 1:100	ID_{50}	% 1:100
426c	C	2	<100	0	<100	0	<100	0	<100	0	–	–	<100	0	<100	0
25710	B	2	<100	0	<100	0	<100	0	<100	0	–	–	<100	0	<100	0
CNE8	AE	1	<100	0	<100	0	<100	0	<100	0	–	–	<100	0	<100	0
CNE8 N276A	AE	1	<100	26	<100	0	<100	0	<100	12	–	–	<100	0	<100	0
CNE20	BC	2	<100	23	<100	0	<100	40	<100	0	–	–	<100	0	<100	0
CNE20 N276A	BC	2	338	83	610	79	903	88	<100	16	–	–	2,017	98	<100	0
JRCSF	B	2	<100	0	<100	0	<100	0	<100	0	–	–	<100	0	<100	0
Q23.17	A	1	120	57	<100	30	<100	28	<100	0	–	–	<100	0	<100	0
YU2	B	2	<100	0	<100	0	<100	0	<100	0	–	–	<100	0	<100	0
BG505 T332N	A	2	<100	0	<100	0	<100	0	<100	0	–	–	<100	0	<100	0
6535.5	B	1	165	67	<100	0	<100	0	<100	0	–	–	<100	0	<100	0
3415_V1_C1	A	2	<100	0	<100	40	<100	0	<100	0	–	–	<100	0	108	50
CAAN5 342.A2	B	2	<100	0	<100	0	<100	0	<100	0	–	–	<100	0	<100	0
PVO.4	B	3	<100	43	<100	45	<100	12	<100	35	–	–	115	50	<100	0
Q842.D 12	A	2	<100	0	<100	0	<100	0	<100	0	–	–	<100	0	<100	0
RHPA4 259.7	B	2	<100	0	<100	0	<100	0	<100	0	–	–	<100	0	<100	0
WITO4 160.33	B	2	<100	28	145	53	<100	0	<100	48	–	–	<100	40	<100	0
ZM214 M.PL15	C	2	<100	0	<100	0	<100	0	<100	0	–	–	<100	0	<100	0
MuLV			<100	0	<100	0	<100	0	<100	0	–	–	<100	0	<100	0

Table S4: Mutational analysis of antibodies isolated from IOMA iGL transgenic mice.

VH1-2*02 amino acid	VH Position	amino acid substitution	Random Frequency	# of IGT2-induced mAbs with this SHM	IGT2 Frequency	IOMA Substitution	Critical Interaction	VRC01 Substitution
Q	1		–	67	100.0	E		
		E	0.0	0	0.0			
V	2			67	100.0	V		
Q	3			67	100.0	Q		
L	4			67	100.0	L		
V	5			67	100.0	V		
Q	6			67	100.0	E		
		E	0.1	0	0.0			
S	7			67	100.0	S		
G	8			67	100.0	G		
A	9			67	100.0	A		G
E	10			67	100.0	Q		Q
		Q	0.2	0	0.0			
V	11			66	98.5	V		M
		M	3.3	1	1.5			
K	12			56	83.6	K		
		R	6.9	11	16.4			
K	13			67	100.0	K		
P	14			67	100.0	P		
G	15			67	100.0	G		E
A	16			67	100.0	A		
S	17			67	100.0	S		
V	18			67	100.0	V		M
K	19			22	32.8	T	**YES**	R
		T	2.3	31	46.3			
		R	9.6	14	20.9			
V	20			67	100.0	V		I
S	21			67	100.0	S		
C	22			67	100.0	C		
K	23			55	82.1	T		R
		A	0.2	1	1.5			
		T	2.3	0	0.0			
		E	3.3	5	7.5			
		R	4.6	6	9.0			
A	24			61	91.0	A		
		T	13.5	6	9.0			
S	25			67	100.0	S		
G	26			67	100.0	G		

Y	27			67	100.0	Y		
T	28			65	97.0	K		E
		K	0.6	0	0.0			
		N	2.0	2	3.0			
F	29			66	98.5	F		
		L	3.8	1	1.5			
T	30			58	86.6	T		I
		A	1.7	1	1.5			
		I	7.2	8	11.9			
G	31			32	47.8	G		D
		E	0.8	1	1.5			
		A	11.7	6	9.0			
		D	34.3	28	41.8			
Y	32			65	97.0	Y		C
		H	8.5	2	3.0			
Y	33			27	40.3	H	**YES**	T
		E	0.1	14	20.9			
		D	0.6	9	13.4			
		S	1.9	2	3.0			
		H	4.5	8	11.9			
		F	8.4	7	10.4			
M	34			33	49.3	M		L
		L	13.8	7	10.4			
		I	48.4	27	40.3			
H	35			61	91.0	H		N
		Q	2.2	1	1.5			
		Y	3.5	5	7.5			
W	36			67	100.0	W		
V	37			67	100.0	V		I
R	38			67	100.0	R		
Q	39			66	98.5	Q		L
		R	1.1	1	1.5			
A	40			65	97.0	A		
		V	2.0	2	3.0			
P	41			67	100.0	P		
G	42			67	100.0	G		
Q	43			66	98.5	R		K
		R	1.5	1	1.5			
G	44			67	100.0	G		R
L	45			64	95.5	L		P
		F	1.9	3	4.5			
E	46			66	98.5	E		

		D	0.5	1	1.5			
W	47			67	100.0	W		
M	48			62	92.5	M		
		L	4.9	4	6.0			
		V	6.4	1	1.5			
G	49			67	100.0	G		
W	50			52	77.6	W		
		R	0.0	14	20.9			
		L	0.8	1	1.5			
I	51			66	98.5	I		L
		S	0.5	1	1.5			
N	52			58	86.6	N		K
		H	2.2	3	4.5			
		S	4.4	6	9.0			
P	(52A)			67	100.0	P		
N	53			15	22.4	F	**YES**	R
		F	0.1	30	44.8			
		E	1.0	2	3.0			
		T	1.4	5	7.5			
		R	1.8	7	10.4			
		Y	3.5	5	7.5			
		D	8.0	1	1.5			
		K	13.5	2	3.0			
S	54			12	17.9	R	**YES**	G
		F	0.2	7	10.4			
		R	2.7	45	67.2			
		N	11.9	1	1.5			
		T	14.8	2	3.0			
G	55			67	100.0	G		
G	56			31	46.3	A	**YES**	A
		R	0.9	2	3.0			
		N	0.9	8	11.9			
		V	6.3	5	7.5			
		A	11.3	20	29.9			
		D	22.4	1	1.5			
T	57			21	31.3	V	**YES**	V
		V	0.4	21	31.3			
		R	0.9	3	4.5			
		P	1.3	2	3.0			
		I	1.4	18	26.9			
		S	1.9	2	3.0			
N	58			18	26.9	K	**YES**	

		G	0.7	10	14.9			
		E	1.4	15	22.4			
		D	7.2	8	11.9			
		K	16.5	16	23.9			
Y	59			52	77.6	Y		
		C	0.7	2	3.0			
		S	5.6	13	19.4			
A	60			42	62.7	P		
		R	0.1	3	4.5			
		E	1.6	3	4.5			
		T	1.9	6	9.0			
		P	2.1	0	0.0			
		V	2.2	8	11.9			
		S	3.0	5	7.5			
Q	61			56	83.6	Q		R
		R	2.8	3	4.5			
		E	4.3	8	11.9			
K	62			64	95.5	N		P
		R	7.5	1	1.5			
		N	9.4	2	3.0			
F	63			66	98.5	F		L
		L	2.4	1	1.5			
Q	64			56	83.6	R		
		R	4.8	11	16.4			
G	65			67	100.0	G		
R	66			67	100.0	R		
V	67			66	98.5	V		
		L	2.3	1	1.5			
T	68			64	95.5	S		
		I	2.4	2	3.0			
		S	4.4	1	1.5			
M	69			64	95.5	M		
		L	12.3	3	4.5			
T	70			67	100.0	T		
R	71			67	100.0	R	**YES**	
D	72			67	100.0	D		
T	73			66	98.5	T		V
		P	0.8	1	1.5			
S	74			66	98.5	S		Y
		T	0.7	1	1.5			
I	75			67	100.0	M		S
		M	1.5	0	0.0			

S	76			37	55.2	E		D
		E	0.1	0	0.0			
		I	0.3	1	1.5			
		K	0.6	1	1.5			
		R	3.1	1	1.5			
		T	13.3	20	29.9			
		N	18.0	7	10.4			
T	77			64	95.5	I		
		I	0.6	3	4.5			
A	78			60	89.6	F		
		F	0.5	0	0.0			
		T	2.1	1	1.5			
		V	15.3	6	9.0			
Y	79			67	100.0	Y		F
M	80			64	95.5	M		L
		L	9.1	3	4.5			
E	81			65	97.0	E		
		V	0.4	2	3.0			
L	82			66	98.5	L		
		M	2.3	1	1.5			
S	(82A)			45	67.2	S		R
		K	1.2	1	1.5			
		R	8.1	2	3.0			
		N	8.9	16	23.9			
		T	12.8	3	4.5			
R	(82B)			59	88.1	R		S
		G	13.4	8	11.9			
L	(82C)			66	98.5	L		
		V	0.9	1	1.5			
R	83			60	89.6	T		T
		N	0.7	1	1.5			
		I	1.7	1	1.5			
		K	7.9	2	3.0			
		T	29.6	3	4.5			
S	84			66	98.5	S		V
		Y	2.3	1	1.5			
D	85			66	98.5	D		
		N	1.0	1	1.5			
D	86			67	100.0	D		
T	87			67	100.0	T		
A	88			67	100.0	A		
V	89			60	89.6	V		

		R A M I	0.1 0.3 4.6 10.8	1 1 1 4	1.5 1.5 1.5 6.0			
Y	90			67	100.0	Y		
Y	91	 N F	 0.0 14.6	48 2 17	71.6 3.0 25.4	Y		F
C	92			67	100.0	C		
A	93	 T V	 3.5 5.1	65 1 1	97.0 1.5 1.5	A		T
R	94			67	100.0	R		

VL2-23*02 amino acid	VL Position	amino acid substitution	Random Frequency	# of IGT2 induced mAbs with this SHM	IGT2 Frequency	IOMA Substitution	Critical Interaction	VK3-20*01 Residue	VL Position	VRC01 Substitution	Random Frequency	Critical Interaction
Q	1			67	100.0	Q		Q	1	Q	100.0	
S	2			66	98.5	S		S	2	S	98.5	
		F	0.1	1	1.5						1.5	
A	3			67	100.0	A		A	3	A	100.0	
L	4			67	100.0	L		L	4	L	100.0	
T	5			67	100.0	T		T	5	T	100.0	
Q	6			67	100.0	Q		Q	6	Q	100.0	
P	7			67	100.0	P		P	7	P	100.0	
A	8			67	100.0	A		A	8	A	100.0	
S	9			67	100.0	S		S	9	S	100.0	
V	11			67	100.0	V		V	11	V	100.0	
S	12			66	98.5	S		S	12	S	98.5	
		F	0.1	1	1.5						1.5	
G	13			67	100.0	G		G	13	G	100.0	
S	14			67	100.0	S		S	14	S	100.0	
P	15			67	100.0	P		P	15	P	100.0	
G	16			62	92.5	G		G	16	G	92.5	
		E	0.1	5	7.5						7.5	
Q	17			67	100.0	Q		Q	17	Q	100.0	
S	18			67	100.0	S		S	18	S	100.0	
I	19			65	97.0	I		I	19	I	97.0	
		S	0.1	1	1.5						1.5	
		T	0.1	1	1.5						1.5	
T	20			67	100.0	T		T	20	T	100.0	
I	21			67	100.0	I		I	21	I	100.0	
S	22			67	100.0	S		S	22	S	100.0	
C	23			67	100.0	C		C	23	C	100.0	
T	24			67	100.0	A		T	24	A	100.0	
		A	2.3	0	0.0						0.0	
G	25			63	94.0	G		G	25	G	94.0	
		V	0.1	4	6.0						6.0	
T	26			65	97.0	S		T	26	S	97.0	
		P	0.6	1	1.5						1.5	
		A	2.6	1	1.5						1.5	
		S	7.2	1	1.5						1.5	
S	27			65	97.0	S		S	27	S	97.0	
		G	2.2	1	1.5						1.5	

		R	2.5	1	1.5						1.5	
S	(27A)			63	94.0	R	**YES**	S	(27A)	R	94.0	**YES**
		R	2.4	2	3.0						3.0	
		N	6.1	2	3.0						3.0	
D	(27B)			67	100.0	D		D	(27B)	D	100.0	
V	(27C)			53	79.1	V		V	(27C)	V	79.1	
		F	1.9	1	1.5						1.5	
		I	17.0	13	19.4						19.4	
G	28			67	100.0	G		G	28	G	100.0	
S	29			51	76.1	G	**YES**	S	29	G	76.1	**YES**
		I	2.0	1	1.5						1.5	
		R	3.2	4	6.0						6.0	
		G	5.3	4	6.0						6.0	
		T	14.3	1	1.5						1.5	
		N	14.5	6	9.0						9.0	
Y	30			56	83.6	F	**YES**	Y	30	F	83.6	**YES**
		S	3.0	4	6.0						6.0	
		F	4.1	7	10.4						10.4	
N	31			35	52.2	D	**YES**	N	31	D	52.2	**YES**
		Y	1.3	4	6.0						6.0	
		D	10.2	28	41.8						41.8	
L	32			65	97.0	L		L	32	L	97.0	
		F	8.2	2	3.0						3.0	
V	33			67	100.0	V		V	33	V	100.0	
S	34			66	98.5	S		S	34	S	98.5	
		P	0.0	1	1.5						1.5	
W	35			67	100.0	W		W	35	W	100.0	
Y	36			67	100.0	Y		Y	36	Y	100.0	
Q	37			67	100.0	Q		Q	37	Q	100.0	
Q	38			67	100.0	Q		Q	38	Q	100.0	
H	39			67	100.0	H		H	39	H	100.0	
P	40			67	100.0	P		P	40	P	100.0	
G	41			67	100.0	G		G	41	G	100.0	
K	42			66	98.5	K		K	42	K	98.5	
		N	0.7	1	1.5						1.5	
A	43			61	91.0	A		A	43	A	91.0	
		T	0.8	5	7.5						7.5	
		V	7.6	1	1.5						1.5	
P	44			67	100.0	P		P	44	P	100.0	
K	45			67	100.0	K		K	45	K	100.0	
L	46			66	98.5	L		L	46	L	98.5	
		F	2.4	1	1.5						1.5	

M	47			63	94.0	I		M	47	I	94.0	
		L	10.7	2	3.0						3.0	
		I	34.4	2	3.0						3.0	
I	48			66	98.5	I		I	48	I	98.5	
		L	2.6	1	1.5						1.5	
Y	49			66	98.5	Y		Y	49	Y	98.5	
		H	1.8	1	1.5						1.5	
E	50			51	76.1	E		E	50	E	76.1	
		K	0.3	4	6.0						6.0	
		D	6.5	12	17.9						17.9	
V	51			67	100.0	V		V	51	V	100.0	
S	52			46	68.7	N		S	52	N	68.7	
		I	3.2	1	1.5						1.5	
		N	19.8	14	20.9						20.9	
		T	29.2	6	9.0						9.0	
K	53			38	56.7	K		K	53	K	56.7	
		A	0.2	1	1.5						1.5	
		R	3.8	23	34.3						34.3	
		Q	4.9	4	6.0						6.0	
		E	7.1	1	1.5						1.5	
R	54			67	100.0	R		R	54	R	100.0	
P	55			67	100.0	P		P	55	P	100.0	
S	56			67	100.0	S		S	56	S	100.0	
G	57			67	100.0	G		G	57	G	100.0	
V	58			61	91.0	I		V	58	I	91.0	
		I	10.9	6	9.0						9.0	
S	59			66	98.5	S		S	59	S	98.5	
		Y	0.0	1	1.5						1.5	
N	60			65	97.0	S		N	60	S	97.0	
		S	7.3	1	1.5						1.5	
		D	17.3	1	1.5						1.5	
R	61			67	100.0	R		R	61	R	100.0	
F	62			67	100.0	F		F	62	F	100.0	
S	63			65	97.0	S		S	63	S	97.0	
		A	0.4	2	3.0						3.0	
G	64			65	97.0	A		G	64	A	97.0	
		D	0.1	1	1.5						1.5	
		A	5.3	1	1.5						1.5	
S	65			67	100.0	S		S	65	S	100.0	
K	66			67	100.0	K		K	66	K	100.0	
S	67			65	97.0	S		S	67	S	97.0	
		C	0.0	1	1.5						1.5	

		A	0.5	1	1.5						1.5	
G	68			65	97.0	G		G	68	G	97.0	
		D	3.3	2	3.0						3.0	
N	69			66	98.5	N		N	69	N	98.5	
		K	0.8	1	1.5						1.5	
T	70			64	95.5	T		T	70	T	95.5	
		M	0.8	2	3.0						3.0	
		S	0.8	1	1.5						1.5	
A	71			67	100.0	A		A	71	A	100.0	
S	72			67	100.0	S		S	72	S	100.0	
L	73			67	100.0	L		L	73	L	100.0	
T	74			56	83.6	T		T	74	T	83.6	
		P	0.0	2	3.0						3.0	
		I	0.5	9	13.4						13.4	
I	75			67	100.0	I		I	75	I	100.0	
S	76			67	100.0	S		S	76	S	100.0	
G	77			66	98.5	G		G	77	G	98.5	
		D	0.5	1	1.5						1.5	
L	78			32	47.8	L		L	78	L	47.8	
		F	0.0	35	52.2						52.2	
Q	79			65	97.0	Q		Q	79	Q	97.0	
		R	2.5	2	3.0						3.0	
A	80			59	88.1	E		A	80	E	88.1	
		E	0.1	0	0.0						0.0	
		D	0.3	1	1.5						1.5	
		T	4.9	6	9.0						9.0	
		P	5.1	1	1.5						1.5	
E	81			67	100.0	E		E	81	E	100.0	
D	82			67	100.0	D		D	82	D	100.0	
E	83			57	85.1	E		E	83	E	85.1	
		V	0.0	3	4.5						4.5	
		K	0.1	2	3.0						3.0	
		G	0.2	5	7.5						7.5	
A	84			66	98.5	A		A	84	A	98.5	
		G	4.2	1	1.5						1.5	
D	85			61	91.0	H		D	85	H	91.0	
		G	0.2	2	3.0						3.0	
		Y	0.9	1	1.5						1.5	
		N	2.1	1	1.5						1.5	
		H	2.6	0	0.0						0.0	
		E	4.1	2	3.0						3.0	
Y	86			65	97.0	Y		Y	86	Y	97.0	

		N		2	3.0						3.0	
Y	87			45	67.2	Y		Y	87	Y	67.2	
		E	0.0	1	1.5						1.5	
		D	0.0	5	7.5						7.5	
		H	4.3	12	17.9						17.9	
		F	6.2	4	6.0						6.0	
C	88			67	100.0	C		C	88	C	100.0	
C	89			57	85.1	Y		C	89	Y	85.1	
		W	0.8	1	1.5						1.5	
		Y	1.8	4	6.0						6.0	
		S	10.3	5	7.5						7.5	
S	90			60	89.6	S		S	90	S	89.6	
		L	0.7	6	9.0						9.0	
		T	1.0	1	1.5						1.5	
Y	96			61	91.0	Y		Y	96	Y	91.0	
		C	0.7	1	1.5						1.5	
		S	2.1	3	4.5						4.5	
		F	7.4	2	3.0						3.0	
A	97			48	71.6	A		A	97	A	71.6	
		E	1.4	1	1.5						1.5	
		T	5.8	3	4.5						4.5	
		G	7.2	9	13.4						13.4	
		V	8.8	6	9.0						9.0	

Table S5: Serum neutralization in wildtype mice

			M1		M3		M4		M5		M13		M14		M15		M21	
			B3 (week 18)		B3 (week 18)		B3 (week 18)		B3 (week 18)		B3 (week 18)		B3 (week 18)		B3 (week 18)		B4 (week 23)	
Virus	**Clade**	**Tier**	**ID_{50}**	**% 1:100**	**ID_{50}**	**% 1:100**	**ID_{50}**	**% 1:100**	**ID_{50}**	**% 1:100**	**ID_{50}**	**% 1:100**	**ID_{50}**	**% 1:100**	**ID_{50}**	**% 1:100**	**ID_{50}**	**% 1:100**
426c	C	2	<100	0	<100	0	<100	0	<100	0	<100	0	<100	0	<100	0	<100	0
25710	B	2	<100	0	<100	0	<100	0	<100	0	<100	0	<100	0	<100	0	<100	0
CNE8	AE	1	<100	0	<100	0	<100	0	<100	0	<100	0	<100	0	<100	0	225	56
CNE8 N276A	AE	1	<100	0	<100	0	<100	0	<100	0	<100	0	<100	0	<100	0	<100	0
CNE20	BC	2	<100	0	<100	0	<100	0	<100	0	<100	0	<100	0	<100	40	<100	0
CNE20 N276A	BC	2	<100	0	<100	0	<100	0	<100	0	<100	0	<100	0	<100	0	<100	0
JRCSF	B	2	<100	0	<100	0	<100	0	<100	0	<100	0	<100	0	<100	0	<100	0
Q23.17	A	1	<100	0	<100	0	<100	0	<100	0	<100	0	<100	0	<100	40	<100	0
YU2	B	2	<100	0	<100	0	<100	0	<100	0	<100	0	<100	0	<100	0	<100	0
BG505 T332N	A	2	<100	0	<100	0	<100	0	<100	0	<100	0	<100	0	<100	0	<100	0
6535.5	B	1	<100	0	<100	0	<100	0	<100	0	<100	0	<100	0	<100	47	<100	0
3415_V1_C1	A	2	<100	0	<100	0	<100	0	<100	0	<100	0	<100	0	<100	0	<100	0
CAAN5342.A2	B	2	<100	0	–	–	<100	0	<100	0	<100	0	<100	0	<100	0	<100	0
PVO.4	B	3	113	57	–	–	<100	0	<100	0	<100	41	<100	0	145	58	<100	0
Q842.D12	A	2	<100	43	–	–	<100	0	<100	0	<100	0	<100	0	<100	0	<100	0
RHPA4259.7	B	2	<100	0	–	–	<100	0	<100	0	<100	0	<100	0	<100	0	<100	0
WITO4160.33	B	2	<100	47	–	–	<100	0	<100	0	<100	0	<100	0	<100	0	<100	0
ZM214M.PL15	C	2	<100	0	–	–	<100	0	<100	0	<100	0	<100	0	<100	0	<100	0
MuLV			<100	0	–	–	<100	0	<100	0	<100	0	<100	0	<100	0	<100	0
			M22		**M23**		**M24**		**M25**		**M26**		**M27**		**M28**		**M29**	
			B4 (week 23)		**B4 (week 23)**		**B4 (week 23)**		**B4 (week 23)**		**B4 (week 23)**		**B4 (week 23)**		**B4 (week 23)**		**B4 (week 23)**	
Virus	**Clade**	**Tier**	**ID_{50}**	**% 1:100**	**ID_{50}**	**% 1:100**	**ID_{50}**	**% 1:100**	**ID_{50}**	**% 1:100**	**ID_{50}**	**% 1:100**	**ID_{50}**	**% 1:100**	**ID_{50}**	**% 1:100**	**ID_{50}**	**% 1:100**
426c	C	2	<100	0	<100	0	<100	0	<100	0	<100	0	<100	0	<100	0	<100	0
25710	B	2	<100	0	<100	0	<100	0	<100	0	<100	0	<100	0	<100	0	<100	0
CNE8	AE	1	<100	0	<100	0	100	50	<100	0	729	70	<100	0	841	61	242	71
CNE8 N276A	AE	1	<100	0	<100	0	<100	0	<100	0	<100	0	<100	0	<100	0	<100	0
CNE20	BC	2	<100	0	<100	0	<100	0	<100	0	<100	0	<100	0	<100	0	<100	0
CNE20 N276A	BC	2	<100	0	<100	0	<100	0	<100	0	<100	0	<100	0	<100	0	<100	0

JRCSF	B	2	<100	0	<100	0	<100	0	<100	0	<100	0	<100	0	<100	0	<100	0
Q23.17	A	1	<100	0	<100	0	<100	0	<100	0	<100	0	<100	0	<100	0	<100	0
YU2	B	2	<100	0	<100	0	<100	0	<100	0	<100	0	<100	0	<100	0	<100	0
BG505 T332N	A	2	<100	0	<100	0	<100	0	<100	0	<100	0	<100	0	<100	41	<100	0
6535.5	B	1	<100	0	<100	0	<100	0	<100	0	<100	0	<100	0	<100	0	<100	0
3415_V1_C1	A	2	<100	0	<100	0	<100	0	<100	0	<100	0	<100	0	<100	0	<100	0
CAAN5342.A2	B	2	<100	0	<100	0	<100	0	<100	0	<100	0	<100	0	<100	0	<100	0
PVO.4	B	3	<100	0	<100	0	<100	0	<100	0	<100	0	<100	0	<100	43	<100	0
Q842.D12	A	2	<100	0	<100	0	<100	0	<100	0	<100	0	<100	0	<100	0	<100	0
RHPA4259.7	B	2	<100	0	<100	0	<100	0	<100	0	<100	0	<100	0	<100	0	<100	0
WITO4160.33	B	2	<100	0	<100	0	<100	0	<100	0	<100	0	<100	0	<100	0	<100	0
ZM214M.PL15	C	2	<100	0	<100	0	<100	0	<100	0	<100	0	<100	0	<100	0	<100	0
MuLV			<100	0	<100	0	<100	0	<100	0	<100	0	<100	0	<100	0	<100	0

Table S6: Oligonucleotides used to generate yeast display gp120 libraries.

Oligo Name	Fragment	Sequence
426c Library 1 For	1	GTCTGGAAAGAGGCTAAGACCACACTG
426c Library 1 Rev	1	CAGGTTTTTTGATCTGATCACAATCTCTTC
426c Library 1 - 1 For	2	GAAGAGATTGTGATCAGATCAAAAAACCTGNNKAACAATGCCAAGATCATTATCGTGC
426c Library 1 - 2 Rev	2	ATCTCCACACTCTTATTCAGCTGCACGATAATGATCTTGGCATT
426c Library 1 - 3 For	2	AGCTGAATAAGAGTGTGGAGATCGTCTGCACACGACCTAACA
426c Library 1 - 4 Rev	2	GCCTGCCGAATATCTCCCCCAGATCCGCTGCCGCCATTGTTAGGTCGTGTGCAGACG
426c Library 1 - 5 For	2	GGAGATATTCGGCAGGCTTATTGTAACATCAGTGGCAGAAATTGGTCAGAAGCCGTGAA
426c Library 1 - 6 Rev	2	TGGGGGAAGTGCTCTTTCAGCTTTTTCTTGACCTGGTTCACGGCTTCTGACCAATTT
426c Library 1 - 7 For	2	AAAGAGCACTTCCCCCATAAGAATATTAGCTTTCAGTCTAGTTCAGGCGGGGAC
426c Library 1 - 8 Rev	2	TCGCCTCCGCAGTTGAAGGAGTGTGTGGTGATTTCCAGGTCCCCGCCTGAACTA
426c Library 1 - 9 For	2	ACTGCGGAGGCGAGTTCTTTTACTGTAATACATCCGGCCTGTTTAACG
426c Library 1 - 10 Rev	2	CCGGCAAGGCAGCATGATTGTGGCATTAGAAATGGTATCGTTAAACAGGCCGGATGTA
426c Library 1 - 11 For	2	GCTGCCTTGCCGGATCAAGCAGATTATCAACATGTGGCAGGAA
426c Library 1 - 12 Rev	2	TGCCCTTGATGGGTGGTGCATAGATAGCCTTTCCMNNTTCCTGCCACATGTTGATAATC
426c Library 1 - 13 For	2	CCACCCATCAAGGGCAATATCACCTGTAAGAGTGACATTACAGGGCTGCTGCTGCTGAGA
426c Library 1 - 14 Rev	2	GCCGGAAAATCTCGGTmnnmnnmnnmnnmnnTCCCCCATCTCTCAGCAGCAGCAGCC
426c Library 1 - 15 For	2	ACCGAGATTTTCCGGCCTAGCGGAGGAGACATGCGAGATAATTGGCGGTCTGAACTG
426c Library 1 - 16 Rev	2	GGATCCCAGAGGCTTGATCTCGACCACCTTATATTTGTACAGTTCAGACCGCCAATTA
426c Library 1 For	3	CTGGTGGAGGCGGTAGCGGAGGCGGAGGGTCGGCTAGCGTCTGGAAAGAGGCTAAGACCA
426c Library 1 Rev	3	TTACAAGTCCTCTTCAGAAATAAGCTTTTGTTCGGATCCCAGAGGCTTGATCTCGACCAC
426c Library 2 For	1	GTCTGGAAAGAGGCTAAGACCACACTG
426c Library 2 Rev	1	CAGGTTTTTTGATCTGATCACAATCTCTTC
426c Library 2 - 1 For	2	GAAGAGATTGTGATCAGATCAAAAAACCTGNNKAACAATGCCAAGATCATTATCGTGC
426c Library 2 - 2 Rev	2	ATCTCCACACTCTTATTCAGCTGCACGATAATGATCTTGGCATT
426c Library 2 - 3 For	2	AGCTGAATAAGAGTGTGGAGATCGTCTGCACACGACCTAACA
426c Library 2 - 4 Rev	2	GCCTGCCGAATATCTCCCCCAGATCCGCTGCCGCCATTGTTAGGTCGTGTGCAGACG
426c Library 2 - 5 For	2	GGAGATATTCGGCAGGCTTATTGTAACATCAGTGGCAGAAATTGGTCAGAAGCCGTGAA
426c Library 2 - 6 Rev	2	TGGGGGAAGTGCTCTTTCAGCTTTTTCTTGACCTGGTTCACGGCTTCTGACCAATTT
426c Library 2 - 7 For	2	AAAGAGCACTTCCCCCATAAGAATATTAGCTTTCAGTCTAGTTCAGGCGGGGAC
426c Library 2 - 8 Rev	2	TCGCCTCCGCAGTTGAAGGAGTGTGTGGTGATTTCCAGGTCCCCGCCTGAACTA
426c Library 2 - 9 For	2	ACTGCGGAGGCGAGTTCTTTTACTGTAATACATCCGGCCTGTTTAACG
426c Library 2 - 10 Rev	2	CCGGCAAGGCAGCATGATTGTGGCATTAGAAATGGTATCGTTAAACAGGCCGGATGTA
426c Library 2 - 11 For	2	GCTGCCTTGCCGGATCAAGCAGATTATCAACATGTGGCAGGAA
426c Library 2 - 12 Rev	2	TGCCCTTGATGGGTGGTGCATAGATAGCCTTTCCMNNTTCCTGCCACATGTTGATAATC
426c Library 2 - 13 For	2	CCACCCATCAAGGGCAATATCACCTGTAAGAGTGACATTACAGGGCTGCTGCTGCTGAGA
426c Library 2 - 14 Rev	2	GCCGGAAAATCTCGGTmnnmnnmnnmnnmnnTCCCCCATCTCTCAGCAGCAGCAGCC
426c Library 2 - 15 For	2	ACCGAGATTTTCCGGCCTAGCGGAGGAGACATGCGAGATAATTGGCGGTCTGAACTG
426c Library 2 - 16 Rev	2	GGATCCCAGAGGCTTGATCTCGACCACCTTATATTTGTACAGTTCAGACCGCCAATTA
426c Library 2 For	3	CTGGTGGAGGCGGTAGCGGAGGCGGAGGGTCGGCTAGCGTCTGGAAAGAGGCTAAGACCA
426c Library 2 Rev	3	TTACAAGTCCTCTTCAGAAATAAGCTTTTGTTCGGATCCCAGAGGCTTGATCTCGACCAC

Table S7: Flow cytometric reagents

Reagent	Target species	Antibody clone	Company / Source	Cat.#	RRID
CD16/32	mouse	2.4G2	BD Biosciences	553142	AB_394657
CD4-APCeF780	mouse	RM4-5	Thermo Fisher	47-0042-82	AB_1272183
CD8a-APCeF780	mouse	53-6.7	Thermo Fisher	47-0081-82	AB_1272185
NK1.1-APCeF780	mouse	PK136	Thermo Fisher	47-5941-82	AB_2735070
F4/80-APCeF780	mouse	BM8	Thermo Fisher	47-4801-82	AB_2735036
Ly-6G/C (Gr1)-APCeF780	mouse	RB6-8C5	Thermo Fisher	47-5931-82	AB_1518804
CD11b-APCeF780	mouse	M1/70	Thermo Fisher	47-0112-82	AB_1603193
CD11c-APCeF780	mouse	N418	Thermo Fisher	47-0114-82	AB_1548652
CD93-APC	mouse	AA4.1	Thermo Fisher	17-5892-82	AB_469466
TER-119-APCCy0	mouse	TER-119	BD Pharmingen	560509	AB_1645230
CD95 (FAS)-FITC	mouse	SA367H8	BioLegend	152606	AB_2632901
CD38-AF700	mouse	90	Thermo Fisher	56-0381-82	AB_657740
CD45R/B220-BV421	mouse / human	RA3-6B2	BD Horizon	562922	AB_2737894
CD45R/B220-BV605	mouse / human	RA3-6B2	BioLegend	103244	AB_2563312
IgD-BV786	mouse	11-26c.2a	BD Horizon	563618	AB_2738322
CD19-PECy7	mouse	6D5	BioLegend	115520	AB_313655
CD2-PE	mouse	RM2-5	BioLegend	100108	AB_2073690
CD23-PE	mouse	B3B4	BioLegend	101607	AB_312832
Ig light chain lambda-APC	mouse	RML-42	BioLegend	407306	AB_961363
Ig light chain kappa-BV421	mouse	187.1	BD Horizon	562888	AB_2737867
CD21/CD35	mouse	7G6	BD Horizon	562756	AB_2737772
IgM Fab-FITC	mouse	polyclonal	Jackson Immunoresearch	115-097-020	AB_2338618
Zombie NIR	N/A*	N/A	BioLegend	423105	N/A
Streptavidin-PE	N/A	N/A	BD Pharmingen	554061	AB_10053328
Streptavidin-AF647	N/A	N/A	BioLegend	405237	N/A
Streptavidin-PECy7	N/A	N/A	BioLegend	405206	N/A

RC1-biotin	N/A	N/A	in house	N/A	N/A
CNE8 N276A-biotin	N/A	N/A	in house	N/A	N/A
426c degly2 D279N-biotin	N/A	N/A	in house	N/A	N/A
426c degly2 D279N CD4bs-KO -biotin	N/A	N/A	in house	N/A	N/A
Human Fc Block	human	N/A	BD Horizon	564220	AB_2869554
Ig light chain lambda-APC	human	MHL38	BioLegend	316610	AB_493629
CD19-PECy7	human	SJ25C1	BioLegend	363012	AB_2564203
IgM-FITC	human	MHM88	BioLegend	314506	AB_493009
Ig light chain kappa-BV421	human	MHK-49	BioLegend	316518	AB_2561581

*N/A not applicable

Table S8: Single cell antibody cloning reaction conditions.

PCR1 IgH	Primer sequence
HH_1FL (forward, leader)	CCATGGGATGGTCATGTATCA
HH_1RG (reverse, IgG)	GGACAGGGATCCAGAGTTCC
HH_1RM (reverse, IgM)	CCCATGGCCACCAGATTCTT
PCR1 IgK	**Primer sequence**
HH_1FL (forward, leader)	CCATGGGATGGTCATGTATCA
HH_1RK (reverse, IgK)	GACTGAGGCACCTCCAGATG

PCR1 mastermix		
Reagent	**Volume/plate (µL)**	**Concentration**
nuclease free water	3328	
10x buffer	384	1x
dNTP (25 mM)	48	0.3 mM
5' forward Primer (50 µM)	HC 15; LC 19	HC 0.25 µM; LC 0.25 µM
3' reverse Primer (50 µM)	HC 23 (IgG/IgM 1:1); LC 19	HC 0.30 µM; LC 0.25 µM
HotStar DNA Polymerase (5 U/µL)	42	0.055 U/µL
total	3840	

PCR2 IgH	Primer sequence
HH_2FL (forward, leader)	GTAGCAACTGCAACCGGTGTACATTCT
HH_2RG (reverse, IgG)	GCTCAGGGAARTAGCCCTTGAC
HH_2RM (reverse, IgM)	AGGGGGAAGACATTTGGGAAGGAC
PCR2 IgK	**Primer sequence**
HH_2FL (forward, leader)	GTAGCAACTGCAACCGGTGTACATTCT
HH_2RK (reverse, IgK)	AACTGCTCACTGGATGGTGG

PCR2 mastermix		
Reagent	**Volume/plate (µL)**	**Concentration**
nuclease free water	2536	
loading buffer*	800	
10x buffer	384	1x
dNTP (25 mM)	48	0.3 mM
5' forward Primer (50 µM)	HC 12; LC 15	HC 0.16 µM; LC 0.2 µM
3' reverse Primer (50 µM)	HC 18 (IgG/IgM 1:1); LC 15	HC 0.23 µM; LC 0.2 µM
HotStar DNA Polymerase (5 U/µL)	42	0.055 U/µL
total	3840	
*loading buffer: 40% (w/v) sucrose in nuclease free water with cresol red added to dark red color.		